POLITECNICO
MILANO 1863

DIPARTIMENTO DI
INGEGNERIA CIVILE E AMBIENTALE

Undrained shear strength of soft Finnish clay

TESI DI LAUREA MAGISTRALE IN
CIVIL ENGINEERING-INGEGNERIA CIVILE

Author: **Reza Khalili**

Student ID:	10745666
Advisor:	Cristina Jommi
Co-advisor:	Wojciech Solowski
Academic Year:	2023-24

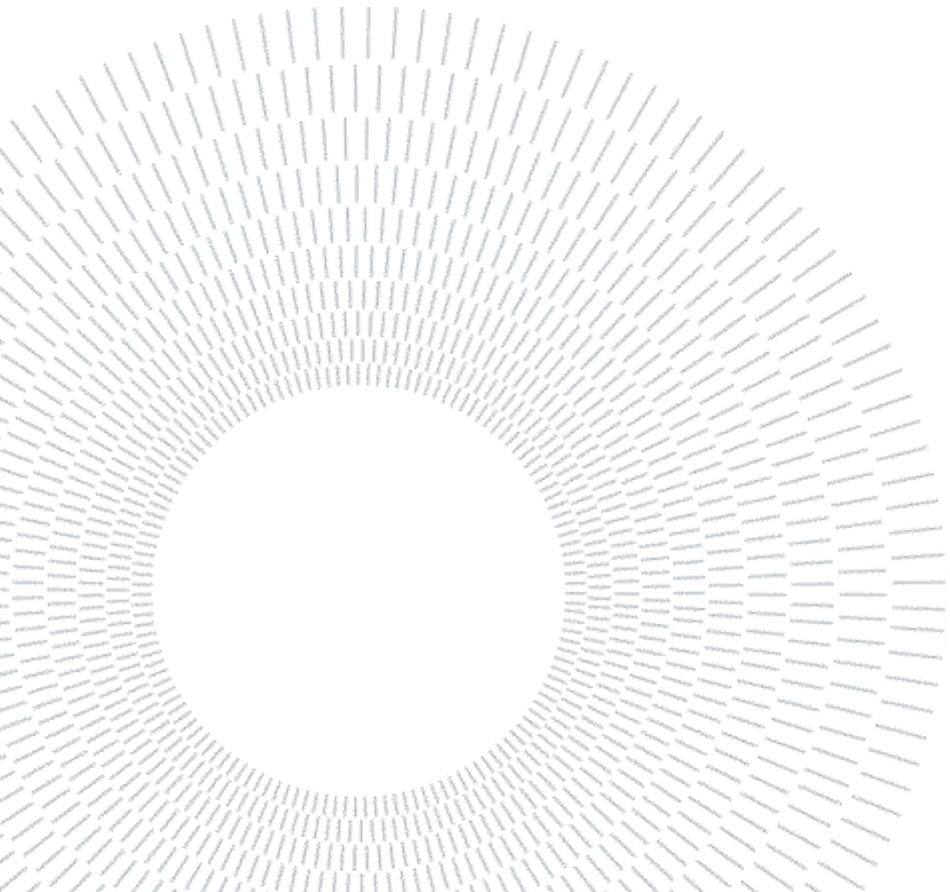

Abstract

This thesis investigates experimentally marine deposits from the gulf of Finland. It established the properties of the deposits, such as the water content, density, undrained shear strength, organic content, and sensitivity. Furthermore, the research investigated both undisturbed and remoulded samples of the deposits with oedometric and triaxial tests. Those help to further assess the effects of structure on compressibility and shear strength. Both isotropic and anisotropic triaxial tests are done and for anisotropic conditions, the case $\eta < k_0$ are investigated. Finally, undrained shear strength is estimated by three approaches such as fall cone tests, oedometric and triaxial tests and then make a comparison between approaches is done and the error of each method is investigated. At the end, the interpretation of the result is done by using two constitutive modelling framework such as Modified Cam Clay model and S-CLAY1 model.

Keywords: Undrained shear strength, Fall cone test, Oedometric test, Undrained consolidated triaxial test, Soft Finnish clay.

Abstract in lingua italiana

Questa tesi indaga sperimentalmente i depositi marini del Golfo di Finlandia. Ha stabilito le proprietà dei depositi, come il contenuto di acqua, la densità, la resistenza al taglio non drenata, il contenuto organico e la sensibilità. Inoltre, la ricerca ha indagato sia campioni indisturbati che rimodellati dei depositi con prove edometriche e triassiali. Questi aiutano a valutare ulteriormente gli effetti della struttura sulla compressibilità e sulla resistenza al taglio. Vengono eseguiti entrambi i test triassiali isotropi e anisotropi e per condizioni anisotrope vengono studiati il case $\eta < k_0$. Infine, la resistenza al taglio non drenata è stimata mediante tre approcci come i test del cono di caduta, i test edometrici e triassiali e quindi si effettua un confronto tra gli approcci e si studia l'errore di ciascun metodo. Alla fine, l'interpretazione del risultato viene effettuata utilizzando due framework di modellazione costitutiva come il modello Modified Cam Clay e il modello S-CLAY1.

Parole chiave: Resistenza al taglio non drenata, Prova del cono di caduta, Edometrico test, Prova triassiale consolidata non drenata, Argilla morbida finlandese.

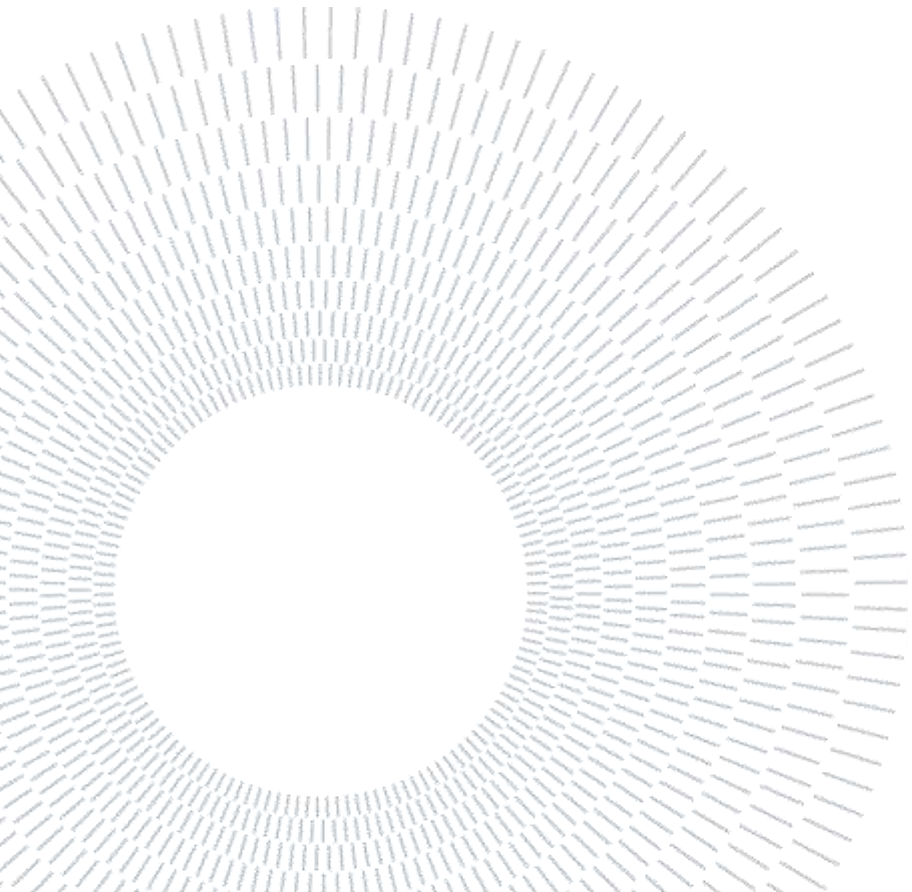

Contents

Abstract ..... **i**

Abstract in lingua italiana ..... **iii**

Contents ..... **v**

1. Introduction **7**

1.1 Research background 7

1.2 Research problem 7

1.3 Research questions 8

2. Materials and methods **11**

2.1 Geo classification of fine-grained materials 11

2.1.1 Marine clay 12

2.1.2 Soft Finnish fine-grained sediments 12

2.2 Physical properties of the soil 12

2.2.1 Hydrometer test 12

2.2.2 Pycnometer test 15

2.2.3 Organic Matters 15

2.3 Geotechnical laboratory tests 16

2.3.1 Fall cone test 16

2.3.2 Oedometric test 19

2.3.3 Consolidated undrained Triaxial test 28

3. Results **33**

3.1 Images and Tomography 33

3.2 Sampling profile 36

3.3 Profile of physical properties 37

3.4 Fall Cone test 39

3.4.1 Undrained shear strength 39

3.4.2 Sensitivity ..... **Error! Bookmark not defined.**
3.5 Oedometric test 41
3.5.1 Remoulded sample 41
3.5.2 Undisturbed sample 43
3.5.3 Oedometric result curve 43
3.6 Triaxial test 52
3.6.1 Remoulded sample for ~~$(\eta = k0)$~~ $(\eta = 0)$ 52
3.6.2 Undisturbed sample for $(\eta = 0)$ 52
3.6.3 Undisturbed sample for $(\eta < k0)$ 52
3.6.4 Specimen and test information 53
3.6.5 Test results 54
4. Analysis of the results 57
4.1 Statistics on penetration depth in Fall Cone test 57
4.2 Errors in the determination of undrained shear strength 63
4.2.1 Fall Cone test 63
4.2.2 Oedometric test 65
4.2.3 Triaxial test 65
4.3 Comparisons and Recommendations 68
5. Conclusions 73
Bibliography 75
A. Appendix 79
B. List of Figures 131
C. List of Symbols 134

1. Introduction

1.1 Research background

In the near future, offshore wind energy will become increasingly popular as a renewable source of energy in Finland because it can reduce carbon emissions and confront climate change. The Baltic Sea wind energy potential is significant and currently estimated at up to 93 GW (European Commission, 2019). The sediments of the Baltic Sea in the Kytö site which is located in an Island in Espoo consist often of thick soft clay layers although the seabed conditions especially in the Gulf of Finland are less known. One of the most basic parameters used in engineering practice to characterize soils is the undrained shear strength (C_u). The particular importance of C_u is in the case of clay soil. Furthermore, According to ISO standard, this parameter also determines soil classification. Some phenomena such as underwater landslide and bearing capacity failure are common in clays in the seabed, hence, by undrained shear strength the capability or bearing capacity of soils can be estimated. In this research, the marine sediments extracted from the seabed of the Baltic sea and then the numerical estimation of the undrained shear strength of the deposit are done. Then the results of undrained shear strength obtained from the Free Fall Cone Penetrometer (FF-CPT) data are compared with those from laboratory tests including triaxial tests, oedometric tests and fall cone tests.

1.2 Research problem

Undrained shear strength of soil can be determined by using different methods (SFS-EN ISO 17892-9, 2017, SFS-EN ISO 17892-9, 2017, SFS-EN ISO 17892-6, 2017). Fall Cone test (SFS-EN ISO 17892-6, 2017) is one of the easiest and quickest method to obtain undrained shear strength of clay. However, this method has several drawbacks. One of the most obvious ones that can be mentioned is human errors. Furthermore, this method includes a lot of uncertainties such as the roughness of cone with soil as well as stem with device and also the smoothness of the surface can

affect our result because it can directly influence on penetration depth. Therefore, for obtaining more reliable undrained shear strength value, Triaxial (SFS-EN ISO 17892-9, 2017) test and Oedometric (SFS-EN ISO 17892-5, 2017) test are performed to clarify the accuracy of Fall Cone test.

In addition, laboratory tests are advantageous for their controlled conditions, accurate results, detailed analysis, time-saving, and cost-effectiveness. Therefore, it is favorable to perform laboratory tests such as triaxial and oedometric tests to obtain properties of materials like undrained shear strength.

1.3 Research questions

1. How can we characterize the physical properties of an offshore site in the northern Gulf of Finland?
2. What is the level of accuracy and reliability of fall cone tests in determining undrained shear strength values of marine sediments, and how do these results compare to those obtained from laboratory tests, including triaxial tests and oedometric tests?
3. How does the mean value of penetration depth can be accurate compare to other methods, such as empirical correlations based on statistics for obtaining undrained shear strength?
4. How do you obtain the undrained shear strength by oedometric tests for structured and destructuration parts, and what are the main hypothesis in this method?

1. For determining the type of soil, grain size distribution and hydrometer tests will be done. Since in this research, we are working on fine-grained soils, a total of 15 series of hydrometer tests are done in two different locations in order to obtain, for instance, the percentage of fine-grained particles like clay and silt. For one location, the percentage of clay was approximately 85%, while for the other location, it was approximately 65%. Therefore, it is clear that soil is realized as clay. In addition, it is obvious that the two locations are a little bit different. Finally, according to the ASTM Standard, since our clay content is greater than 50%, we can call it "fat clay".
2. The fall cone test is a quick and easy method for estimating undrained shear strength. In this work for evaluating the value of undrained shear strength by fall cone test, Houlsby's method is used, which depends on different parameters such as cone factor, penetration depth, and the cone's weight. The

major problem related to this method is that we deal with a lot of uncertainties. For example, the cone tip, friction of the stem, lack of lateral boundary, the roughness of the surface, heterogeneity of the sample, and above all, human error, all can introduce a lot of uncertainties and seem to give us an overestimated value of undrained shear strength, which is not economical from a design point of view and can roughly influence the results. But this kind of test can be useful just to get an idea about the range of the undrained shear strength, especially on a large scale, in a rough way. For these reasons, oedometric and triaxial tests are implemented to get more realistic results. For oedometric tests, Modified Cam Clay (MCC) and S-CLAY constitutive models are employed. There are some differences between each of the constitutive models, which are explained in the next few chapters, but the main difference is that the MCC model is a purely isotropic model, while the S-Clay model considers anisotropy.The results of these two models show that the values of undrained shear strength are very close to each other. One of the bottleneck of this method is correctly defining the pre-consolidation pressure, and if this parameter is defined correctly, we can say that the results of this method are ~~very~~ close to those of the triaxial test. The percentage of error between the fall cone test and the oedometric test is approximately 50-60%. Finally, for the triaxial test, two types of calculations are taken into account. The first one is a typical triaxial test, and the second one is doing a triaxial test while considering pre-consolidation pressure from an oedometric test; this pre-consolidation pressure is something that soil has in the field, and the results of these are very close to each other, and in the shallower layer, these two are coincident. It would seem that this type of test is the most realistic one because in this test we confined the sample by a membrane as well as applied different confining pressures to the sample, which is very similar to the soil in the field. In this case, the percentage of error concerning the fall cone test is approximately 35–40%, and for the oedometric test, it is 20–25%. In the shallower layer, this error is smaller, and vice versa.

3. In practical applications, the mean number of penetration depths is typically utilized as a criterion, despite its inadequacy in calculations due to the heterogeneity of the sample. This heterogeneity can manifest in the presence of water or stone particles in some portions of the sample, which may impact the depth of penetration. Therefore, statistical analyses are employed in this research to demonstrate that the penetration depth can vary across different locations. Specifically, a t-student test is conducted, and a probability mass function is constructed to show that the data clusters around the mean value. The uncertainty of the mean value in relation to the first penetration (i.e., the

center of the sample) is then calculated, indicating an error of approximately 5%. It is important to note that this error can be reduced with an increase in the amount of data available. Consequently, the uncertainty associated with all the penetrations is also considered, revealing a reduction in uncertainty to approximately 2%, which is in close proximity to the mean value.

4. In this method, first, the coefficient of earth pressure (k_0) and the value of the critical state line (M) is determined by triaxial tests. Following a thorough analysis of multiple test results, it is hypothesized that the coefficient of earth pressure (k_0) and the critical state line (M) are constant values across all tests. furthermore, It is postulated that the slope of the normal consolidation line (λ), derived from the oedometric test conducted on remoulded samples, is a constant value. In the next step, the pre-consolidation pressure is ascertained through the oedometric test, and the initial effective stress and deviatoric stress are computed. As the soil is anticipated to be non-normally consolidated, the undrained shear strength demonstrates a linear increase, resulting in additional volumetric changes. Thus, it becomes necessary to undergo an unloading process from the k_0-line toward the critical state line (CSL). (Further elucidation is provided in Section 2.3.2.). Finally, the effective and deviatoric stresses are computed in the critical state line (CSL), followed by the estimation of the undrained shear strength based on these new stress values.

   For the destructuration part, a similar approach is employed. Initially, two points that have experienced significant structure are identified, typically at the final part of the loading phase. Subsequently, a line is drawn parallel to the normal consolidation line (NCL) with a slope of λ, while maintaining the same volume as in the previous phase. Thus, by determining the effective stress at the most structured point and its corresponding volume, as well as the volume at the critical state line (CSL) corresponding to the pre-consolidation pressure point, and the slope of the CSL, the effective stress in this line can be calculated. Following this step, the subsequent procedure is identical to that of the previous part.

2. Materials and methods

2.1 Geo classification of fine-grained materials

The location of the site that samples are taken is shown in the Figure 2-1. This is in the Kytö site which is located at about five kilometers south of Suvisaaristo.

Figure 2-1 Map of the site

2.1.1 Marine clay

A soft soil known as marine clay is common along the coast and offshore. This kind of soil is typically characterized by significant settlement and instability, poor soil qualities, and an inability to meet engineering requirements. Because of the high moisture content, this type of soil is usually considered detrimental.

Furthermore, marine clay is typically composed of soil minerals such as chlorite, kaolinite, montmorillonite, and illite, as well as stone minerals such as quartz and feldspar, all of which are bonded together by the presence of organic matter (Hj Ali & Ahmad, 2013). Marine clays are highly vulnerable to changes in moisture content, and when found underneath the pavements or foundations, they are unreliable and frequently unforeseen in performance (Marto et al., 2014).

Through the flocculation process, the structure of marine clay deposited on the ocean can be changed by which fine particles are caused to clump or floc together. Relating to the interaction of clay particles, the flocculation can be edge to edge or edge to face. Clays can also be aggregated or shifted in their structure besides being flocculated.

Physical properties of marine clay like liquid limit, plastic limit, water content, depth from which the marine clay is obtained, organic content, and specific gravity are the most important parameters that affect the strength and stability of marine clays.

2.1.2 Soft Finnish fine-grained sediments

The majority of Finnish fine-grained sediments are NC or lightly OC, with an over-consolidation ratio ranging between 1 and 2. Clays with high sensitivity are found in all sediments (Gardemeister R, 1975). Finland's soft, fine-grained sediments were deposited either at the end of the last ice age (late glacial sediment) or later (post-glacial sediment). The structure of the marine sediments varies which is mainly based on the stages of evolution of the Baltic Sea (Hyyppä, 1963). The stratification of the sediments is weak due to the salinity of the water. Variation in the significance of the varves occurs as a result of the mixing of fresh and saline water (Gardemeister R, 1975).

2.2 Physical properties of the soil

2.2.1 Hydrometer test

According to (SFS-EN ISO 17892-4, 2016), Hydrometer tests are performed.

Samples were collected from two distinct locations at the Kytö site in the Baltic Sea, called KU1 (LAT 60°00.625 and LONG 24°44.382) and KU4 (LAT 60°02.155 and LONG 24°42.368). Consequently, two sets of hydrometer tests were conducted: seven tests were performed for 40 days in the first series to obtain an optimal range of readings, while eight tests were conducted for 20 days in the second series. The disparity in the duration of the tests indicates that the characteristics of the two locations are dissimilar. Figure 2-2 displays one of the hydrometer tests.

Figure 2-2 Hydrometer test

Figures 2-3 and 2-4 display the outcomes of the hydrometer test, demonstrating the grain size distribution of the Kytö site's KU1 and KU2 locations, respectively. If the fine-grained soil's clay content exceeds 10%, it is categorized based on the clay content.

- If clay content is between 10 to 30 percent, it calls **clayey silt**.
- If clay content is between 30 to 50 percent, it calls **lean clay**.
- If clay content is larger than 50%, it calls **fat clay** (ASTM Committee D-18 on Soil and Rock, 2017).

It is clear that most part of the soil contains clay and soft silt. In both cases, since clay contents are more than 50%, therefore, they are some types of fat clay.

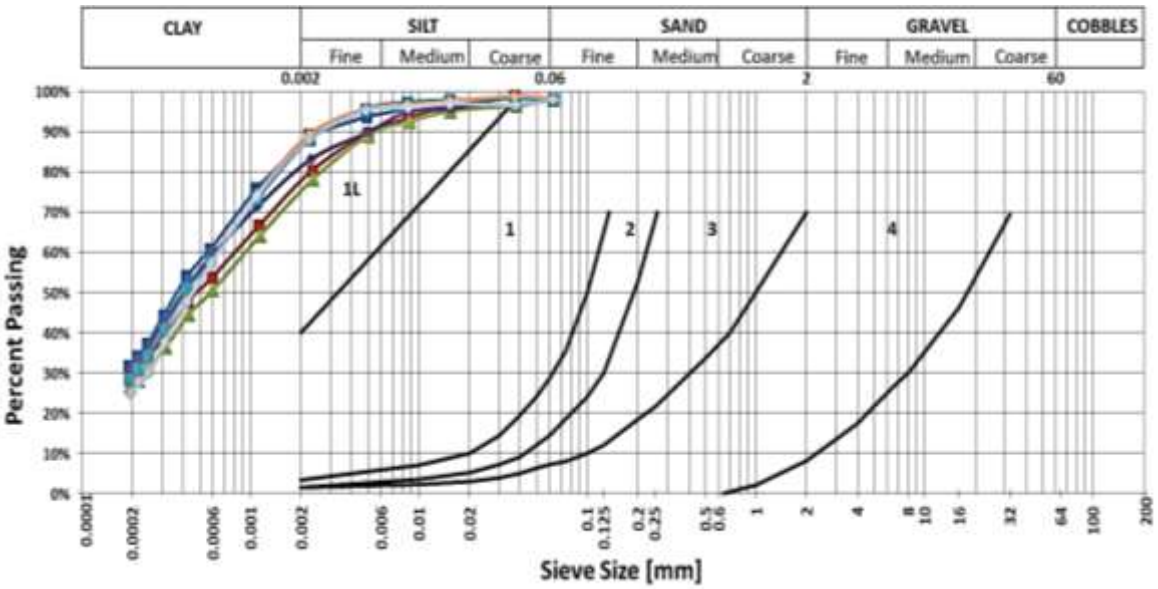

Figure 2-3 Hydrometer test for the site KU1

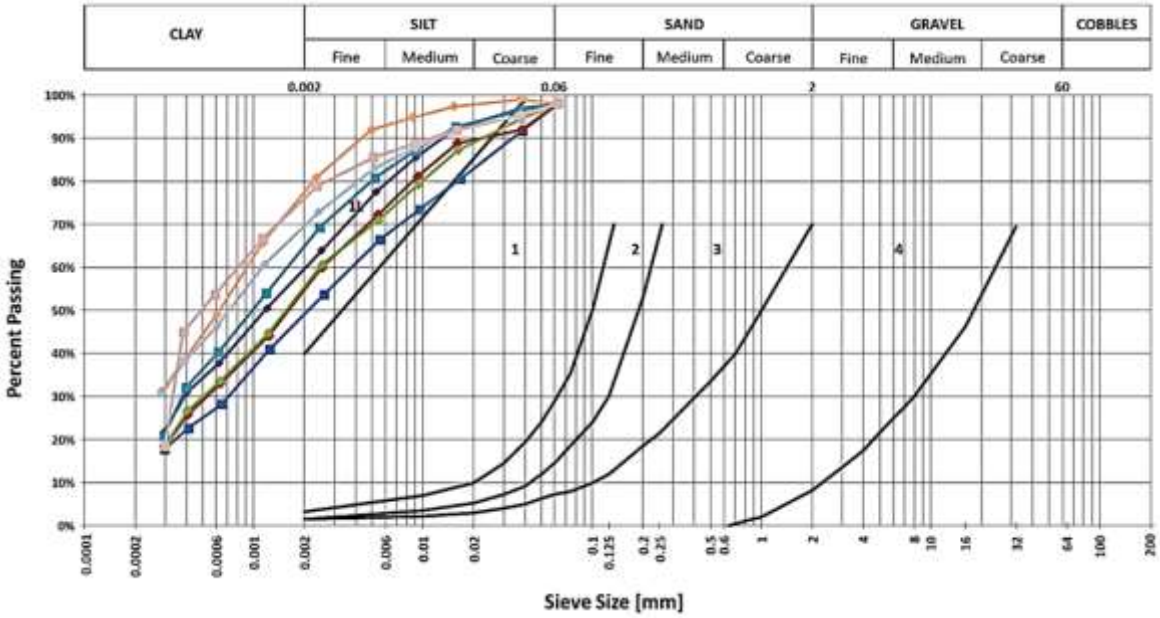

Figure 2-4 Hydrometer test for the site KU1

The result of the Hydrometer experiment of two sites (KU1 and KU4) are given in Table A.1 to Table A.8 in the Appendix.

2.2.2 Pycnometer test

The pycnometer is a widely utilized instrument for quantifying the density of substances in both solid and liquid states. To carry out this measurement, a standardized pycnometer test procedure, the (SFS-EN ISO 17892-3, 2015) standard is typically employed.

Figure 2-5 Pycnometer glass

The outcomes of the measurements of solid density have been documented in the Appendix, where Tables A.9 and A.10 respectively display the relevant data.

2.2.3 Organic Matters

Soil organic matter is an organic component of soil and consists of three primary parts including humus (plant material that has rotted down to create the rich, black substance in soil that helps hold water and nutrients), roots of living trees and plants, and living soil organisms. It is included 4% to more than 5% of the soil (Magdoff F. & van ES H., 2021).

There are two commonly used methods for the determination of the organic matter in sediment: (EN 1997-2, 2007)

1) For accurate determination, organic nitrogen and organic carbon are estimated.
2) For rough estimation, measuring the loss of weight on ignition can be used.

The second method is only used in ecological studies where the organic matter in marine sediment is needed for environmental issues (Luczak et al., 1997).

We caution that, when CaCO3 is high in marine sediments, loss of weight on ignition be used with great care by keeping furnace temperatures below 5oo°C, and that the method was checked (Hirota J. & Szyper JP., 1975) by determining the loss of weight after baking prepared samples of pure CaCO3.

The results of Organic Matters are shown in Table A.11 and Table A.12 in the Appendix.

2.3 Geotechnical laboratory tests

This research involved conducting three distinct types of tests, specifically the Fall Cone, Oedometric, and Triaxial tests.

2.3.1 Fall cone test

The first time, the fall cone test was developed by Swedish state railways between 1914 and 1922, and after that, it was widely used in Scandinavian countries (Hansbo, 1957). In this test, a metal cone is vertically placed in the contact with surface sample, and it is dropped freely by its weight to penetrate the sample. Then the penetration depth is recorded. In Figure 2.6 the apparatus is shown.

Figure 2-6 Fall cone apparatus for undisturbed sample

Before starting this test, first, it should be checked that the cone is not corroded and that the friction between the stem and apparatus shall be reduced as much as possible by lubricating. Furthermore, for the test, the depth of the specimen shall be specified in advance. To obtain an undisturbed sample, the first part of the sample at

the tube which is at the top shall be cut off with a wire cutter because it may be disturbed (SFS-EN ISO 17892-6, 2017).

For measuring the penetration depth of remoulded sample, the structure of the soil should be completely broken down. Then cup shall be filled with a sample without entrapping air bubbles and smooth the surface with a spatula (SFS-EN ISO 17892-6, 2017) The apparatus used for remoulded samples is as Figure 2.7.

Figure 2-7 Fall cone apparatus for remoulded sample

The samples used in this research have a five-centimeter diameter and a 10-centimeter height. The cone has radius of 60° degrees and a mass of 60 grams. The penetration depth in all samples is almot four to 12 mm. For the undisturbed sample, five tests are done, and for remoulded sample, three tests are done. The ISO standard suggests getting the mean values of them and if any values deviate more than 0.5 mm, they should be removed. Since in this research, the values have some irregular differences, for the matter of using mean value, statistical analyses were performed ~~are done~~ in the next chapter to determine the uncertainty of the penetration depth of our tests. This study involves 32 fall cone tests in total.

One of the objective of the fall cone test is determining undrained shear strength Generally, for obtaining undrained shear strength, equation (1) is used (Hansbo, 1957):

$$S_u = \frac{KQ}{h^2} \quad (1)$$

Where Q is the weight of the cone, h is the penetration depth, and K is the fall cone factor, which depends on the degree of roughness and cone angle. In Table 2.1, values of K for different cone apex angles (β) and different roughnesses (α) are presented by (Koumoto T & Houlsby G. T, 2001).

β	30°	45°	60°	75°	90°
Smooth α=0	2	0.835	0.4	0.216	0.120
Semi-rough α=0.5	1.33	0.580	0.305	0.171	0.097
Rough α=1	1.03	0.495	0.250	0.152	0.090

Table 2.1 Calculated values of K for different values of β and α

In Figure 2.8, a comparison is presented between theoretical values of K derived by (Koumoto T & Houlsby G. T, 2001) and experimental values obtained from studies conducted by (Hansbo, 1957; Karlsson, 1961; Wood D. M., 1982, 1985). The comparison was made for different cone apex angles, and it was observed that for a cone apex 60 degrees, the theoritical and experimental results were found to be in close agreement. For the present research, a cone apex angle of 60°/60 gr was selected, and while the roughness results for this cone were similar to those observed in previous studies, a value of α equal to one was assumed. Based on the values presented in Table 2.1, the coefficient K was determined to be 0.25 for the current research.

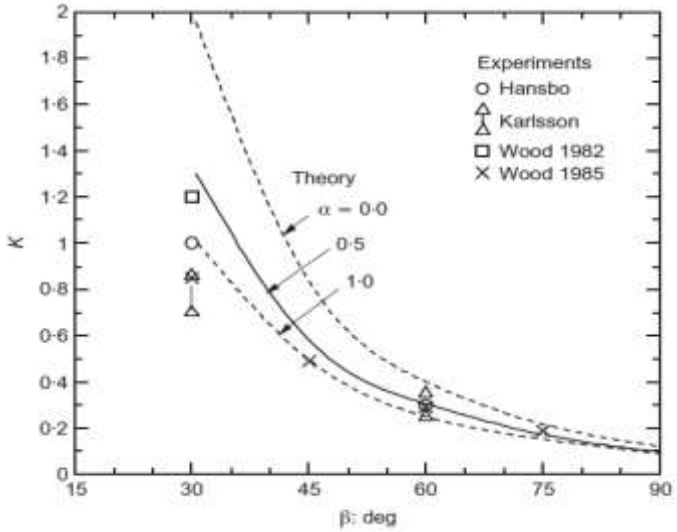

Figure 2-8 Comparison between theoretical and experimental values by different researchers

2.3.2 Oedometric test

Incremental loading tests are used in these types of tests. By increasing effective stress, the pore water pressure decreases and as a result, the void ratio decreases.

In this research, 14 Oedometric tests are done, 12 of which are for undisturbed samples and two of them for remoulded samples.

The samples that are used have a 2 cm height and 5 cm diameter. At first, the ring shall be greased, and then a 2 cm sample is taken from the required tube. In the next step, the side of the ring shall be cleaned and the surface must be smoothed. Next, the porous stone and filter paper is put at the bottom of the cell, then the sample is put in the cell and after that filter paper, porous stone, and loading cap are put on the sample, respectively.

After finishing the preparation of the sample and substituting it in the cell, the loading apparatus should be put in the center of the loading cap. The loop of unloading/reloading is considered two times. The reading of the deformation gauge is done in the intervals 6 sec, 15 sec, 30 sec, 1 min, and 1 day. The procedure of loading is such that first, we apply 62.5-gram weight, and readings are started for each interval until 1 minute. Then immediately after that, we add another 62.5-gram weight and write readings until 1 minute and the last reading is red after 45 minutes. Then, the 125-gram weight is added, and written reading until one minute. Next, we have to wait one day and then write the last reading. The same procedure should be repeated for weights 250 gr, 500 gr, 1 kg, 2kg, 4kg and 8 kg. After that, the unloading procedure will be started. In this part, after one hour we bring a load and write the readings and the unloading procedure will be continued until the weight 500 gr. The next day, the same procedure is done each hour for reloading. Finally, on the last day, we unload the weights each minute, and then the last readings are written (SFS-EN ISO 17892-5, 2017).

In this research, two constitutive models are used for obtaining undrained shear strength which are Modified Cam Clay Model (MCC Model) and S-CLAY1 Model.

2.3.2.1 MCC Model

This is a very simple model which considers the same shape as the yield surface and the change of this yield surface only depends on volumetric deformation.

For formulation of this model the following assumptions is considered:

- Elastic deformation

$$\delta\varepsilon_p^e = \frac{\kappa}{\nu}\frac{\delta p'}{p'} \tag{2}$$

$$\delta\varepsilon_q^e = \frac{\delta q}{3G'} \tag{3}$$

- Yield surface

The yield surface is assumed to be elliptical and as follows:

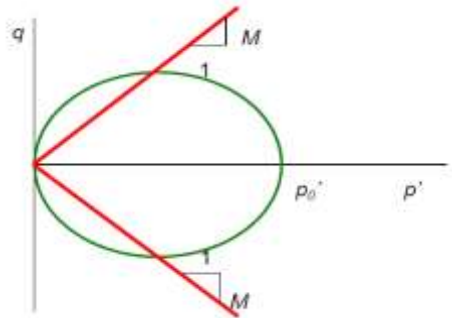

Figure 2-9 Yield surface in MMC Model

And also can be expressed in terms of $\eta = \frac{q}{p'}$ as follows:

$$\frac{p'}{p'_0} = \frac{M^2}{M^2 + \eta^2} \tag{4}$$

- Flow rule

According to MCC Model, since the flow rule is associated, therefore f=g

$$g = f \equiv q^2 - M^2 p'\left(p'_0 - p'\right) = 0 \tag{5}$$

- Hardening law

In this model, all deformations are existed and can have both elastic and plastic components, but only volumetric plastic strain affects hardening which describes the changes in the size of the yield surface.

$$\frac{\partial p'_0}{\partial \varepsilon_p^p} = \frac{v p'_0}{\lambda - \kappa} \tag{6}$$

$$\frac{\partial p'_0}{\partial \varepsilon_q^p} = 0 \tag{7}$$

2.3.2.2 S-CLAY1 Model

Since MCC model assumes Drucker-Prager failure condition which does not considered lode angle dependency on shear strength, so it gives an overestimated value of undrained shear strength. Furthermore, real soils are anisotropic and both the shape and size of the yield surface would need to change. Hence, for these reasons, S-CLAY1 is introduced. S-CLAY1 is a critical state type of model that incorporates an inclined yield surface to account for initial anisotropy and a rotational component of hardening to describe the soil's deformation behavior. (Koskinen M., 2014).

For formulation of this model the following assumptions is considered:

- Elastic deformation

To simplify the characterization of elastic behavior, an isotropic elastic relationship, similar to that of the Modified Cam Clay model (MCC) proposed by (Roscoe & Burland, 1968) is utilized.

- Yield surface

The shape of the yield surface is sheared ellipse as in Figure 2.10 and α is the scalar value of the inclination of the yield surface.

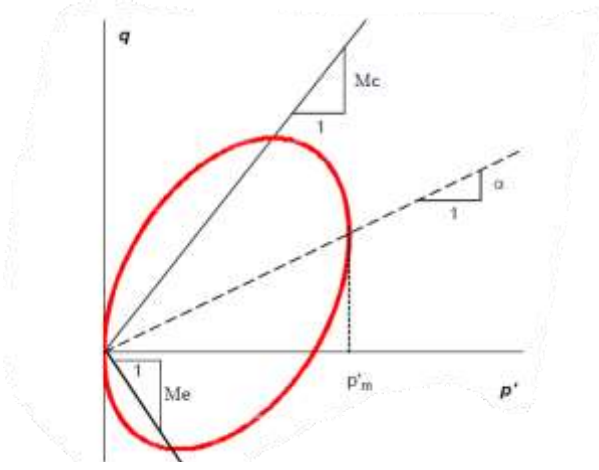

Figure 2-10 Yield surface in S-CLAY1 Model (Koskinen M., 2014)

- Flow rule

The S-CLAY1 model includes an associated flow rule, which has been proposed as a plausible assumption by (Korhonen & Lojander, 1987), taking into account experimental evidence.

$$g = f \equiv (q - \alpha p')^2 - (M^2 - \alpha^2)(p'_m - p')p' = 0 \quad (8)$$

In the above equation α is the inclination of the yield curve and calculated as follows:

$$\alpha_{k0} = \frac{\eta_{k0}^2 + 3\eta_{k0} - M^2}{3} \quad (9)$$

And p'_m defines the size of the yield surface and defines as Figure 2.11:

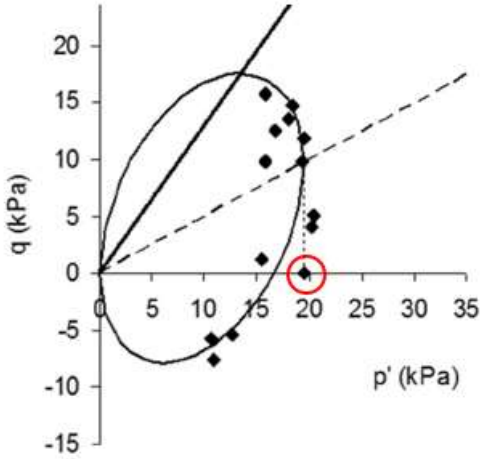

Figure 2-11 definition of p'_m (Koskinen M., 2014)

To compute p'_m using Equation 8, knowledge of the friction angle (to determine values of M and α) and at least one yield point on the yield curve is necessary.

- Hardening law

The model employs two types of hardening laws: a volumetric hardening law, similar to that used in the MCC model, which characterizes the size of the yield curve; and a rotational hardening law, which accounts for changes in the orientation of the yield surface.

2.3.2.3 Procedure for obtaining undrained shear strength by Oedometric test

In this context, two constitutive models, namely the MCC model and the S-CLAY1 model, are employed to characterize both structured and destructuration part.

2.3.2.3.1 MCC Model/Structured part

The procedure is as follows:

- Estimation of λ and κ

The determination of the slope of the normal compression line (NCL), λ, and the slope of the swelling line, κ, is accomplished through analysis of the ln p' – v plot obtained from an oedometer test. For natural soils, the value of λ is stress ratio-dependent; thus, it considers this value to be the slope of natural structured soils. In all calculations, the value of λ assumed to be constant and correspond to the inclination of the slope of NCL for a remoulded sample.

- Estimation of critical state line position

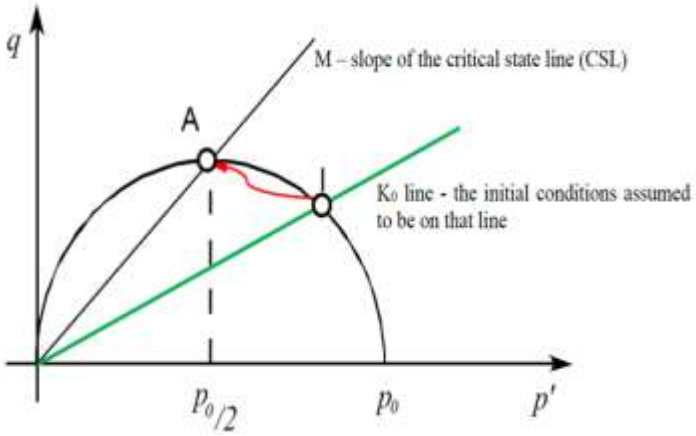

Figure 2-12 Position of critical state line

Since the soil has been expected to not normally consolidated, undrained shear strength increases linearly, and we have further volume change. The red line is the unloading line for the critical state line. The summary calculation about the above point is as follows:

$$p'_{ini} = \frac{\sigma_1 + 2 * \sigma_3}{3} \tag{10}$$

$$q = \sigma_1 - \sigma_3 \tag{11}$$

$$F = q^2 - M^2 p'(p'_0 - p') = 0 \rightarrow p'_0 = \cdots \tag{12}$$

$$p'_{CSL} = \frac{p'_0}{2} \tag{13}$$

$$q_{CSL} = Mp'_{CSL} \quad (14)$$

- Determination of specific volume (No destructuration)

$$v_{CSL} = \nu + \kappa \ln(\frac{p'_{ini}}{p'_{CSL}}) \quad (15)$$

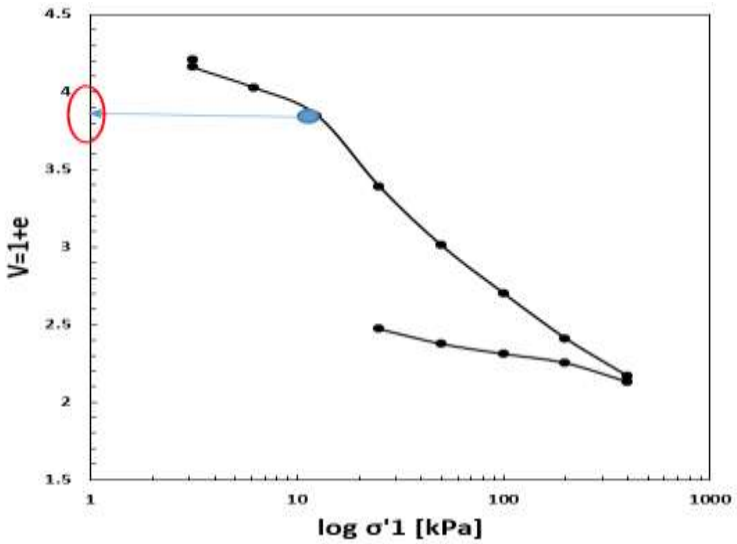

Figure 2-13 Position of v in the above formula

- Calculation of p′ during shearing at constant volume

$$v = v_{CSL} + \lambda \ln\left(\frac{p'_{CSL}}{p'_{structured}}\right) \rightarrow p'_{structured} = \frac{p'_{CSL}}{e^{\frac{v - v_{CSL}}{\lambda}}} \quad (16)$$

$$q = M * p'_{structured} \quad (17)$$

- Calculation of undrained shear strength

$$Cu_{struct} = \frac{q}{2} \quad (18)$$

2.3.2.3.2 MCC Model/Destructuration part

The procedure is as follows:

- Estimation of λ and κ (exactly the same value as before)

- Estimation of critical state line position

In this study, particular attention was given to the highly structured region of the material under investigation, which is characterized by the last part of the loading curve. This region is of significant interest as it experiences the most severe destructuration. The values of v and P' were assumed to be known for this region. To establish the CSL (Critical State Line) for this zone, a line was drawn parallel to the NCL (Normal Compression Line) while maintaining a constant value of v. This was achieved by setting the coordinates of the first point (by same λ) and the value of v for the second point. Using this information, the value of P' for the second point was determined. The process is illustrated in Figure 2.14.

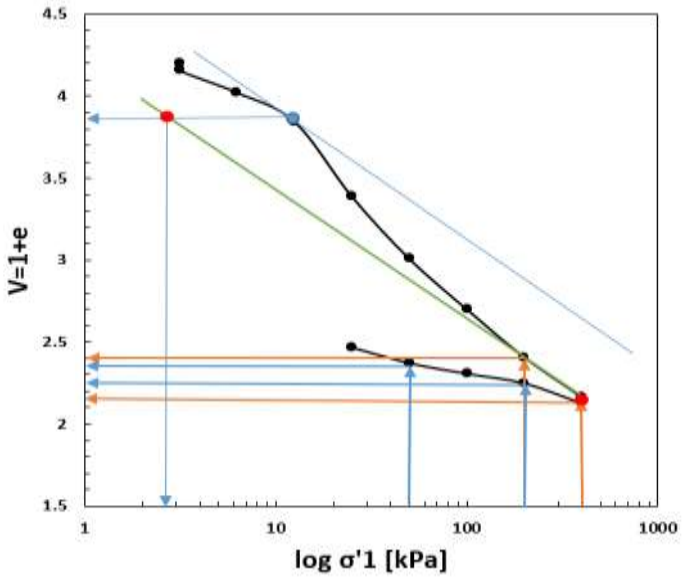

Figure 2-14 determination of p′ at destructuration part

Thus, by finding out P′ at red point, the other parameters like σ_1, σ_3, P'_{ini}, q, P'_0, P'_{CSL} and q_{CSL} will be calculated as before.

- Determination of specific volume (Destructuration)

$$\upsilon_{CSL} = \nu + \kappa \ln\left(\frac{p'_{ini}}{p'_{CSL}}\right) \tag{19}$$

- Calculation of p′ during shearing at constant volume

$$\upsilon = \upsilon_{CSL} + \lambda \ln\left(\frac{p'_{CSL}}{p'_{destruct}}\right) \rightarrow p'_{destruct} = \frac{p'_{CSL}}{e^{\frac{\upsilon - \upsilon_{CSL}}{\lambda}}} \quad (20)$$

$$q = M * p'_{destruct} \quad (21)$$

- Calculation of undrained shear strength

$$Cu_{destruct} = \frac{q}{2} \quad (22)$$

2.3.2.3.3 S-CLAY1 Model/Structured part

The procedure is as follows:

- Estimation of λ and κ (exactly as before)
- Determination of σ_1, σ_3, p'_{ini} and q as before.
- Calculation of α

$$\alpha_{k0} = \frac{\eta_{k0}^2 + 3\eta_{k0} - M^2}{3} \quad (23)$$

Which η_{k0} is equal to $\eta_{k0} = \frac{q}{p'}$

For calculation of p'_m, at first, we needed to know the value of the friction angle (for calculating the values of M and α) and one point on the yield curve.

- Estimation of p'_m

$$F = (q - \alpha P')^2 - (M^2 - \alpha^2)(P'_m - P')P' = 0 \rightarrow P'_m = \frac{(q - \alpha P')^2}{[P'(M^2 - \alpha^2)] + P'} \quad (24)$$

p'_m defines the size of the yield surface.

- Calculation of p' and q

$$P'_{CSL} = \frac{(M^2 - \alpha^2)P'_m}{M^2 - 2M\alpha + M^2} \quad (25)$$

$$q_{CSL} = M * p'_{CSL} \quad (26)$$

- Determination of specific volume (No destructuration)

$$v_{CSL} = \nu + \kappa \ln(\frac{p_{ini}^{'}}{p_{CSL}^{'}}) \quad (27)$$

- Calculation of p′ during shearing at constant volume

$$v = v_{CSL} + \lambda \ln\left(\frac{p'_{CSL}}{p'_{structured}}\right) \rightarrow p'_{structured} = \frac{p'_{CSL}}{e^{\frac{v - v_{CSL}}{\lambda}}} \quad (28)$$

$$q = M * p'_{structured} \quad (29)$$

- Calculation of undrained shear strength

$$Cu_{struct} = \frac{q}{2} \quad (30)$$

2.3.2.3.4 S-CLAY1 Model/destructuration part

This section involves the same calculations as the MCC section, the only difference is that instead of calculating p'_0, p'_m based on equation (24) must be calculated.

2.3.3 Consolidated undrained Triaxial test

2.3.3.1 Types of tests

For the aim of Triaxial tests, Wykeham Farrance system is used. In Figure 2.15, the system is shown:

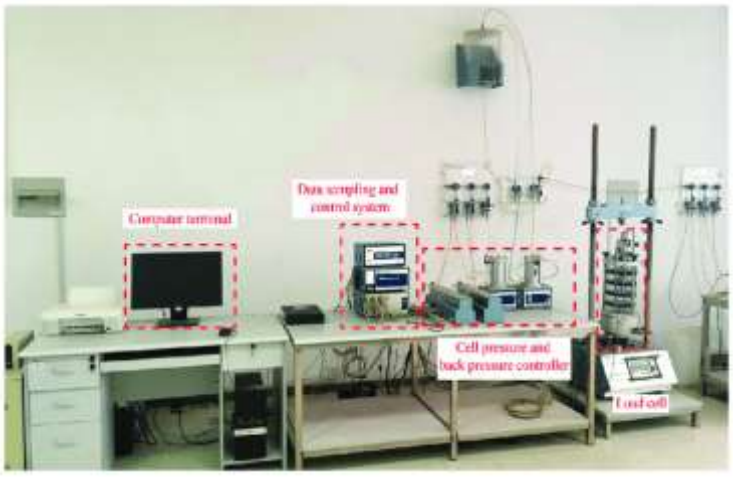

Figure 2-15 Wykeham Farrance system for Triaxial test

This device only measures the applied pressure. In addition, the back volume change is measured with a burette.

This test has two major stages, consolidation and shearing. Consolidation can be divided into isotropic and anisotropic, whereas shearing can be drained or undrained.

In this research two types of Triaxial tests are performed:

- Isotropic consolidation and undrained compression (CIUC)
- Anisotropic consolidation and undrained compression (CAUC)

The experimental conditions for this study involved conducting 16 triaxial tests, where isotropic materials were tested to determine their physical properties, which remained consistent in all directions during the testing process. Conversely, anisotropic materials were tested to assess their varying material properties in different directions. Furthermore, undrained conditions were maintained during the tests to ensure that water could not escape from the specimen, while a back pressure pump was used to control the back volume and maintain a constant pressure. Of the 16 tests conducted, 12 were performed on CIUC specimens, while the remaining four were conducted on CAUC specimens.

2.3.3.2 Preparation of specimen in the Laboratory

The soil samples under study are stored in a controlled environment at a temperature of 6°C, simulating the in-situ soil temperature in Finland. The samples

are then trimmed to a dimension of 10 cm height and 5 cm diameter, following which their weight is determined. Given the low permeability of clayey soils, the specimens are equipped with five wet filter papers arranged in a radial direction, serving as side drains to promote water drainage from the outer edges. The specimens are subsequently fully saturated to eliminate any entrapped air, and then inserted into a triaxial apparatus. Porous stones are carefully selected for the top and bottom of the sample to avoid any entrapment of soil particles or air bubbles, followed by sterilization in boiling water for 30 minutes and then subsequent vacuum chambering. The external surface of the specimen is covered with a membrane to prevent water ingress, with the top and bottom of the membrane sealed using four O-rings. Finally, the cell is positioned on the triaxial machine, the piston is set at the cap load, water is added to the cell, and the test is ready to commence.

The isotropic consolidation tests were conducted at confining pressures of 30 kPa, 60 kPa, and 90 kPa, while anisotropic consolidation tests were conducted at confining pressures of 30 kPa and 60 kPa. Each test lasted for approximately four days, with two days allocated for consolidation and two days for shearing.

2.3.3.3 Procedure for obtaining undrained shear strength by Triaxial test

The procedure is as follows:

- Determination of M and K_0

  In this study, a value of M=1.1 and a simplified equation $k_0 \approx 1 - sin\emptyset'$ were assumed to calculate K_0 for all models. While K_0 was approximately 0.55 in most cases, it was considered a fixed value of 0.6 for all cases. However, there were instances where K_0 deviated from 0.6 due to factors such as the sample originating from a different site. Furthermore, undergoing remoulding, resulting in a smaller K_0 value. Additionally, in one case, K_0 was estimated using only one triaxial test, reaching a value of 0.49.

- Using λ and κ from Oedometric test

  In all models, λ assumed to be 0.23

- Estimation of σ_1 and σ_3

$$\sigma_1 = \gamma'.H \tag{31}$$

$$\sigma_3 = K_0.\sigma_1 \tag{32}$$

Given the results of the triaxial test, which provides values for the parameters q_{max} , p'_{mox} and υ at a specific point A, it is assumed that the soil being tested is not in a normally consolidated state. Consequently, the undrained shear strength

of the soil is expected to increase linearly, leading to subsequent changes in volume, as indicated by point B in the graphical representation and the associated equations.

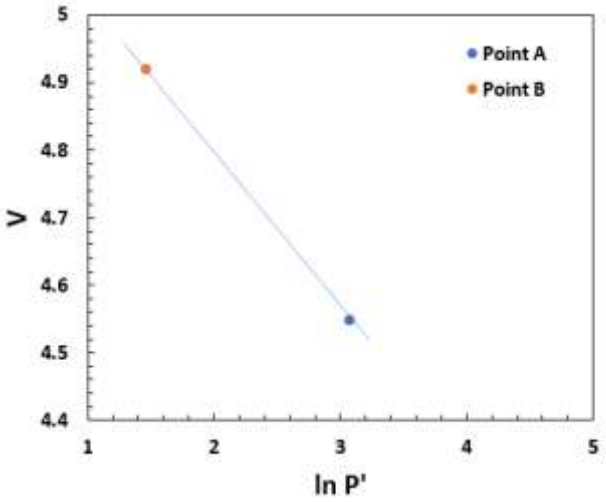

Figure 2-16 New point B for correct calculation

$$p_B^{'} = \frac{\sigma_1 + 2 * \sigma_3}{3} \tag{33}$$

$$q_B = M * p' \tag{34}$$

$$v_B = v_A + \lambda \ln(\frac{p_A^{'}}{p_B^{'}}) \tag{35}$$

$$C_u = \frac{q_B}{2} \tag{36}$$

3. Results

3.1 Images and Tomography

In this part, I investigated some specific depths of clay in two locations (KU1 and KU4) because most research is done in these two specific locations. The reason for choosing some specific depth is that for investigating the whole four meters depth the interpretation is very challenging to present long core, thus, only some specific depth is chosen for better graphical representation and interpretation.

Geological layers of KU1:

KU1 consists of a coarse-grained top layer up to 5 cm depth. Below the coarse-grained layer, there is grey postglacial lake clay to a depth of 210 cm. At the depth of 210 cm begins brownish glaciolacustrine clay which is indicated by silt and clay couplet layers. The lowest part of glaciolacustrine clay consists of debris-flow sediments.

Geological layers of KU4:

KU4 consists of olive-grey brackish-water clay up to 6 cm in depth. Below brackish-water sediment, there is grey postglacial lake clay to a depth of 330 cm. Below, there is brownish-grey glaciolacustrine clay with alternating silt and clay layers.

KU1 181-196 cm lacustrine clay:

Figure 3-1 is from the depth of 181-196 cm of investigation point KU1. According to geological studies, at that depth, there is postglacial lacustrine clay. It is weakly laminated, mostly homogeneous clay with some monosulfide mottlings.

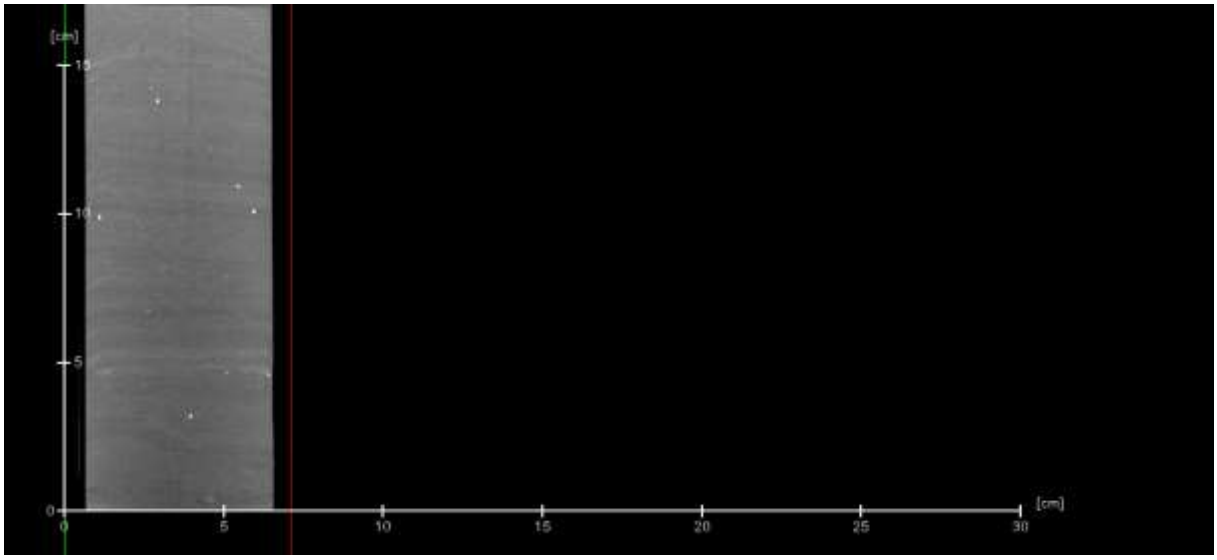

Figure 3-1 KU1 For the depth 181-196 cm

KU1 335-350 cm glaciolacustrine clay and debrite:

Figure 3-2 represents the lowest geological unit in the depth of 335-350 cm. The image shows a chaotic structure in glaciolacustrine clay.

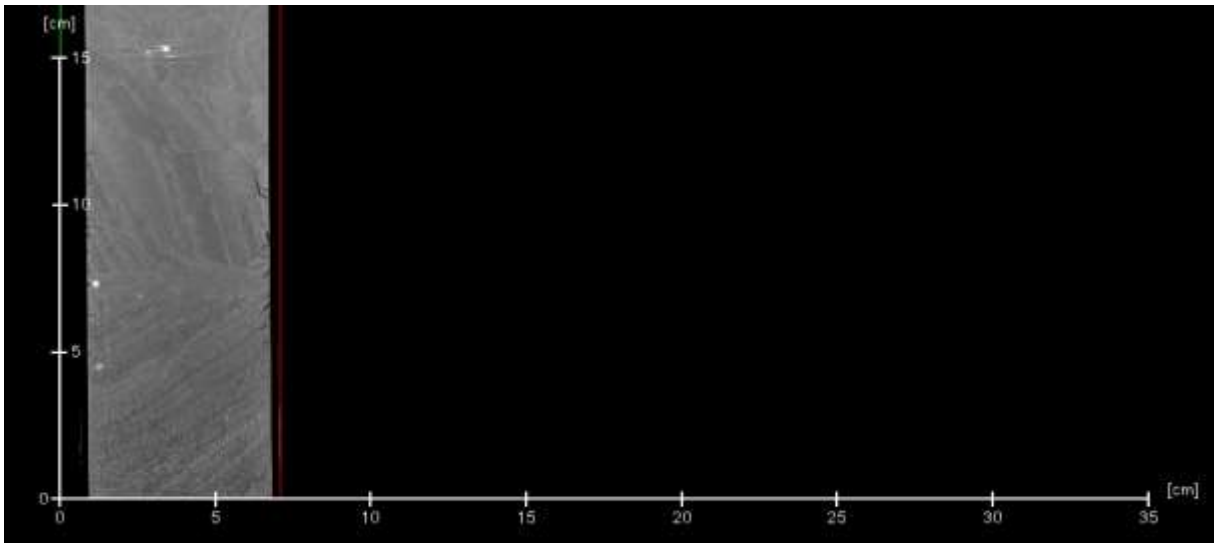

Figure 3-2 KU1 For the depth 335-350 cm

KU4 168-183 cm lacustrine clay:

Figure 3-3 shows postglacial lacustrine clay for point KU4 from depth of 168-183 cm. This sediment is very homogeneous with only few monosulfide mottlings.

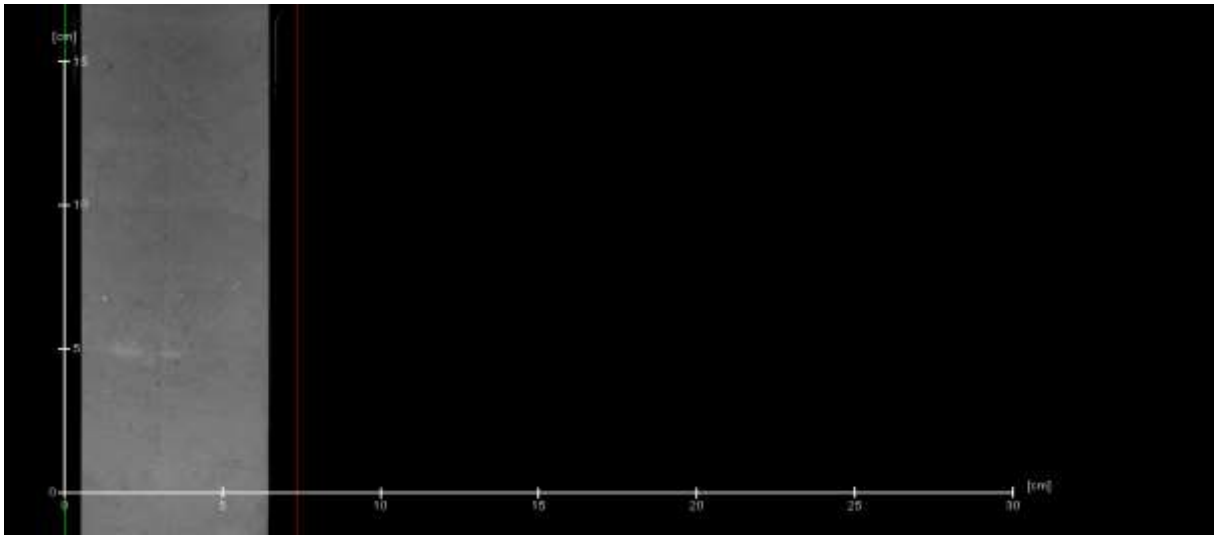

Figure 3-3 KU4 For the depth 168-183 cm

KU4 400-415 cm glaciolacustrine clay:

Figure 3-4 shows typical glaciolacustrine rhythmites with alternating silt and clay couplet layers in the bottom of the core.

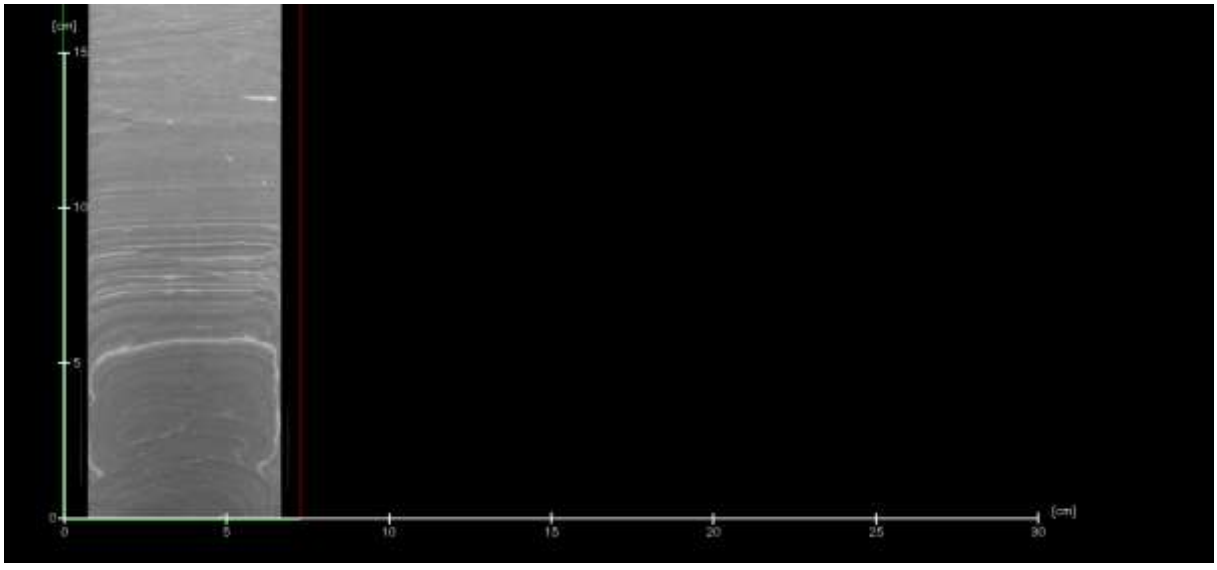

Figure 3-4 KU4 For the depth 400-415 cm

3.2 Sampling profile

The sample is collected by a cone penetrometer device from four meters depth below the seabed in the Kytö site in the Baltic sea. Then, the whole sample is cut into 50 cm height in each separate cylindrical plastic tube for easy storing and transporting. Therefore the sample profile is as follows:

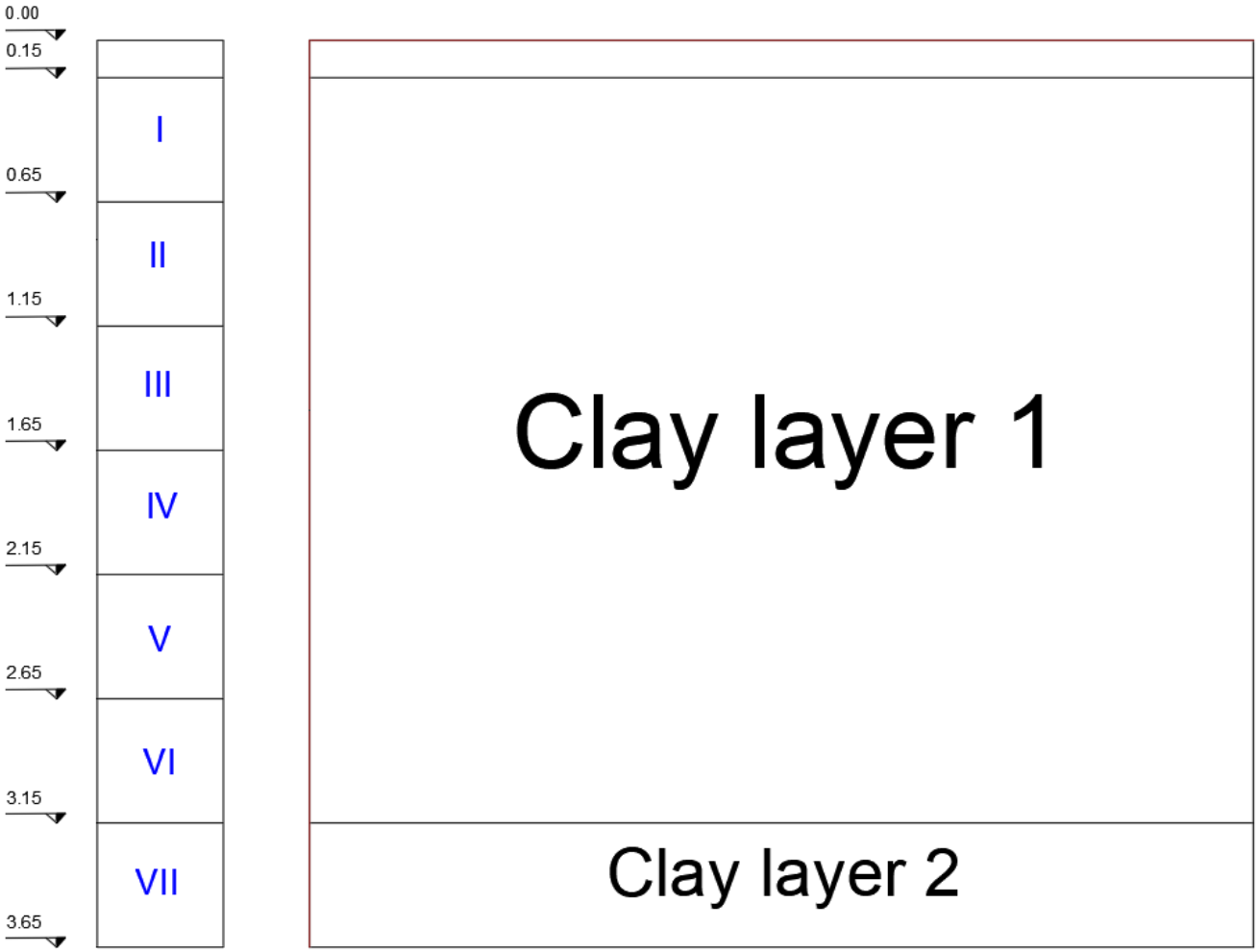

Figure 3-5 Sampling profile

3.3 Profile of physical properties

In this section, some plots of physical properties such as water content, sensitivity, bulk density, grain density and organic content for four different locations of Kytö site: KU1 (LAT 60˚00.625, LONG 24˚44.382), KU2 (LAT 60˚00.773, LONG 24˚45.178), KU3 (LAT 60˚01.489, LONG 24˚44.056) and KU4 (LAT 60˚02.155, LONG 24˚42.368) are demonstrated.

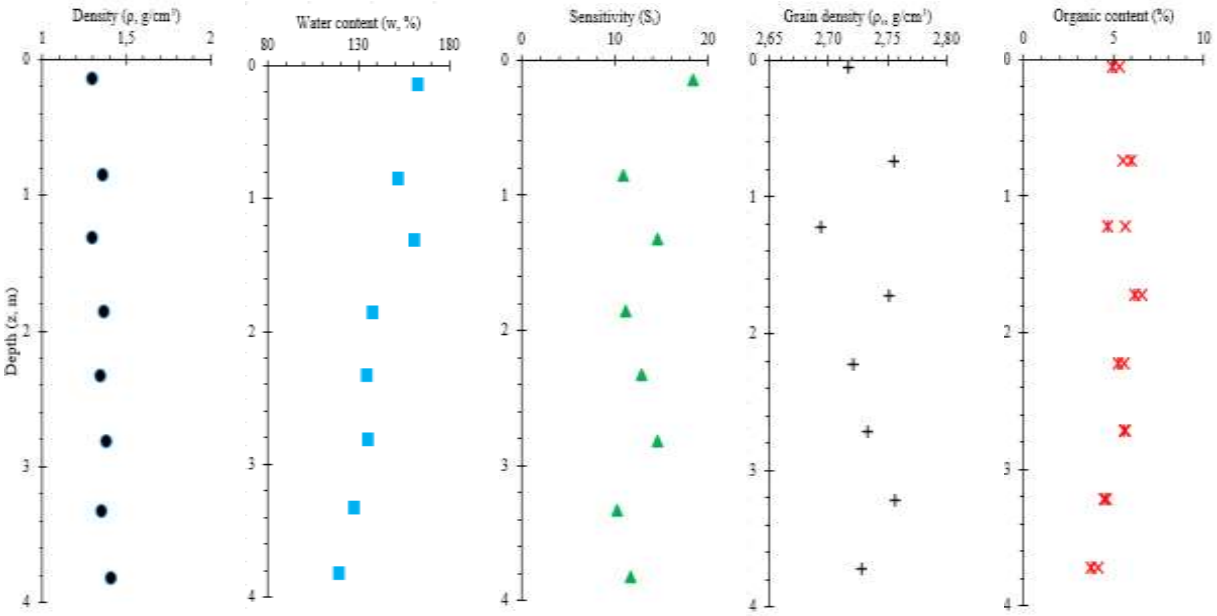

Figure 3-6 Physical property of the KU2 site

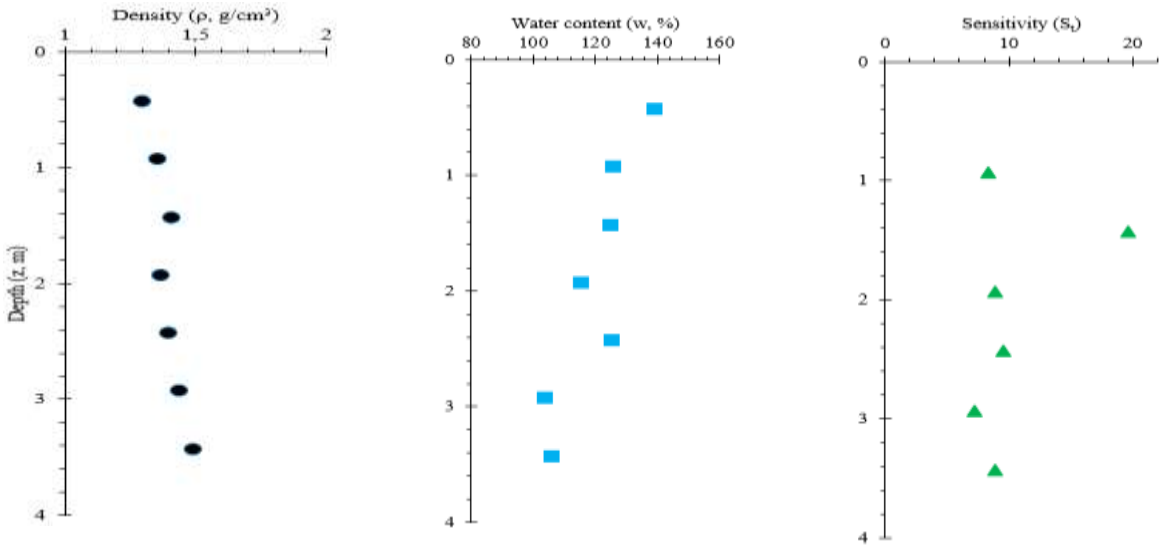

Figure 3-7 Physical property of the KU3 site

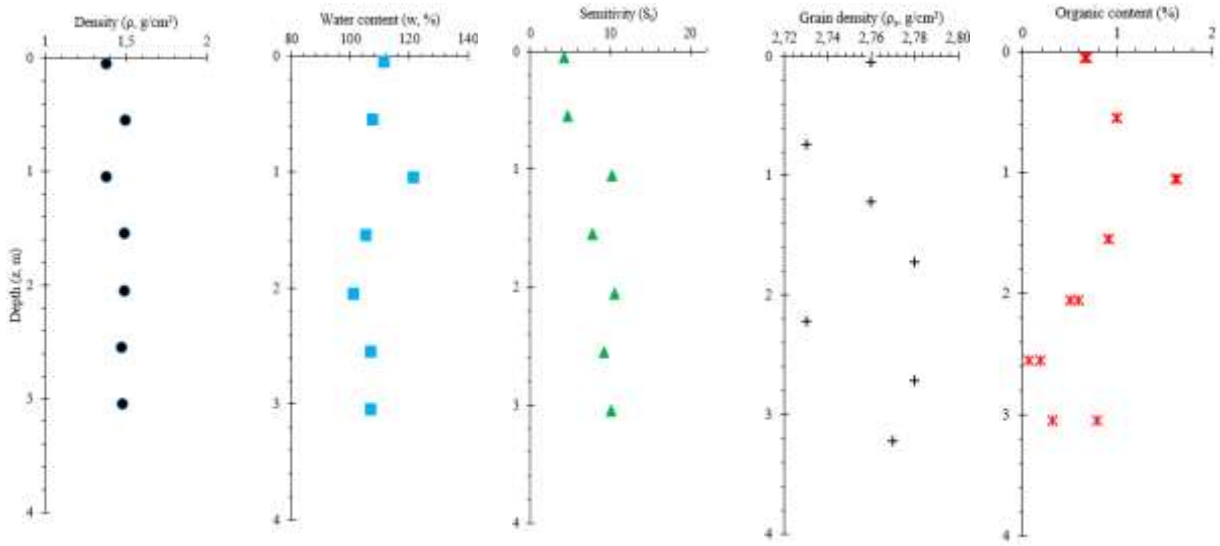

Figure 3-8 Physical property of the KU1 site

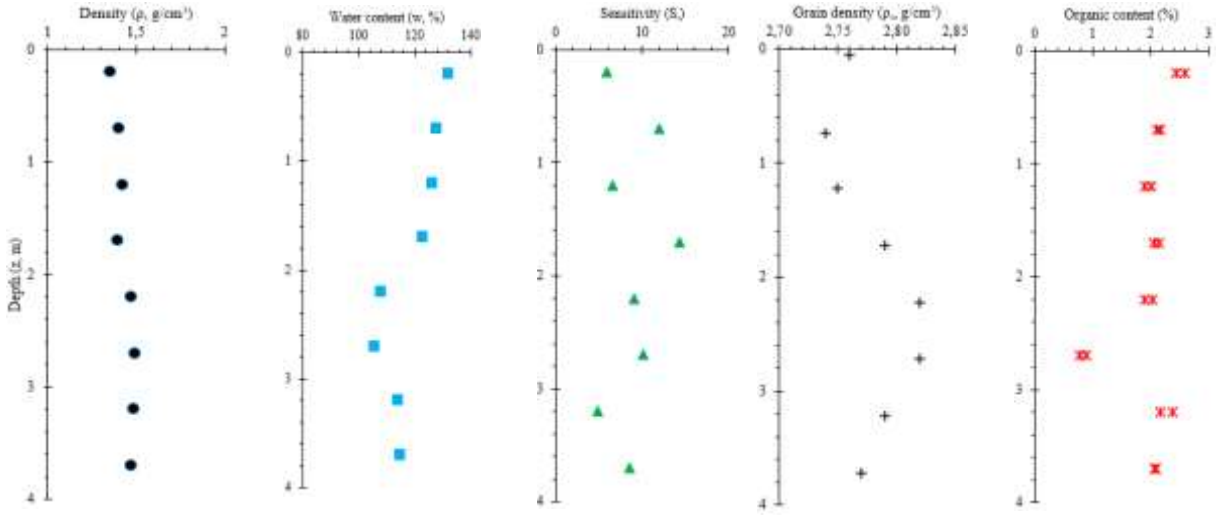

Figure 3-9 Physical property of the KU4 site

3.4 Fall Cone test

The present study involved the execution of 32 fall cone tests at four distinct locations within the Kytö site. Specifically, nine tests were conducted on sample KU2, located at depths ranging between 0.1 and 3.87 meters, eight tests on sample KU3, situated at depths of 0 to 3.48 meters, seven tests on sample KU1, found at depths ranging from 0 to 3.1 meters, and eight tests on sample KU4, positioned at depths between 0.15 and 3.75 meters.

3.4.1 Undrained shear strength

For the estimation of undrained shear strength, the Houlsby's method is used, which is already explained in Section 2.3.1.

The selection of a suitable value for the cone factor (k) in fall cone tests is critical, as it is directly linked to the surface roughness of the cone (α). Depending on the chosen value of k, the obtained results for undrained shear strength may be significantly impacted.

Figure 3.10 illustrates the relationship between penetration and undrained shear strength (S_u) for various cone factors.

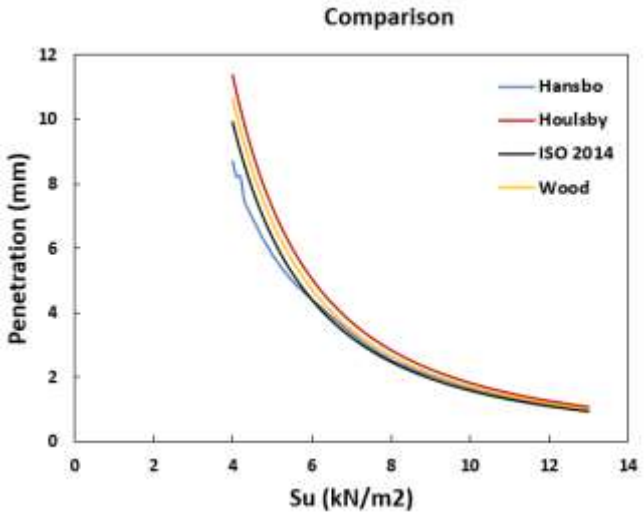

Figure 3-10 Comparison of Undrained shear strength for undisturbed samples by different researchers for different k

Several studies, including those by (Hansbo, 1957; Koumoto T & Houlsby G. T, 2001; SFS-EN ISO 17892-6, 2017; Wood D. M., 1985) have investigated the cone factor (k) for the 60g-60° cone, reporting values of ~0.25, 0.31, 0.27 and 0.29 respectively. Furthermore, for remoulded samples tested using the 10g-60° cone, the cone factor was determined to be 0.3, 0.31, 0.27 and 0.29 by the same researchers, and the results are presented in Figure 3.11:

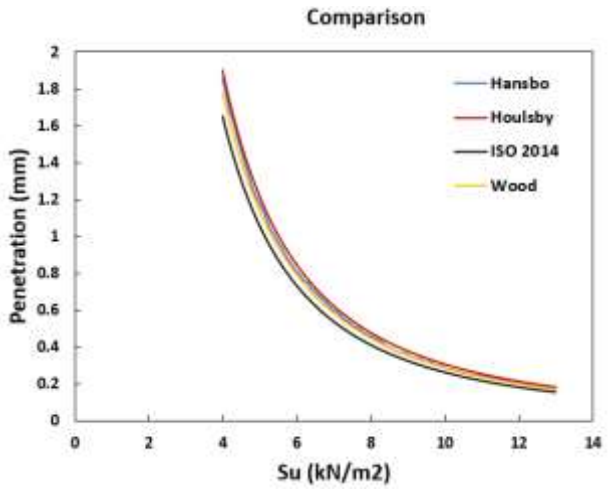

Figure 3-11 Comparison of Undrained shear strength for remoulded samples by different researchers for different k

The findings presented in both figures demonstrate a high degree of similarity between the results obtained by different researchers. However, it is crucial to consider the accuracy of the selected factor, as cone roughness is directly linked to the cone factor. Therefore, it is necessary to assume whether the cone's surface texture is rough, semi-rough, or smooth, as this could potentially influence the cone factor.

The undrained shear strength results obtained from the fall cone tests are presented in Tables A.13 to A.21 of the Appendix.

3.5 Oedometric test

The methodology has been previously elucidated in section 2.3.2 with comprehensive details provided for both the structured and destructuration components.

In this test, some parameters such as water content, porosity, void ratio, bulk density and degree of saturation of a sample can be estimated, both prior to and subsequent to the testing process.

3.5.1 Remoulded sample

For remoulding the sample, the below procedure is conducted:

- The sample is dried in the oven for two days. Then it is crushed into small pieces and after that, a mixer is used to convert these pieces to powder.
- 1.5 of liquid limit is used for obtaining target water content.
- In this step, the sample is put in the vacuum under -1 Bar pressure for almost 30 minutes until all bubbles are disappeared.
- Preparation of the consolidometer in order to consolidate the sample.
- Fill the tube with the soil-water mixture.
- Add loads incrementally and examine the water level every two days.

In the Figure 3.12 the uniaxial test is done for consolidating remoulded sample.

Figure 3-12 Uniaxial test for consolidating remoulded sample

Following a two-month period, the samples were extracted for the purpose of conducting tests. This research involved the implementation of two Oedometric tests on remoulded samples, with the sample dimensions measuring 5 cm in diameter and 1.5 cm in height. The testing depths required for the two tests were within the ranges of 2.65-2.665 meters and 2.77-2.785 meters, respectively. The tests were conducted utilizing a conventional Oedometric device that lacked a pore pressure sensor. The device utilized for the testing process is depicted in Figure 3.13.

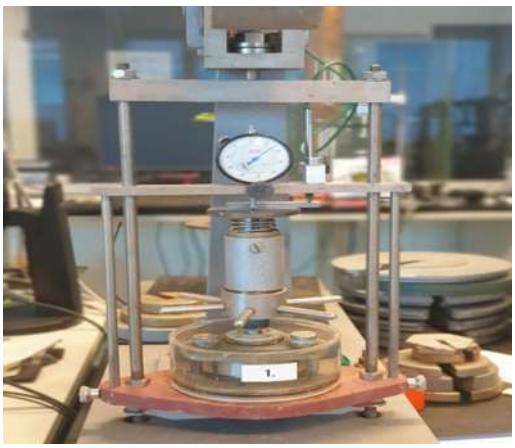

Figure 3-13 Oedometric test without pore pressure sensor

3.5.2 Undisturbed sample

Undisturbed samples were subjected to testing after direct extraction from the tube. These samples measured 5 cm in diameter and 2 cm in height, and a total of 12 tests were performed on them utilizing a conventional Oedometric device equipped with a pore pressure sensor. The tests were conducted at various depths, as depicted by the devices in Figure 3.14.

Figure 3-14 Oedometric test with pore pressure sensor

In the Table A.22 to Table A.35, the results of these tests are shown.

3.5.3 Oedometric result curve

In the Figure 3.15 To Figure 3.28 , the results of the oedometric tests are shown:

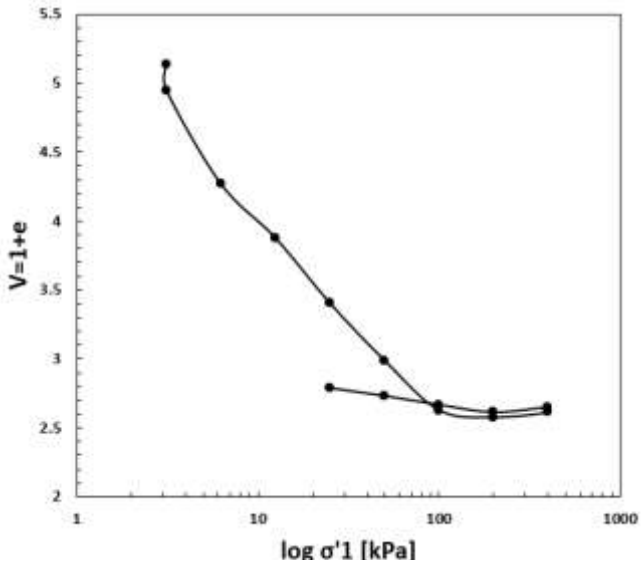

Figure 3-15 The Oedometric result for the depth 0.26 m and the site Kytö (KU 4)

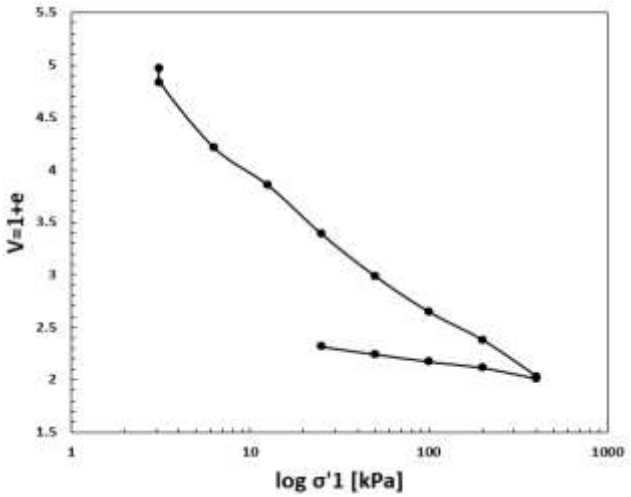

Figure 3-16 The Oedometric result for the depth 0.29 m and the site Kytö (KU 4)

Based on the figures presented above, it appears that pre-consolidation pressure is not available due to an observed elasticity phenomenon, which may be attributed to irreversibility, anolonomy (stiffness depends on loading direction), or failure. This may be due to stress relaxation occurring at the given depth, which is located in close proximity to the surface. Additionally, the high water content at this depth may also be a contributing factor, as it is located in close proximity to the water table.

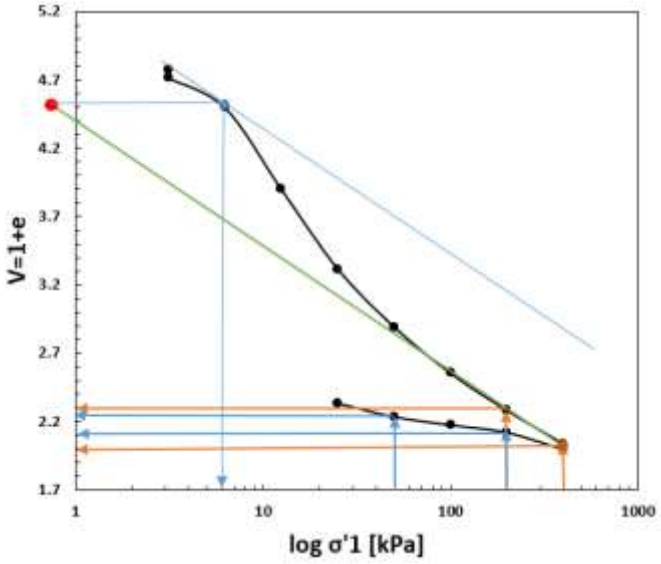

Figure 3-17 The Oedometric result for the depth 1.11 m and the site Kytö (KU 1)

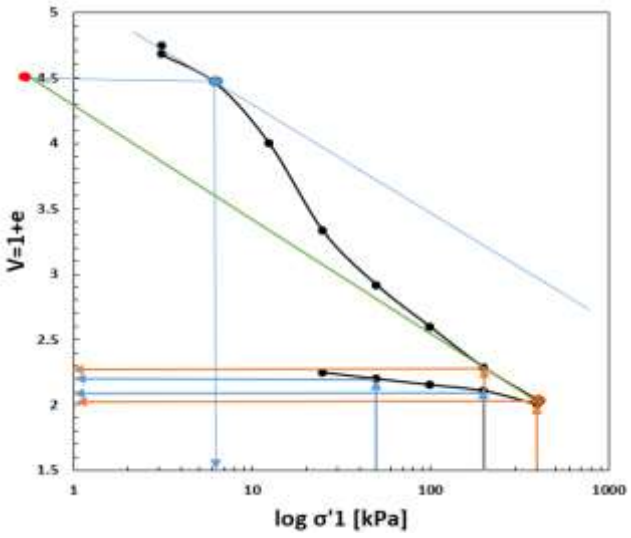

Figure 3-18 The Oedometric result for the depth 1.14 m and the site Kytö (KU 1)

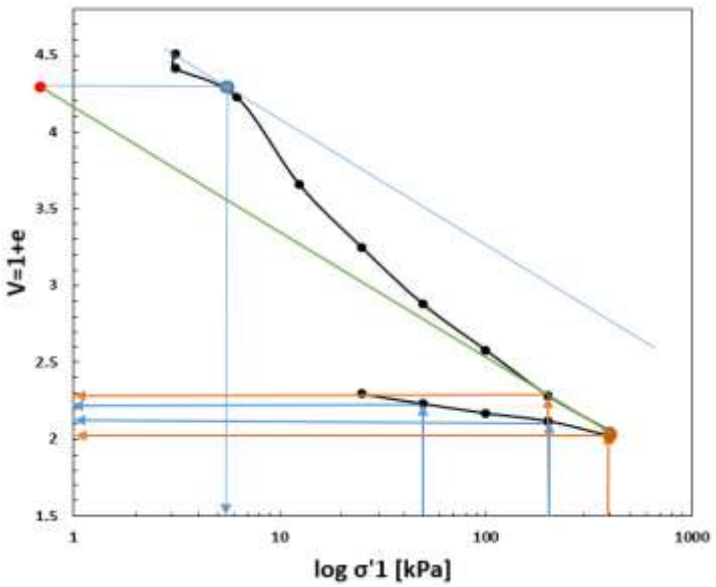

Figure 3-19 The Oedometric result for the depth 1.41 m and the site Kyto (KU 4)

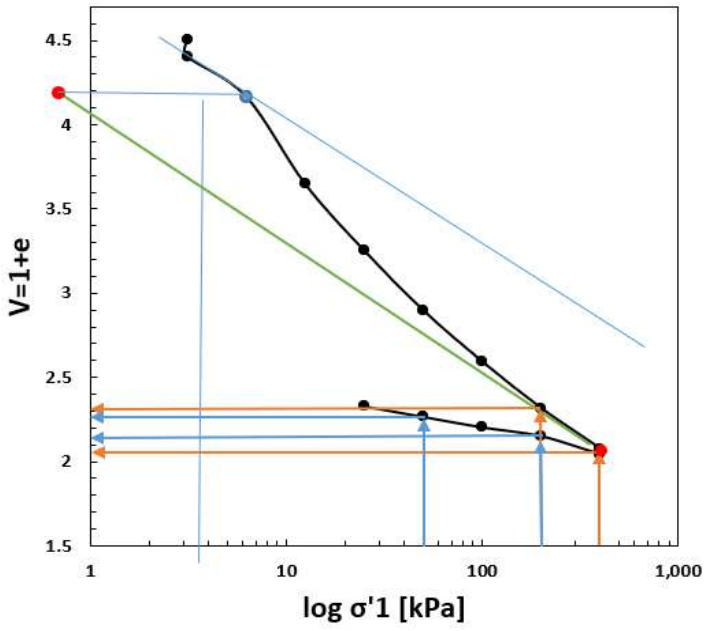

Figure 3-20 The Oedometric result for the depth 1.44 m and the site Kyto (KU 4)

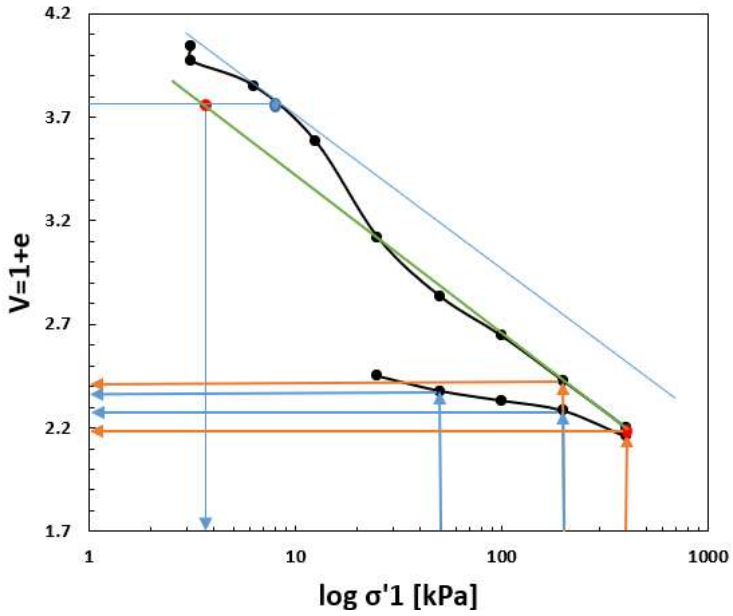

Figure 3-21 The Oedometric result for the depth 2.26 m and the site Kyto (KU 4)

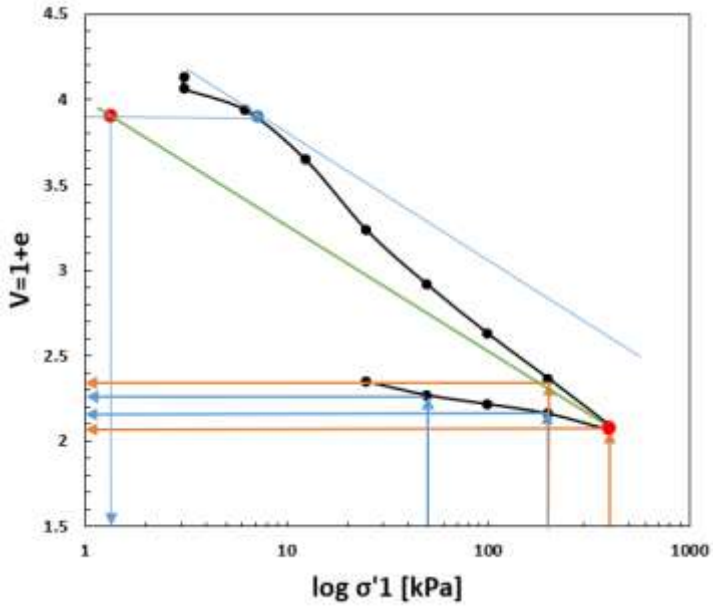

Figure 3-22 The Oedometric result for the depth 2.31 m and the site Kyto (KU 4)

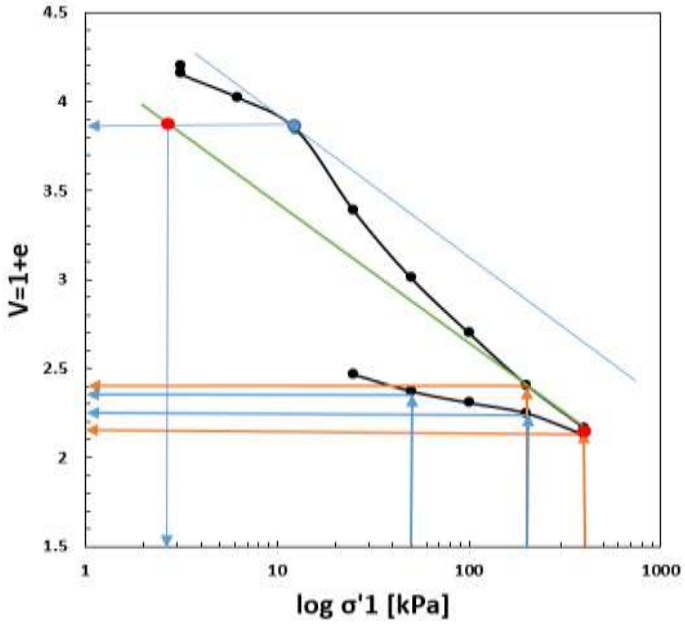

Figure 3-23 The Oedometric result for the depth 2.76 m and the site Kyto (KU 4)

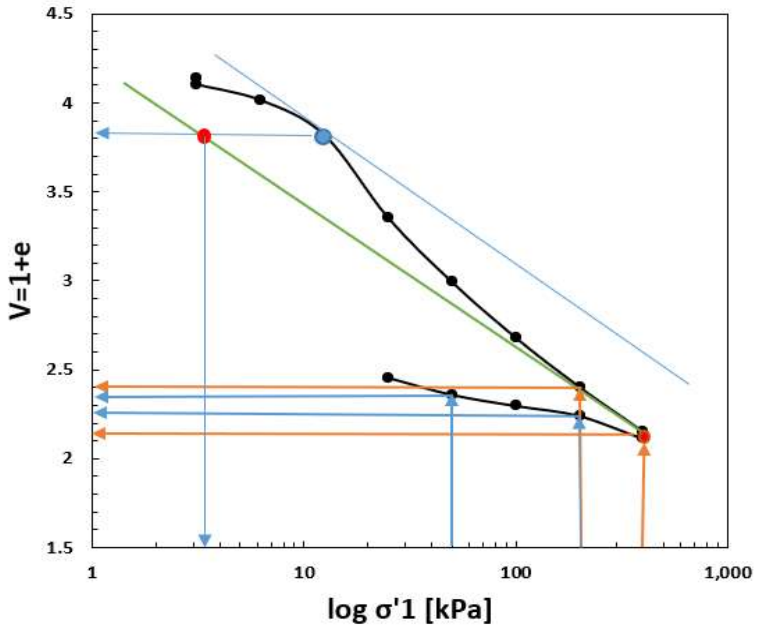

Figure 3-24 The Oedometric result for the depth 2.79 m and the site Kyto (KU 4)

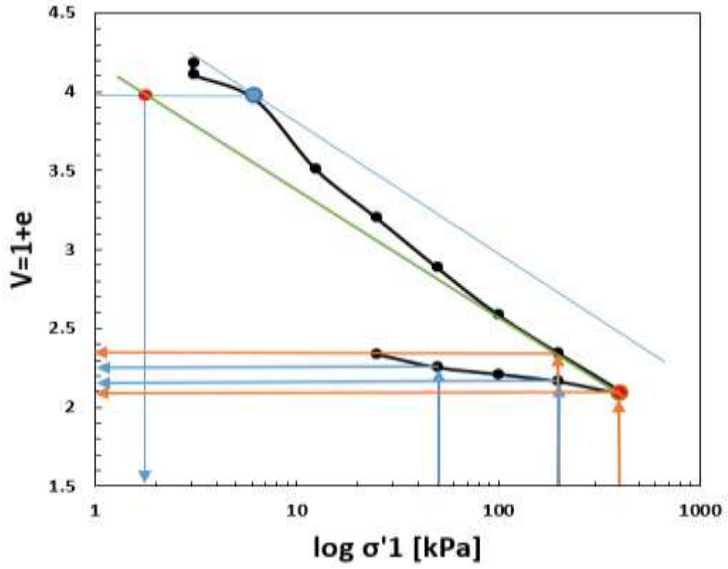

Figure 3-25 The Oedometric result for the depth 3.26 m and the site Kyto (KU 4)

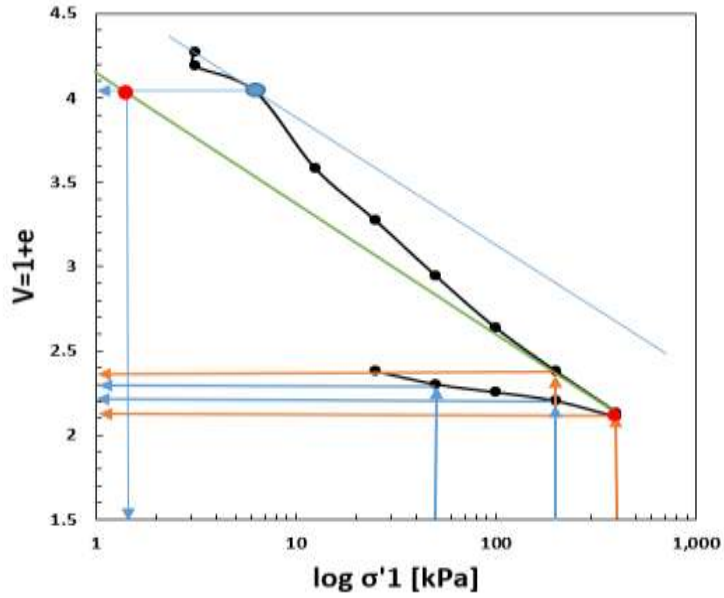

Figure 3-26 The Oedometric result for the depth 3.29 m and the site Kyto (KU 4)

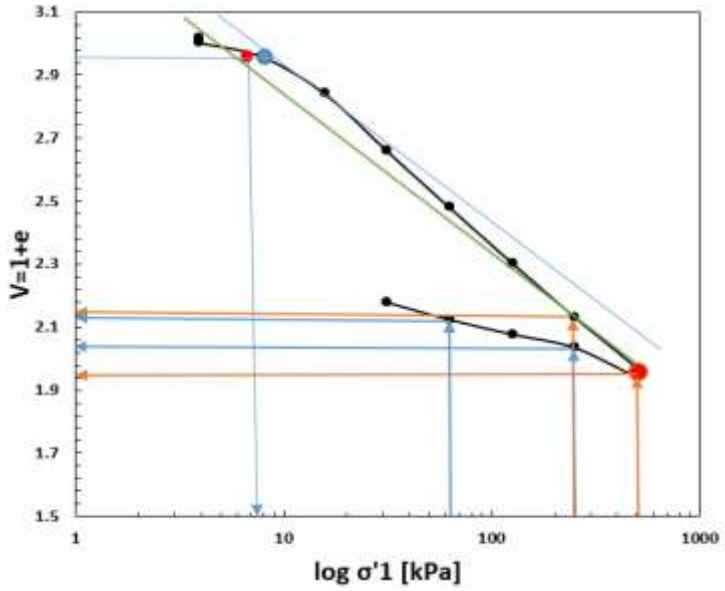

Figure 3-27 The Oedometric result for the depth 2.66 m and the site Kyto (KU 4) (Remoulded sample)

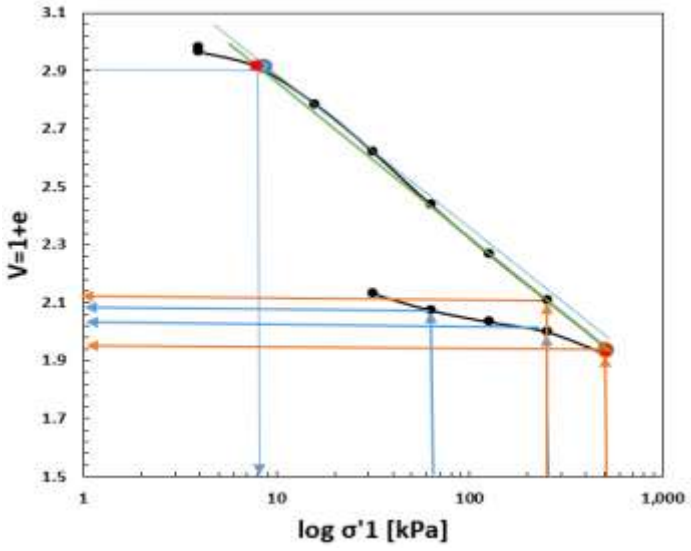

Figure 3-28 The Oedometric result for the depth 2.78 m and the site Kyto (KU 4) (Remoulded sample)

The observed trends in the aforementioned figures indicate that the confining stress generally increases with depth, except for the cases presented in Figures 3.25 and 3.26 where a decreasing trend is evident with increasing depth, likely due to variations in soil layers. Consequently, an accurate determination of the pre-consolidation pressure point is crucial to minimize errors in estimating undrained shear strength.

Figure 3-29 depicts the values of in-situ vertical stress at a specified depth, as determined through both calculation (indicated by green circles) and the oedometer test (indicated by blue stars).

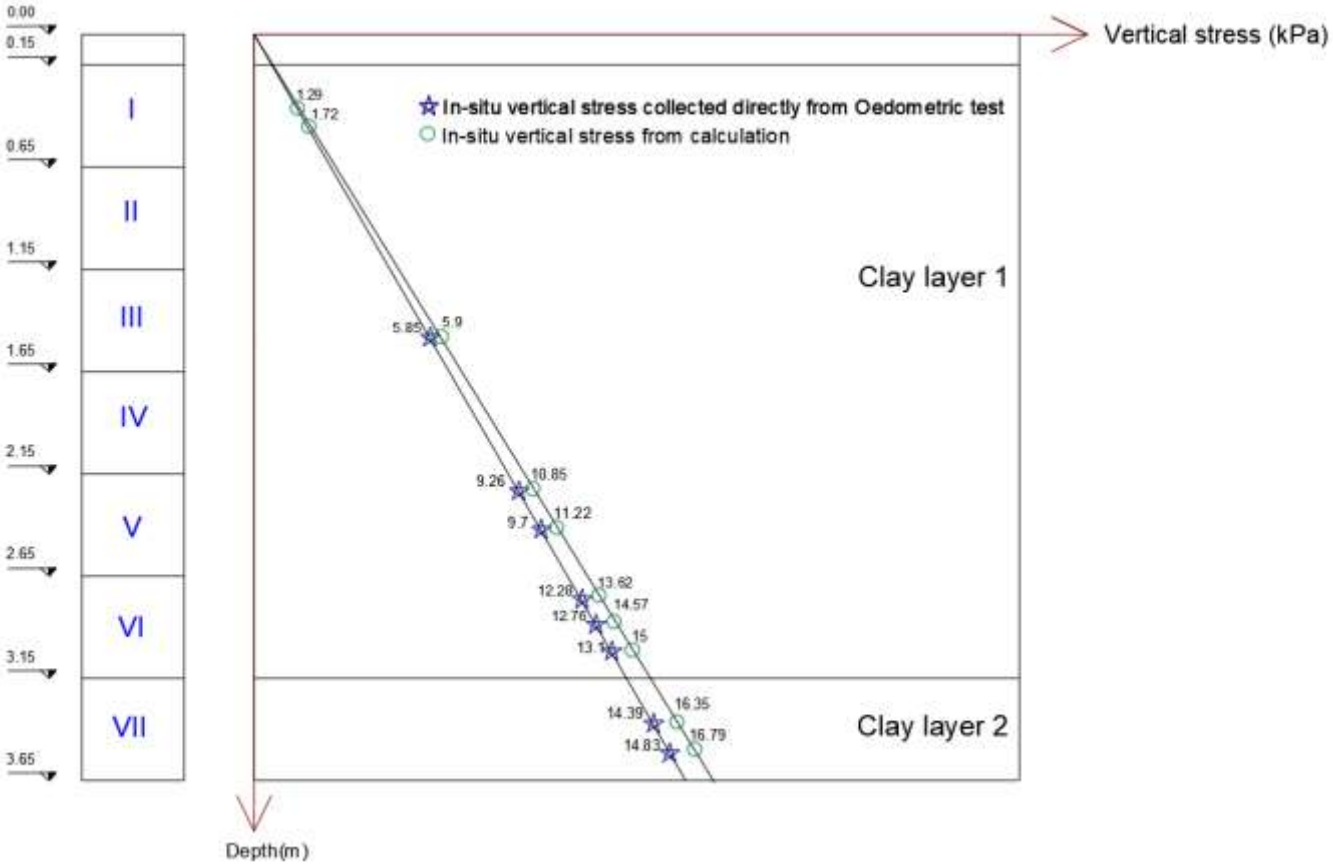

Figure 3-29 Representation of the in-situ vertical stress by Oedometric test and by calculations

3.6 Triaxial test

This study involved conducting a total of 16 triaxial tests, of which 13 were performed on undisturbed samples, while the remaining 3 tests were carried out on remoulded samples.

3.6.1 Remoulded sample for ($\eta = 0$)

Three isotropic triaxial tests were conducted on remoulded samples with stress ratio ($\eta = 0$), using three different confining pressures of 30, 60, and 90 kPa. The outcomes of these tests are presented in Table A.36 to Table A.38.

3.6.2 Undisturbed sample for ($\eta = 0$)

Nine isotropic triaxial tests were done for undisturbed samples. The critical state line is constant in these cases. The results of these tests are illustrated in Table A.39 to Table A.47.

3.6.3 Undisturbed sample for ($\eta < k_0$)

The determination of the yield point in an anisotropic soil specimen can be challenging due to the variations in anisotropy that occur under different stress paths. The selection of stress ratios η was based on initial assessments of k_0, to approximate one-dimensional consolidation which in this research, we only consider ($\eta < k_0$). In addition, The anisotropic consolidation test involves the application of both confining pressure (σ_3) and axial stress (σ_1), necessitating the application of additional weight. The calculation of the required weight for this test is determined as follows:

(As an assumption, η is considered equal to 0.2)

$$\eta = \frac{q}{P'} = \frac{\sigma_1 - \sigma_3}{\frac{\sigma_1 + 2\sigma_3}{3}} \rightarrow \frac{3\sigma_1 - 3\sigma_3}{\sigma_1 + 2\sigma_3} = 0.2 \rightarrow \frac{\sigma_3}{\sigma_1} = 0.82 \tag{37}$$

The following equation can be utilized to determine the required weight for the aforementioned anisotropic consolidation test:

$$\sigma_1 = \sigma_3 + \left[\frac{\left(F + m_p\right) - \left[\left(\frac{\sigma_3}{98.07}\right) * A_p\right]}{A}\right] * 98.07 \tag{38}$$

The equation mentioned above involves the variables A_p and m_p, where A_p represents the area of the piston and is equal to 1 cm^2. The values of m_p for cell 242 and cell 244 are 0.786 g and 0.767 g, respectively.

In each incremental load during the anisotropic consolidation test, it is crucial to calculate the necessary weight. This entails subtracting the previous weight from the newly calculated weight, and adding the resultant value to the testing apparatus. Additionally, it is imperative to keep a detailed record of the displacement and burette readings at each load increment, as changes in area and volume occur. This information is necessary to obtain the updated height and volume measurements for subsequent loading stages.

It is important to carefully select the values of axial stress (σ_1) and confining pressure (σ_3) at each step of the anisotropic consolidation test, such that the ratio of σ_1 to σ_3 is maintained at 0.82.

The results of CAUC tests are shown in Table A.48 to Table A.51.

3.6.4 Specimen and test information

Instant samples were taken from the Kytö site in the bed of the Baltic sea in the Espoo in January 2022 and transported to Aalto University. Their diameter is 5 cm and their height is 10 cm. The specimens tested by triaxial tests were those from site KU1 and site KU4. Table 3.40 summarizes the index properties of the specimens and test information. The test procedure followed the European Committee for Standardization standard, i.e. (SFS-EN ISO 17892-9, 2017).

Sampling site	Sampling date	D (mm)	Z (m)	ρ ($\frac{g}{cm^3}$)	w (%)	Lab test No.	Lab test date	σ'_3 (kPa)	Apparatus
KU1	January	50	1.15-1.25	1.419	124.11	CIUC6950	2022-10-20	30	Wykeham Farrance 242 & 244
			1.25-1.34	1.414	131.68	CIUC6951	2022-10-20	60	
			1.35-1.43	1.458	132.61	CIUC6952	2022-10-26	90	
KU4	January		2.8-2.9	1.497	106.41	CIUC6953	2022-10-26	30	
			2.9-3	1.496	99.71	CIUC6958	2022-11-03	60	
			3-3.1	1.489	123.81	CIUC6959	2022-11-03	90	
			2.33-2.43	1.461	110.90	CAUC6960	2022-11-14	30	
			2.43-2.53	1.450	110.96	CAUC6961	2022-11-14	60	
			3.3-3.4	1.458	119.31	CAUC6962	2022-11-21	30	
			3.4-3.5	1.450	115.93	CAUC6963	2022-11-21	60	
			0.3-0.4	1.396	140.99	CIUC6968	2022-11-25	30	
			0.4-0.5	1.397	133.63	CIUC6969	2022-11-25	60	
			1.45-1.55	1.378	127.10	CIUC6970	2022-11-29	30	
			2.5-2.6	1.581	68.74	**CIUC6971**	2022-11-29	30	
			2.67-2.77	1.624	67.77	**CIUC6974**	2022-12-08	60	
			2.79-2.89	1.603	66.94	**CIUC6975**	2022-12-08	90	

*The bold font presents Triaxial tests for remoulded samples.

Table 3.1 Specimen index properties and test information

3.6.5 Test results

As an illustrative instance, the outcomes of the anisotropic consolidation test on the (CIUC653-6958-6959) sample series are depicted in Figure 3.30 to Figure 3.32. These figures demonstrate the behavior of the deviatoric stress and pore pressure relative to axial strain ε_1, as well as the results depicted on the stress path (p',q) diagram, along with photographic evidence before and after the test.

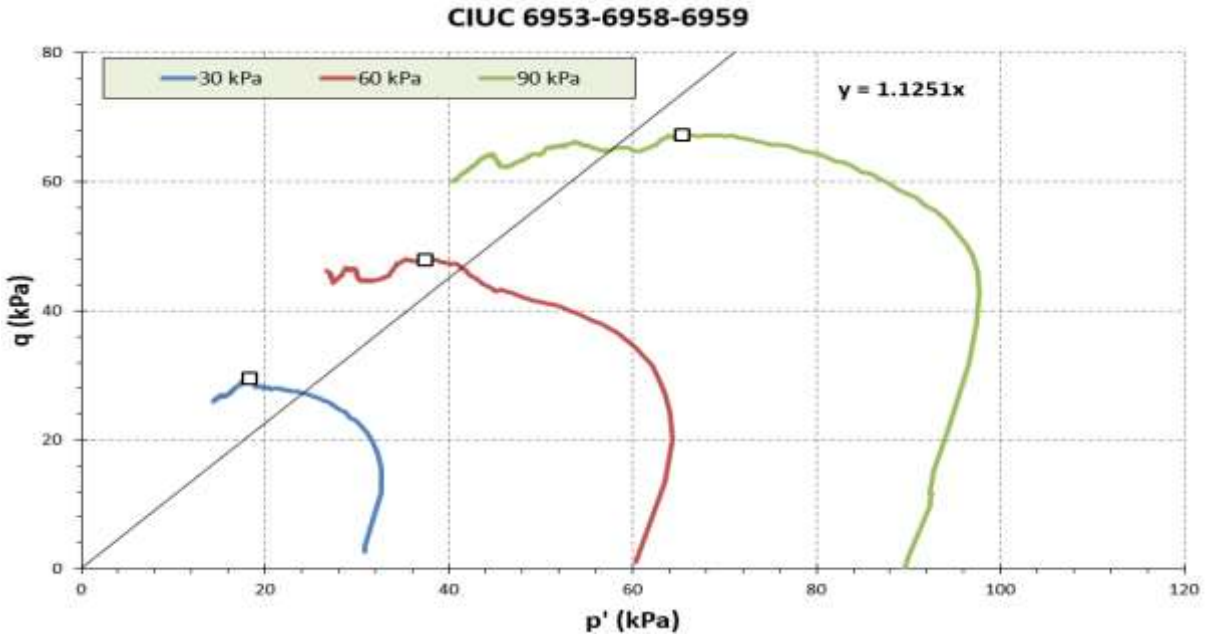

Figure 3-30 Stress path (p',q) diagram for CIUC 6953-6958-6959

It is possible to consider different values for the critical state stress ratios, Mc and Me, in triaxial compression and extension, respectively, or to incorporate any dependence on Lode angle, as previously discussed by (Wheeler et al., 2003) and (Sivasithamparam, 2012). However, the existence of Lode angle dependency remains a topic of debate, as evidenced by conflicting findings in the literature. (Atkinson et al., 1987) presented experimental data that supported Mc=Me, whereas (Kirkgard & Lade', 1993) observed significant Lode angle dependency. Notably, the most recent

implementation of the model by Sivasithamparam (2012) includes the consideration of Lode angle dependency.

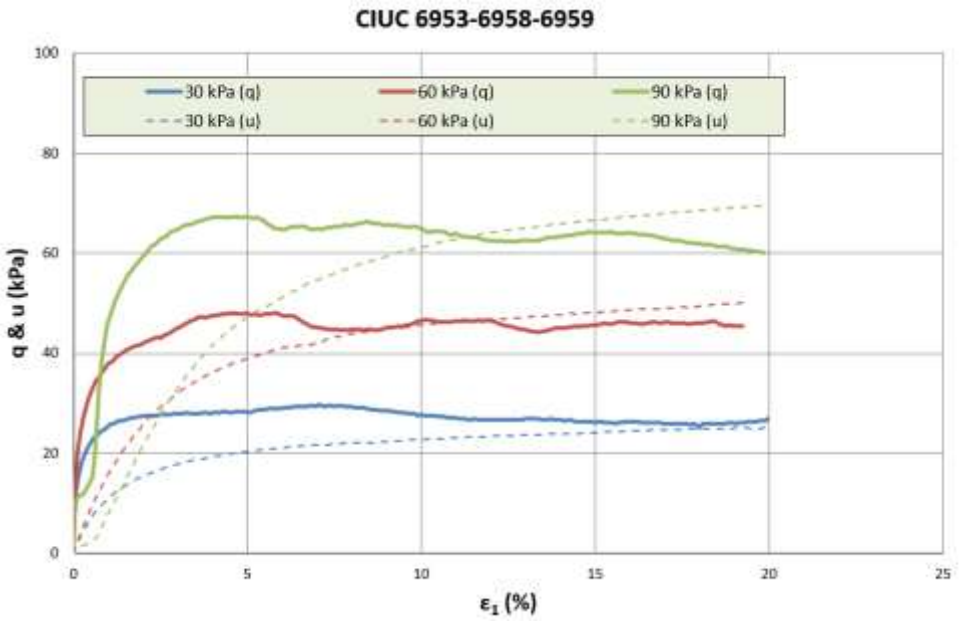

Figure 3-31 Behavior of deviatoric stress and pore pressure wrt axial strain

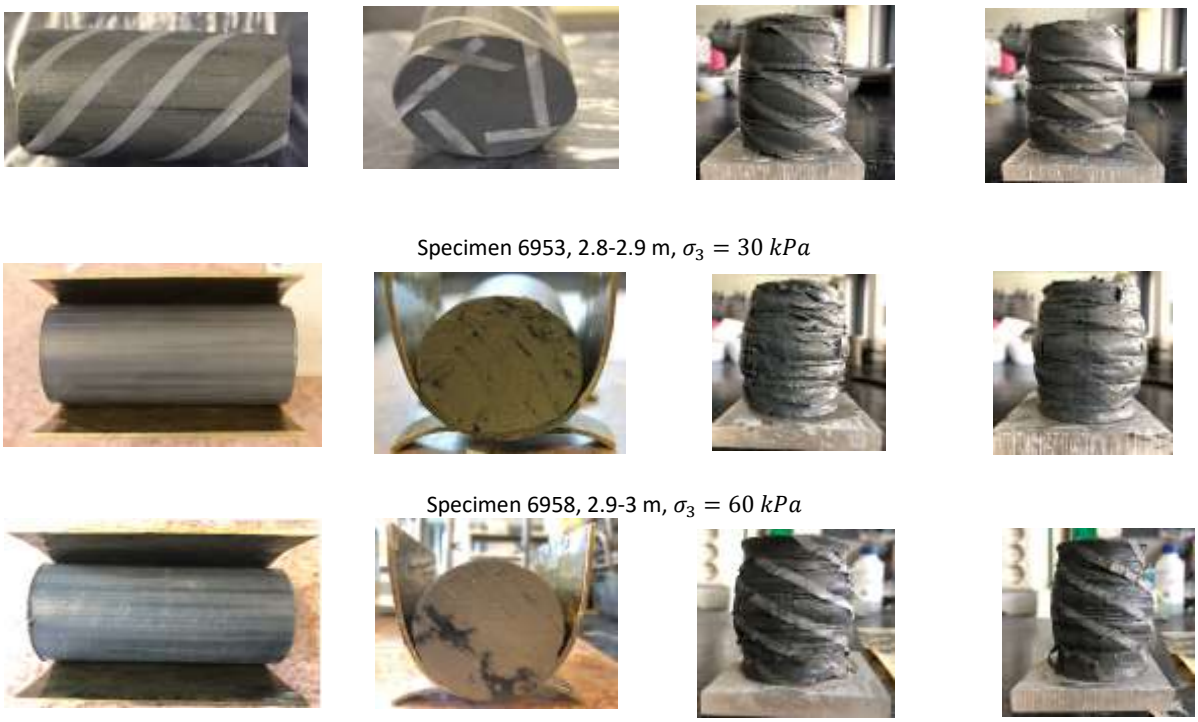

Specimen 6953, 2.8-2.9 m, $\sigma_3 = 30\ kPa$

Specimen 6958, 2.9-3 m, $\sigma_3 = 60\ kPa$

Specimen 6959, 3-3.1 m, $\sigma_3 = 90\ kPa$

Figure 3-32 Specimen before and after Triaxial test

Some key parameters of the results are summarized in Table 3.2. According to this table, the range of M (the slope of the critical state line) is between 0.72-1.55, which in this research was considered 1.1 for all calculations. The k_0 value's range is between 0.38-0.68, which in this research was assumed to be constant and equal to 0.6. About the friction angle, this value is a bit different in two sites; moreover, in the depth near the surface, this value is larger.

Sampling site	Lab test No.	Z (m)	ρ ($\frac{g}{cm^3}$)	w (%)	M	C (kPa)	φ (°)	k_0
KU1	6950	1.15-1.25	1.419	124.11	0.72	0	18.78	0.68
	6951	1.25-1.34	1.414	131.68				
	6952	1.35-1.43	1.458	132.61				
KU4	6953	2.8-2.9	1.497	106.41	1.12	0	28.27	0.53
	6958	2.9-3	1.496	99.71				
	6959	3-3.1	1.489	123.81				
	6960	2.33-2.43	1.461	110.90	1.02	0	25.87	0.56
	6961	2.43-2.53	1.450	110.96				
	6962	3.3-3.4	1.458	119.31	1.04	0	26.22	0.56
	6963	3.4-3.5	1.450	115.93				
	6968	0.3-0.4	1.396	140.99	1.55	0	38.1	0.38
	6969	0.4-0.5	1.397	133.63				
	6970	1.45-1.55	1.378	127.10	1.24	0	30.87	0.49
	6971	2.5-2.6	1.581	68.74	1.35	0	33.44	0.45
	6974	2.67-2.77	1.624	67.77				
	6975	2.79-2.89	1.603	66.94				

Table 3.2 Summary of the Triaxial test results

4. Analysis of the results

4.1 Statistics on penetration depth in Fall Cone test

In the fall cone test, five tests are conducted on each sample to measure the penetration depth. However, the variability in penetration depth across the five tests can be attributed to factors such as heterogeneity, the presence of coarse particles, heave effects, and water in certain areas. As a result, determining the mean value of penetration depth alone may not be a reliable criterion. Statistical analysis is therefore performed on the penetration depth measurements.

To ensure consistency, all penetration depth measurements are first normalized relative to the initial penetration depth, which corresponds to the center of the sample. This normalization process is applied to all five tests and four different locations (KU1, KU2, KU3, and KU4). The results of the statistical analysis are presented in Figure 4.1.

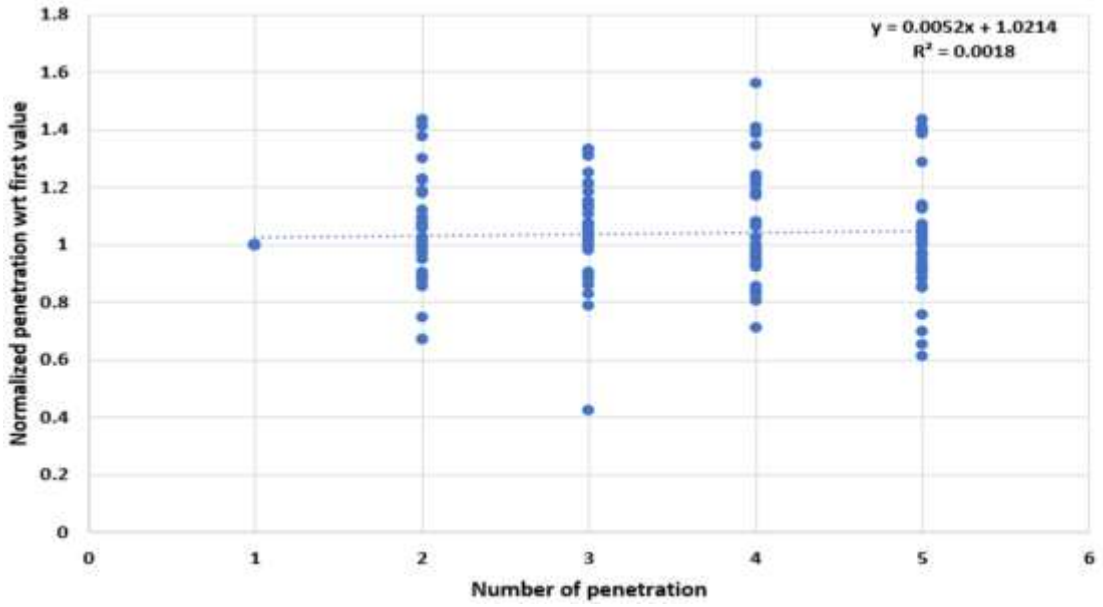

Figure 4-1 Statistics results on penetration depth

The subsequent step involves the estimation of the error associated with the mean value of penetration depth. This involves computing the mean value and standard deviation for each group of penetration measurements. The standard deviation is calculated using the following equation:

$$SD = \sqrt{\frac{\sum_{i=1}^{n}(x_i - \bar{x})^2}{n-1}} \tag{39}$$

where x_i represents the value of the ith data point in the data set, $\bar{x}$ is the mean value of the data set, and n is the total number of data points in the data set.

The result of the error estimation process is illustrated in Figure 4.2:

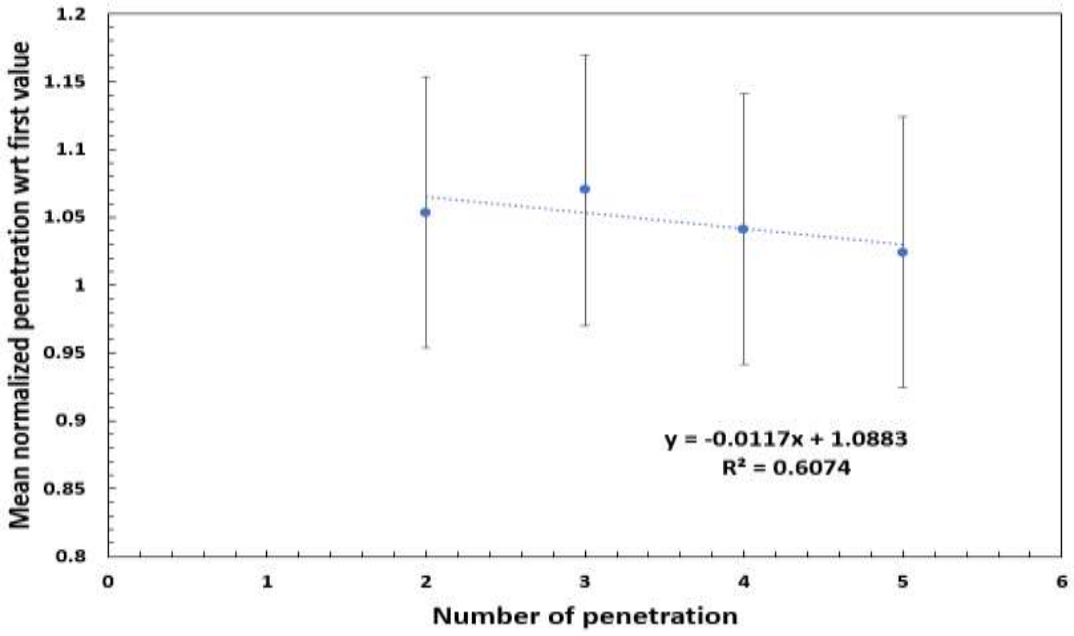

Figure 4-2 Error estimation of penetration depth

The error estimation process resulted in a 40% error for the mean value, which is considered substantial.

In Table 4.1, the mean and standard deviation of four penetrations are illustrated:

Penetration	2	3	4	5
SD	0.19	0.15	0.17	0.21
Mean	1.05	1.07	1.04	1.02

Table 4.1 Necessary data of four penetration

The probability mass function and cumulative density function for the four penetration measurements are presented below:

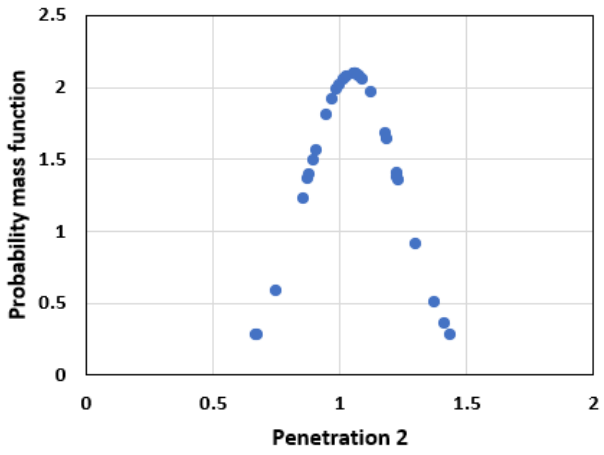

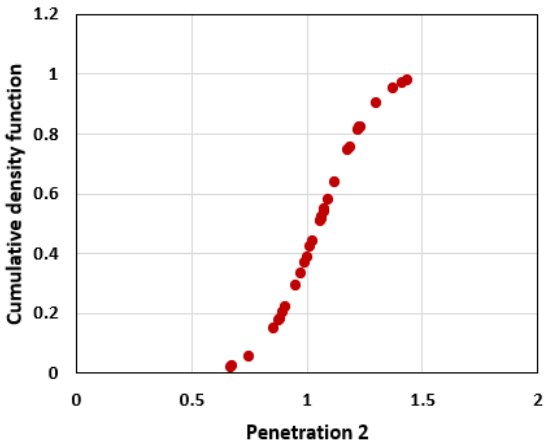

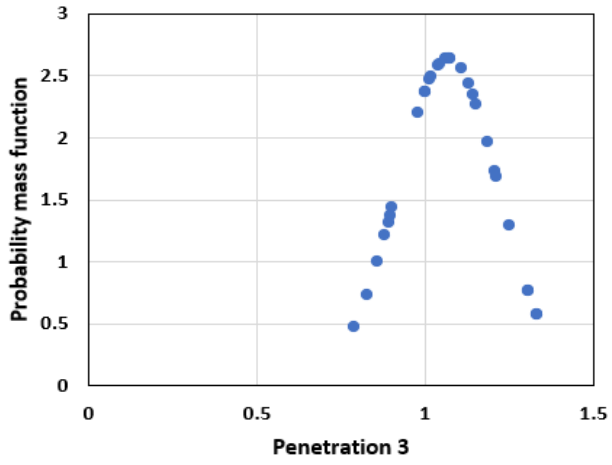

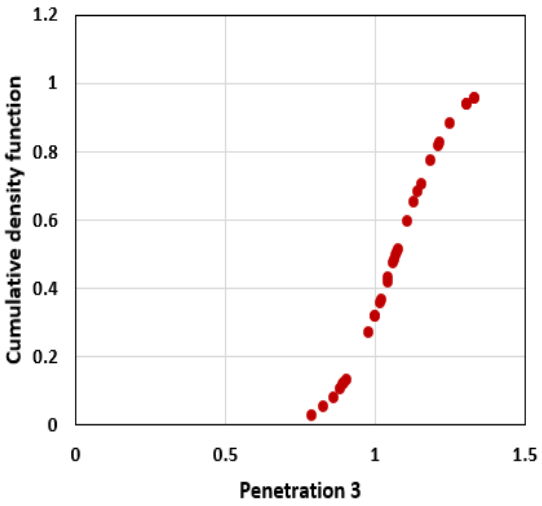

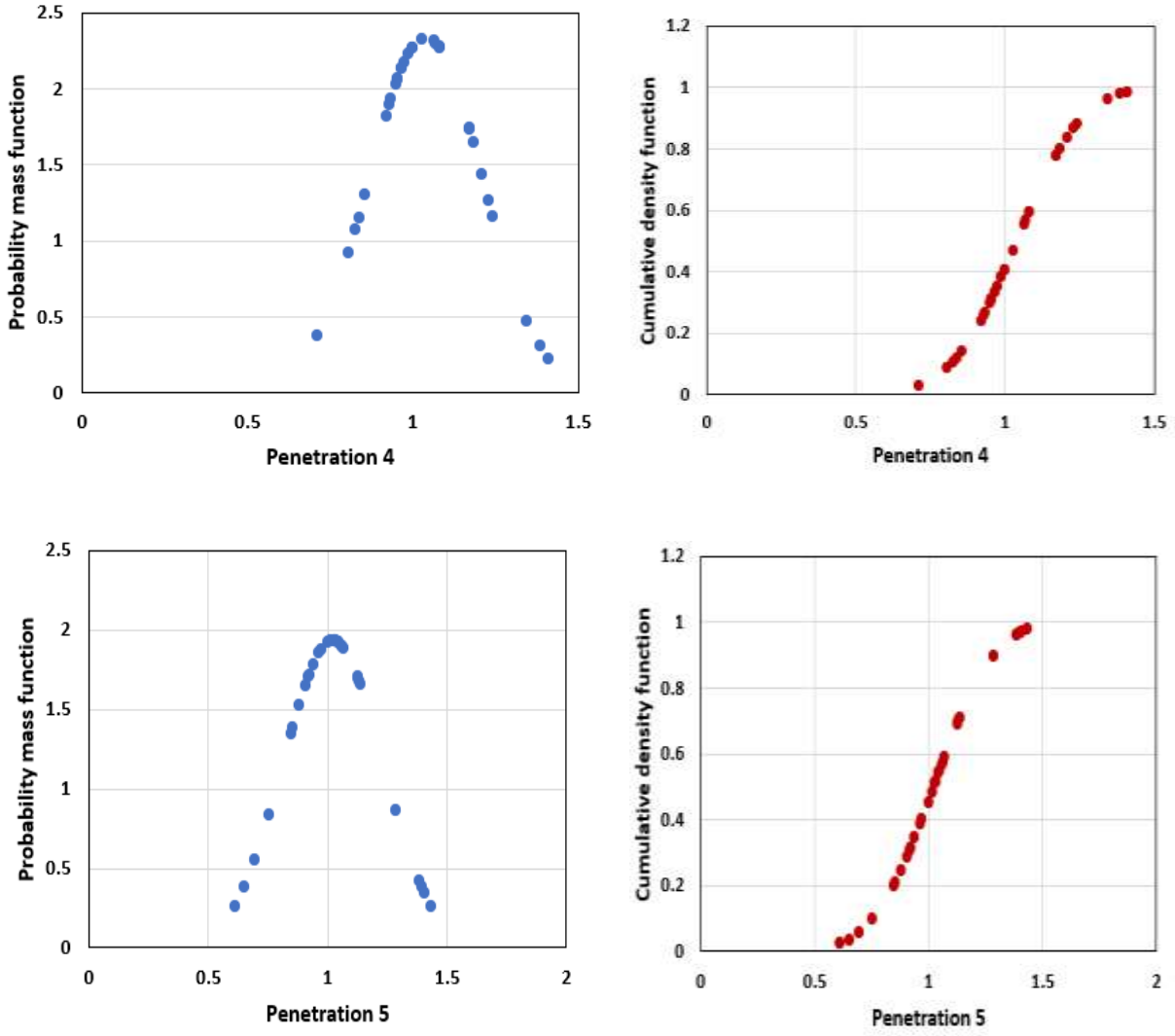

Figure 4-3 Probability mass function and Cumulative density function for four penetration

The probability mass function provides insights into the distribution of values around the mean value. Based on the probability mass function curves presented, it is evident that a significant portion of the data points is concentrated around the mean value.

The final step involves estimating the uncertainty associated with each penetration measurement. The uncertainty is calculated using the following equation:

$$U_m = \frac{ts}{\sqrt{N}} \tag{40}$$

where t represents the student's t-distribution, s is the standard deviation and N is the number of measurements. The results are presented in Table 4.2 to Table 4.5.

Penetration 2	
Mean	1.053603084
N (measurements)	32
N-1 (DOF)	31
S (standard deviation)	0.190431649
SE (standard error)	0.033663878
$t_{0.95}$	1.6957
CI=SE*$t_{0.95}$	0.057083837
Upper CI	1.110686921
Lower CI	0.996519247
U_m (uncertainty)	0.057083837

Table 4.2 Calculation of uncertainty for penetration 2

Penetration 3	
Mean	1.070061754
N (measurements)	31
N-1 (DOF)	30
S (standard deviation)	0.151189062
SE (standard error)	0.027154357
$t_{0.95}$	1.697
CI=SE*$t_{0.95}$	0.046080944
Upper CI	1.116142698
Lower CI	1.02398081
U_m (uncertainty)	0.046080944

Table 4.3 Calculation of uncertainty for penetration 3

Penetration 4	
Mean	1.041380538
N (measurements)	31
N-1 (DOF)	30
S (standard deviation)	0.17076137
SE (standard error)	0.030669647
$t_{0.95}$	1.697
CI=SE*$t_{0.95}$	0.052046392
Upper CI	1.093426929
Lower CI	0.989334146
U_m (uncertainty)	0.052046392

Table 4.4 Calculation of uncertainty for penetration 4

Penetration 5	
Mean	1.024051392
N (measurements)	32
N-1 (DOF)	31
S (standard deviation)	0.206405622
SE (standard error)	0.036487704
$t_{0.95}$	1.6957
CI=SE*$t_{0.95}$	0.061872199
Upper CI	1.085923591
Lower CI	0.962179192
U_m (uncertainty)	0.061872199

Table 4.5 Calculation of uncertainty for penetration 5

The uncertainty associated with each penetration measurement is as follows: 0.06, 0.05, 0.05, and 0.06, respectively. To obtain more accurate results, it is advisable to consider all the penetration measurements together. This is because more data points are available, resulting in more reliable and precise outcomes. The results for all the data points considered together are presented in Table 4.6.

All penetration together	
Mean	1.047140113
N (measurements)	126
N-1 (DOF)	125
S (standard deviation)	0.179802802
SE (standard error)	0.016018107
$t_{0.95}$	1.659595556
CI=SE*$t_{0.95}$	0.026583579
Upper CI	1.073723692
Lower CI	1.020556535
U_m (uncertainty)	0.026583579

Table 4.6 Calculation of uncertainty for all penetration together

In conclusion, statistical analysis was carried out using a t-student test to determine the most favorable penetration depth. Various parameters, including the standard error, confidence interval, and uncertainty, were computed. The uncertainty values associated with each penetration measurement were determined to be approximately 0.06, 0.05, 0.05, and 0.06, respectively. To obtain more accurate results, all the data points were considered together, resulting in an uncertainty value of 0.03, which is smaller than the individual values calculated for each penetration. Therefore, this value is considered more favorable. These findings highlight the importance of having more data points to improve estimation accuracy.

4.2 Errors in the determination of undrained shear strength

4.2.1 Fall Cone test

The fall cone test is used to determine the undrained shear strength of soil by measuring the depth of penetration of a cone that falls with its tip toward the soil specimen. It should be noted that the test does not represent either the vertical triaxial compression test or a horizontal shear test, as it produces a complex shear in the test specimen. While the Fall cone test may be correlated with other laboratory tests that estimate undrained shear strength, it cannot be considered a direct indicator of this property. Additionally, the test is conducted on a small laboratory specimen, which may not yield results that are comparable to those of laboratory tests on larger specimens. Furthermore, the test specimen may not be representative of the natural state of the soil, as the presence of fissures may be spaced differently in situ than in the test specimen. Considering these factors, the fall cone test can be viewed as an estimation rather than a precise measurement of undrained shear strength.

The surface roughness of a cone is a crucial factor that affects the undrained shear strength of the soil. While some studies have shown that the roughness of the cone has a minimal impact on the value of undrained shear strength obtained from the fall cone test, such as the work of (Llano-Serna & Contreras, 2020), generally, it cannot be completely disregarded and should be taken into account in the analysis.

The fall cone test may be susceptible to changes in the soil sample over time and under certain storage conditions, such as drying, oxidation, or biological processes, which can affect the test results unless precautions are taken to minimize these effects.

The undrained shear strength of soil is also affected by the water content, as demonstrated by (Boukpeti et al., 2012). It should be noted that the soil sample used in the fall cone test may have a different water content compared to that in the field, owing to storage and handling procedures in the laboratory. This variability in water content may cause discrepancies in the measured undrained shear strength values.

As the cone angle increases during the fall cone test, the surrounding clay is subjected to more deformation, leading to an increase in the tangent angle between the cone and the surface. However, there is another factor that can potentially have a more significant effect on the shape of the disturbed region. This factor is related to the displacement of the surrounding media, which is required to adjust the volume

of clay that is forced aside by the cone. This phenomenon can be influenced by several factors, including the compression of contained gas bubbles and dilatancy. Consequently, the penetration depth can be affected by these factors, potentially leading to variations in the estimated undrained shear strength (Hansbo, 1957).

Another source of uncertainty in the fall cone test is the condition of the cone tip. If the cone tip is worn or damaged, it can have a significant impact on the results, leading to an overestimation of undrained shear strength and introducing considerable error in the estimation. This introduces additional uncertainty, as it cannot be guaranteed that the cone tip is in perfect condition.

In the case of medium or stiff clay, or even the existence of the sand particle in the clay sample, when a 60g-60° cone is used, the penetration will be very small, hence the accuracy of undrained shear strength is very affected by the accuracy of the readings. Thus, the error of one-tenth of a millimeter at $h = 2\,mm$ will give an error in undrained shear strength of approximately $2\ t/m^2$ (Hansbo, 1957).

In addition, if the cylindrical clay specimen is not bounded around its boundary, the reading of penetrations may not be very accurate because due to the elastic vertical compression caused by the cone impact. However, if the sample is kept in the sampling tube during the test, this effect is minimized.

Friction between the stem and the device can introduce errors in the fall cone test results. In order to minimize this effect, it is recommended to lubricate the stem carefully before each test. In this study, this issue was observed on multiple occasions, highlighting the importance of this precautionary measure.

The smoothness and horizontality of the soil surface is a critical factor that can affect the accuracy of the penetration depth measurement. Therefore, it is essential to ensure that the sample is cut with precision and care, so as to avoid any irregularities or inclined surfaces. However, achieving a perfectly smooth surface in the laboratory may be challenging.

During the fall cone test, it is assumed that the cone penetrates the soil body with a horizontal surface. When the cone penetrates for the first time, the soil around the cone is displaced, resulting in a distorted surface and heave. This phenomenon can affect subsequent penetrations as the soil around the disturbed region becomes more compact. However, in this research, the effect of heave on cone resistance has not been considered, leading to an overestimation of the results.

4.2.2 Oedometric test

In oedometric testing, the analysis of consolidation tests is often conducted under the assumption that the soil being tested is fully saturated. However, in cases where the soil is not completely saturated, some of the derived parameters may be misleading. While it is not always possible to ensure complete saturation of the soil, this assumption is typically made to simplify the analysis; hence, it may affect some parameters in the calculations.

One of the assumptions made in the test involves using λ=0.23 and κ=0.08 for all cases. The value of λ utilized is derived from an Oedometric remoulded sample. While assuming constant values for both factors does not significantly impact the results, there may be some minor errors in the outcomes.

The determination of pre-consolidation pressure is a crucial factor that can significantly impact the accuracy of the results obtained from the test. However, this determination is a complex and challenging task and is subject to a certain level of uncertainty. Hence, it is imperative to take all necessary measures to obtain the pre-consolidation point as accurately as possible.

4.2.3 Triaxial test

Friction between the piston and the cap is a potential source of error in triaxial testing. Adequate lubrication is crucial for reducing friction and ensuring a smooth operation. However, despite taking precautions, a small amount of error may still occur during the calculation process.

The conditions of sampling are a critical aspect to consider in experimental testing. The media must be prepared and maintained under optimal conditions to obtain reliable results. The temperature of the samples should ideally be consistent with natural conditions. Furthermore, the experimental procedures must be conducted precisely to avoid any potential errors that may arise during testing. However, as these tests entail various intricacies, minor errors may occur, especially for non-professionals.

Perhaps the most important factor is the determination of the critical state line (CSL). In this study, M is assumed to be constant and equal to 1.1; however, in reality, each series of samples has a different slope and is not identical. However, in this study, for the sake of simplicity and also because some series of tests are only one or two tests, it is not so reasonable to use the M related to these tests because it is not very accurate. Therefore, one constant value is considered for M, which is a reasonable value for clays, and this constant value can introduce uncertainty into our calculations.

The determination of water content after the triaxial test can be influenced by the location of the sample from which the measurement is taken. In this study, it was observed that the water content of the top and bottom 0.5 cm sections of the sample was similar and higher than the water content measured in the middle section. This discrepancy may be attributed to the friction between the sample and the top and bottom caps. The positions of the sample sections are illustrated in Figure 4.4, and the corresponding results are presented in Figure 4.5.

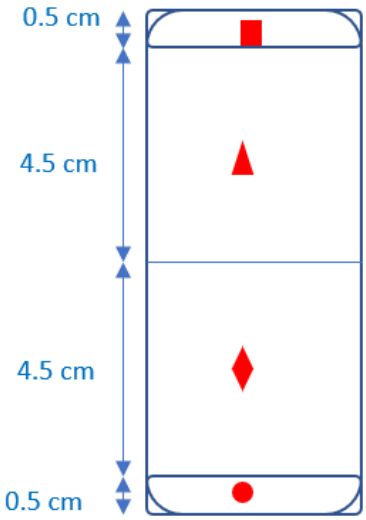

Figure 4-4 Position of each shape

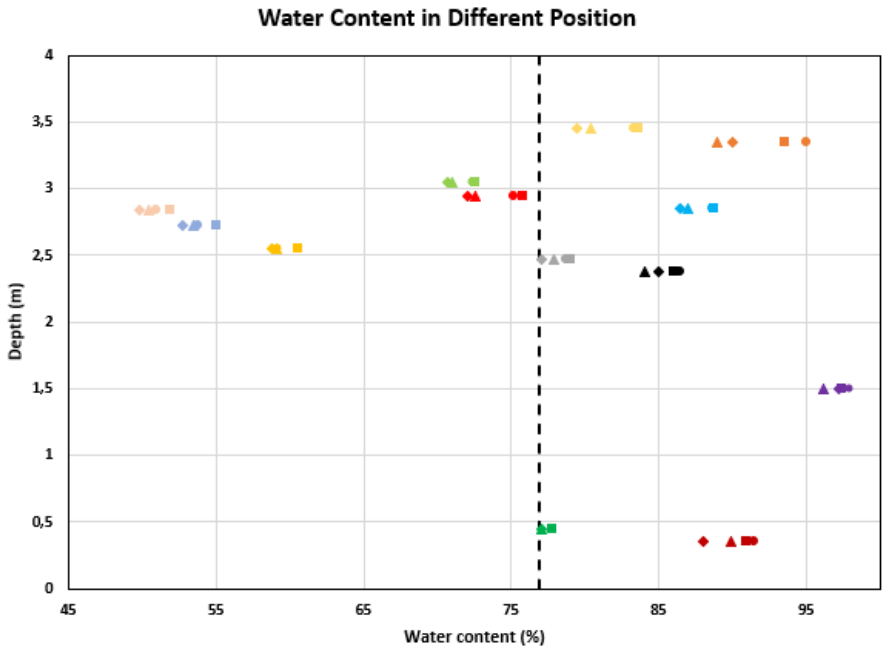

Figure 4-5 Values of water content at 0.5 cm at the top (square shape), 0.5 cm at the bottom (circle shape), 4.5 cm at the middle top (triangle shape) and 4.5 cm at the middle bottom (diamond shape)

The circular symbol corresponds to the water content measurement at the bottom of the sample, while the diamond symbol represents the measurement at the middle-bottom. Likewise, the triangular and square symbols correspond to water content measurements at the middle-top and top of the sample, respectively.

The tests were conducted using a constant sample diameter of 5 cm and a constant sample height of 10 cm. (Muraro & Jommi, 2021) demonstrated that the shear stress at the interface between the sample and the porous stone impedes the lateral expansion of the sample under axial compression. This results in higher average axial stress and stiffness, which may affect the friction between the cap and the sample, potentially influencing the water content measurements.

(Rowe P. W. & Barden L, 1964) showed that the effect of the end restraint on pore pressure depends on the change in the ratio of the diameter and height of the specimen and also on the friction between the cap and specimen. They concluded that the excess pore water pressure at the top and bottom is higher than in the middle. Hence, we can also conclude from this research that water content can be higher at the top and the bottom.

4.3 Comparisons and Recommendations

In this section, the results of undrained shear strength for different methods are illustrated and a comparison are made.

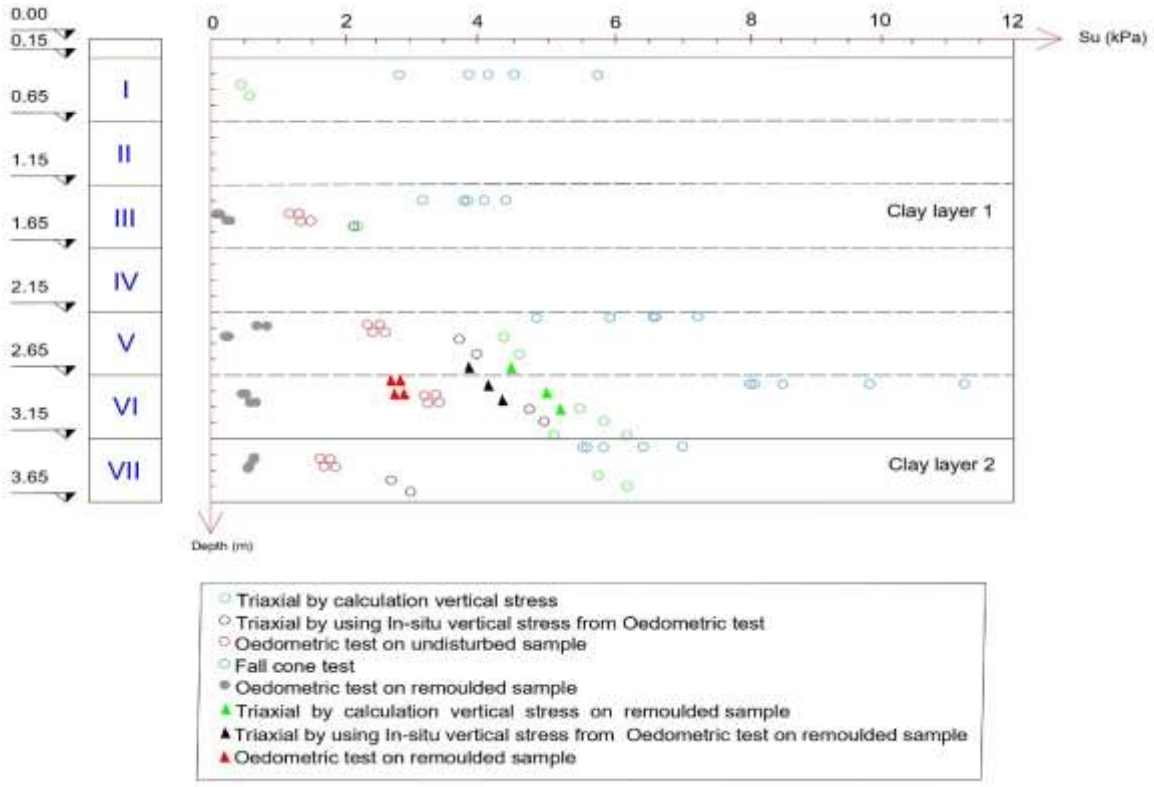

Figure 4-6 Comparison of different methods

The blue circles in the figure represent the undrained shear strength results obtained using the fall cone test. It is evident from the figure that the undrained shear strength values obtained from the fall cone test are greater than those obtained using other methods. This can be attributed to the numerous uncertainties present in the fall cone test, such as the effects of the lateral boundary, confining pressure, surface roughness, cone tip corrosion, and human error, which can introduce significant errors in the estimation. Moreover, significant differences in undrained shear strength values can also be observed between different penetrations at the same depth, particularly in the first layer (0-0.5 meters), where the difference between the minimum and maximum undrained shear strength values is almost twice. This difference may be attributed to the heterogeneity of some parts of the sample or the friction of the stem of the apparatus.

Therefore, to reduce this type of error, it is better to lubricate the stem before each trial. As you see in the picture, by going down to the depth, it is clear that undrained shear strength increases for this type of test, but in the first part of the tube in the shallowest layer (0-0.5 meter), this is not correct because usually in the first layer, we have stress relaxation, and sometimes in geotechnical works the behaviour of the first part of the soil can be considered an exception. In depths of 1–1.5 meters, the values of undrained shear strength are very close to each other, perhaps because we have a very homogenous structure at this depth and also because the human error is reduced to its minimum level. In the depth range of 2.1–2.6 meters, we obtained typical behavior due to some errors in each penetration depth, and in the depth range of 2.6–3.1 meters, we again have the same situation except for the largest value of undrained shear strength, which is around 11.5 kPa. It seems this is more related to human error. An important observation regarding the depth range of 3.1-3.6 meters is that the undrained shear strength values suddenly decreased, indicating a change in the soil layer at this depth. It is noteworthy that in most fall cone tests, the first penetration has a smaller value than subsequent penetrations. This could be attributed to the smooth surface of the soil without any distortion during the first penetration, while subsequent penetrations introduce some degree of roughness on the surface. Furthermore, the penetration of the fall cone into the soil can cause a heave in the surface, which may result in the distortion and breaking of the clay structure. This phenomenon can lead to an increase in the penetration depth in subsequent tries. However, it should be noted that this is not a general criterion, as the structure of the soil is a complex system influenced by numerous factors, including heterogeneity.

The red circles in the provided figure correspond to the outcomes of the oedometric tests for undisturbed samples, modeled by two constitutive models, namely, the Modified Cam Clay model and the S-CLAY model. The results from both models exhibit a close agreement due to their inherent similarities, where the only distinguishable difference is attributed to the value of the parameter α, which determines the inclination of the yield locus. If the value of this parameter is zero, then the two models will converge. The undrained shear strength values obtained from the Modified Cam Clay model and the S-CLAY model were analyzed concerning the depth of the soil. The results indicated that the undrained shear strength values obtained from the S-CLAY model were slightly higher than those obtained from the Modified Cam Clay model due to the effect of the parameter α. However, the difference between the two models was negligible, and the percentage of error was approximately 3-4%, which remained constant with depth. As the depth increased, the undrained shear strength values also increased, with a sudden drop observed in the range of 3.1-3.6 meters due to a change in layering. Overall, the

findings suggest that the S-CLAY model and Modified Cam Clay model can provide reliable estimations of undrained shear strength, with minimal differences observed between the two models. Moreover, it should be noted that as the depth increases, a slight increase in the discrepancy between the outcomes acquired through oedometric and triaxial tests is observed. The black circle in the figure denotes the undrained shear strength obtained through the use of the same constitutive models for the destructured segment. The undrained shear strength values vary from 0.1 to 1 kPa across different depths, and the results obtained from both the Modified Cam Clay and S-CLAY models are nearly identical at each depth. It is noteworthy that the oedometric test results for the shallowest part of the soil (0-0.5 meters) were not apparent. Although the tests were carried out, the pre-consolidation pressure was not observable due to the elasticity phenomenon. Without the pre-consolidation pressure, it is not feasible to estimate the undrained shear strength via the oedometric test.

The green and black circles in the figure denote the undrained shear strengths obtained from a standard triaxial test and a triaxial test with pre-consolidation pressure as the field stress, respectively. In the range of 0-0.5 meters, only the results of the standard triaxial test are available, as the pre-consolidation pressure could not be determined due to the elasticity phenomenon. The results of the two tests are identical in the range of 1-1.5 meters. As the depth increases beyond this range, a discrepancy between the two results is observed, and the undrained shear strength values from the standard triaxial test are higher than those from the test with pre-consolidation pressure. The percentage of error between these two scenarios is found to be in the range of 9-13%. In comparison, the percentage of error between the fall cone test and the triaxial test is approximately 35-40%, while it is 20-25% for the oedometric test. The magnitude of error is relatively lower in the shallower layer and higher in the deeper layer.

In the case of remoulded samples, triangular shapes are used. The results of the oedometric and triaxial tests for both undisturbed and remoulded samples are shown in the above picture. It is evident that the undrained shear strength of the remoulded sample is smaller than that of the undisturbed sample. This can be attributed to the fact that the structure of the sample is destroyed during remoulding, resulting in a lower bearing capacity against loading.

Based on the fewer uncertainties associated with triaxial testing, it is likely to yield more accurate results for undrained shear strength due to its ability to account for the boundary effect by confining the sample with a membrane and its capability to adjust the confining pressure. These factors are crucial for simulating a test that closely resembles the conditions present on the field site. If we assume the triaxial

test as providing the most accurate results, we can infer that the fall cone test tends to overestimate the value of undrained shear strength, while the oedometric test may slightly underestimate the results.

Recommendations-

- Performing fall cone tests with different roughness value (α) and comparing the results with the previous case.
- Taking into account different critical state lines (M) for each analysis based on the results of each series of triaxial tests.
- Examine the impact of varying values of k_0, as its value has been held constant throughout this study.
- Investigating the different values of stress ratio (η) for anisotropic tests, since in this research only $\eta = 0.2$ is discussed.

5. Conclusions

In this research, the undrained shear strength of Finnish clay is estimated by some laboratory tests. The aim is to verify the validity of the Cone penetrometer data concerning Fall Cone, Oedometric, and Triaxial tests. Some important conclusions that we can extract from this Thesis are as follows:

1. The accuracy of fall cone tests is not so reliable and it overestimates the values of undrained shear strength because this type of test includes a lot of uncertainties and this cause to have a lot of errors in our estimation.
2. The study suggests that the mean value of penetration depth obtained from the fall cone test may not be a reliable criterion due to uncertainties associated with the test. These uncertainties could result in errors in the penetration depth measurements at different locations, causing deviations from the mean value. Statistical analysis reveals that the error associated with the mean value is approximately 5%. Therefore, to obtain more accurate results, it is recommended to correct the mean value by accounting for this 5% error.
3. Between the three methods, the oedometric test gives the smallest value of undrained shear strength while the fall cone test gives us the largest.
4. The results for the oedometric test with two constitutive models are very close to each other because the only difference between these two is only due to parameter α which describes the inclination of the yield surface.
5. In a typical triaxial test and triaxial considering pre-consolidation pressure as a field scale, the results are very similar and in the shallower layer, these results tend to be coincident and vice versa in the deeper layer.
6. Analysis of the remoulded samples shows that the value of undrained shear strength decreases concerning to undisturbed sample.
7. After a depth of 3 meters, results suddenly changed and this can be due to a change in the layer.
8. The percentage of error between the fall cone test and the oedometric test is approximately 50-60%, while between the fall cone test and triaxial test, this error is approximately 35–40%, and finally, between the oedometric and triaxial tests it is 20-25%.

9. In the Triaxial results, it is observed that the water content at the top and bottom of the sample is a little bit larger than the middle and the reason can be due to the friction between the specimen and the cap.
10. For determining organic content, two sites are investigated (KU1 and KU2). For KU1, the percentage of organic matter is between 0.07-1.63 while for KU4 this value is between 0.77-2.6.
11. The range of the bulk density for this type of soil is obtained and it was between 2.73-2.82 $g/cm^3$and for the matter of our calculation it is considered 2.76 g/cm^3.
12. For obtaining sensitivity, four sites are used (KU1, KU2, KU3, KU4). The range was between 3.4-22.3 and the mean value of the sensitivity among all values was 10.77, so it can be categorized as active clay. Furthermore, the sites KU2 and KU3 had more active clays concerning KU1 and KU4.

Bibliography

ASTM Committee D-18 on Soil and Rock. (2017). *Standard Practice for Classification of Soils for Engineering Purposes (Unified Soil Classification System)*.

Atkinson, J. H., Richardson, D., & Robinson, P. J. (1987). Compression and extension of K0 normally consolidated kaolin clay. *Journal of geotechnical engineering*, *113*(12), 1468–1482.

Boukpeti, N., White, D. J., Randolph, M. F., & Low, H. E. (2012). Strength of fine-grained soils at the solid-fluid transition. *Geotechnique*, *62*(3), 213–226. https://doi.org/10.1680/geot.9.P.069

EN 1997-2. (2007). *Eurocode 7: Geotechnical design*.

European Commission. (2019). *Study on Baltic offshore wind energy cooperation under BEMIP: final report.*

Gardemeister R. (1975). *On engineering-geological properties of fine-grained sediments in Finland* [Academical Dissertation]. University of Turku.

Hansbo, S. (1957). New approach to the determination of the shear strength of clay by the fall-cone test. *Royal Swedish Geotechnical Institute*.

Hirota J., & Szyper JP. (1975). Separation of total particulate carbon into inorganic and organic components 1. *Limnology and Oceanography*, *20*(5), 896–900.

Hj Ali, F., & Ahmad, E. (2013). Field Behavior and Numerical Simulation of Coastal Bund on Soft Marine Clay Loaded to Failure. *Electronic J. of Geotech. Eng*, *18*, 4027–4042. https://www.researchgate.net/publication/303061691

Hyyppä, E. (1963). On the late-Quaternary history of the Baltic Sea. *Fennia*, *89*(1), 37–48.

Karlsson, R. (1961). Suggested improvements in the liquid limit test, with reference to flow properties of remoulded clays. *Contributions to the Fifth International Conference on Soil Mechanics and Foundation Engineering*.

Kirkgard, M. M., & Lade', P. V. (1993). Anisotropic three-dimensional behavior of a normally consolidated clay. *Canadian Geotechnical Journal* , *30*(5), 848–858. www.nrcresearchpress.com

Korhonen, K. H., & Lojander, M. (1987). Yielding of Perno clay. *Proceedings of 2nd International Conference on Constitutive Laws for Engineering Materials*, 1249–1255.

Koskinen M. (2014). *Plastic anisotropy and destructuration of soft Finnish clays* [Dissertation]. Aalto University.

Koumoto T, & Houlsby G. T. (2001). Theory and practice of the fall cone test. *Géotechnique*, *51*(8), 701–712.

Larsson, R., & Åhnberg, H. (2005). On the evaluation of undrained shear strength and preconsolidation pressure from common field tests in clay. *Canadian Geotechnical Journal*, *42*(4), 1221–1231. https://doi.org/10.1139/t05-031

Llano-Serna, M. A., & Contreras, L. F. (2020). The effect of surface roughness and shear rate during fall-cone calibration. *Geotechnique*, *70*(4), 332–342. https://doi.org/10.1680/jgeot.18.P.222

Luczak, C., Janquin, M.-A., & Kupka, A. (1997). Simple standard procedure for the routine determination of organic matter in marine sediment. *Hydrobiologia*, *345*, 87–94.

Magdoff F., & van ES H. (2021). *Building soils for better crops: ecological management for healthy soils*. Sustainable Agriculture Research & Education.

Marto, A., Mohd Yunus, N. Z., Pakir, F., Latifi, N., Mat Nor, A. H., & Tan, C. S. (2014). Stabilization of Marine Clay by Biomass Silica (Non-Traditional) Stabilizers. *Applied Mechanics and Materials*, *695*, 93–97. https://doi.org/10.4028/www.scientific.net/amm.695.93

Moum, J., & Torrance, J. K. (1971). A GEOCHEMICAL INVESTIGATION OF THE SENSITIVITY OF A NORMALLY CONSOLIDATED CLAY FROM DRAMMEN, NORWAY. *Geotechnique*, *21*(4), 329–340.

Muraro, S., & Jommi, C. (2021). Experimental determination of the shear strength of peat from standard undrained triaxial tests: Correcting for the effects of end restraint. *Geotechnique*, *71*(1), 76–87. https://doi.org/10.1680/jgeot.18.P.346

Nakase A., & Kamei T. (1988). Undrained shear strength of remoulded marine clays. *Soils and Foundations*, *28*(1), 29–40.

Penner E. (1965). A STUDY OF SENSITIVITY IN LEDA CLAY. *Canadian Journal of Earth Sciences*, *2*(5), 424–441. www.nrcresearchpress.com

Roscoe, K. H., & Burland, J. B. (1968). On the generalised stress-strain behaviour of "wet" clay. *Engineering Plasticity:*, 553–569.

Rowe P. W., & Barden L. (1964). Importance of free ends in triaxial testing. *Soil Mechanics and Foundation Engineering*, *90*(1), 1–27.

SFS-EN ISO 17892-3. (2015). *European Standard*.

SFS-EN ISO 17892-4. (2016). *European Standard*.

SFS-EN ISO 17892-5. (2017). *European Standard*.

SFS-EN ISO 17892-6. (2017). *European Standard*.

SFS-EN ISO 17892-9. (2017). *European Standard*.

Shi, X. S., & Herle, I. (2015). Compression and undrained shear strength of remoulded clay mixtures. *Geotechnique Letters*, *5*, 62–67. https://doi.org/10.1680/geolett.14.00089

Sivasithamparam, N. (2012). *Development and Implementation of Advanced Soft Soil Models in Finite Elements*. University of Strathclyde.

Skempton, A. W., & Northey, R. D. (1952). THE SENSITIVITY OF CLAYS. *Geotechnique*, *3*(1), 30–53.

Wheeler, S. J., Näätänen, A., Karstunen, M., & Lojander, M. (2003). An anisotropic elastoplastic model for soft clays. *Canadian Geotechnical Journal*, *40*(2), 403–418. https://doi.org/10.1139/t02-119

Wood D. M. (1982). Cone penetrometer and liquid limit. *Geotechnique*, *32*(2), 152–157.

Wood D. M. (1985). Some fall-cone tests. *Geotechnique*, *35*(1), 64–68.

Yamaguchi S. (1959). *On the sensitivity of clay*.

Yang, S. L., Lunne, T., Andersen, K. H., D'lgnazio, M., & Yetginer, G. (2019). Undrained shear strength of marine clays based on CPTU data and SHANSEP parameters. *17th European Conference on Soil Mechanics and Geotechnical Engineering, ECSMGE 2019 - Proceedings*, *2019-September*. https://doi.org/10.32075/17ECSMGE-2019-0048

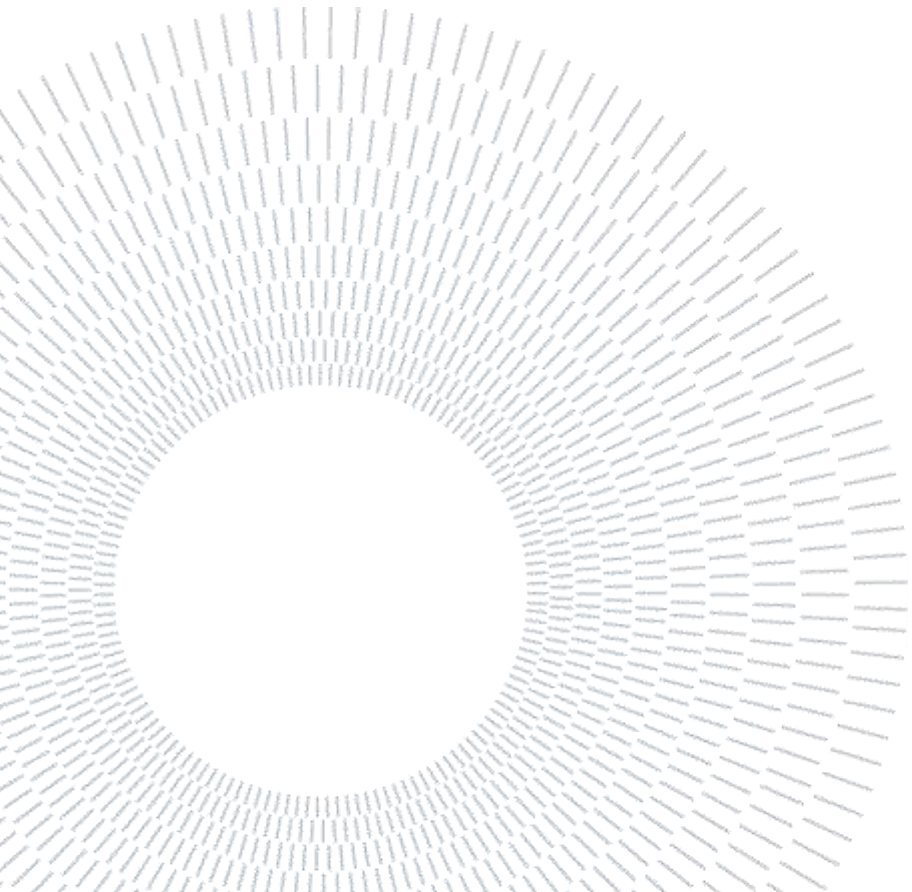

A. Appendix

		Page (1)			Date 29/9/2022		
Laboratory of soil mechanics		Hydrometer Test			Project num.		
Sample		August Part 1 2022					
Research		GTK					
Cup No.		E17			E23		
Tube No.		1			2		
Depth	**m**	0-0.1			0.5-0.6		
Weight of sample for Hydrometer	**g**	50			50		
Time	**Date**	**at**	**T**	**Hyd-Reading**	**at**	**T**	**Hyd-Reading**
1 min	29.9.2022	10:12	23.4	1.0317		10:12	1.0325
6 min	29.9.2022		23.4	1.0316			1.0317
19 min	29.9.2022		23.4	1.0315			1.0308
1 h	29.9.2022		23.4	1.0309			1.0296
5 h	29.9.2022		23.4	1.0295			1.0267
1 day	30.9.2022	10:12	23	1.0254		10:12	1.0125
4 days	2.10.2022	10:08	22.8	1.0207		10:08	1.0185
8 days	6.10.2022	11:23	23.3	1.0185		11:23	1.0165
16 days	14.10.2022	9:33	22.9	1.0155		9:33	1.0139
26 days	24.10.2022	16:00	22.9	1.0133		16:00	1.0123
35 days	2.11.2022	9:21	22.6	1.0124		9:21	1.0113
42 days	9.11.2022	10:12	22.7	1.0116		10:12	1.0106

Table A.1: Hydrometer reading of the site of KU1 2022

	Page (2)	Date 29/9/2022
Laboratory of soil mechanics	Hydrometer Test	Project num.
Sample	August Part 1 2022	
Research	GTK	
Cup No.	E13	E4
Tube No.	3	4
Depth m	1-1.1	1.5-1.6
Weight of sample for Hydrometer g	50	50

Time	Date	at	T	Hyd-Reading	at	T	Hyd-Reading
1 min	29.9.2022	10:12	23.4	1.0318		10:12	1.0325
6 min	29.9.2022		23.4	1.0313			1.0315
19 min	29.9.2022		23.4	1.0305			1.0313
1 h	29.9.2022		23.4	1.0294			1.0297
5 h	29.9.2022		23.4	1.0260			1.0276
1 day	30.9.2022	10:12	23	1.0217		10:12	1.0240
4 days	2.10.2022	10:08	22.8	1.0175		10:08	1.0201
8 days	6.10.2022	11:23	23.3	1.0155		11:23	1.0176
16 days	14.10.2022	9:33	22.9	1.0130		9:33	1.0150
26 days	24.10.2022	16:00	22.9	1.0115		16:00	1.0129
35 days	2.11.2022	9:21	22.6	1.0105		9:21	1.0119
42 days	9.11.2022	10:12	22.7	1.0100		10:12	1.0114

Table A.2: Hydrometer reading of the site of KU1 2022

		Page (3)			Date 29/9/2022		
Laboratory of soil mechanics		Hydrometer Test			Project num.		
Sample		August Part 1 2022					
Research		GTK					
Cup No.		E18			E11		
Tube No.		5			6		
Depth	**m**	2-2.1			2.5-2.6		
Weight of sample for Hydrometer	**g**	50			50		
Time	**Date**	**at**	**T**	**Hyd-Reading**	**at**	**T**	**Hyd-Reading**
1 min	29.9.2022	10:12	23.4	1.0323		10:12	1.0325
6 min	29.9.2022		23.4	1.0322			1.0321
19 min	29.9.2022		23.4	1.0320			1.0318
1 h	29.9.2022		23.4	1.0315			1.0315
5 h	29.9.2022		23.4	1.0291			1.0295
1 day	30.9.2022	10:12	23	1.0246		10:12	1.0249
4 days	2.10.2022	10:08	22.8	1.0198		10:08	1.0196
8 days	6.10.2022	11:23	23.3	1.0175		11:23	1.0166
16 days	14.10.2022	9:33	22.9	1.0145		9:33	1.0135
26 days	24.10.2022	16:00	22.9	1.0124		16:00	1.0112
35 days	2.11.2022	9:21	22.6	1.0114		9:21	1.0104
42 days	9.11.2022	10:12	22.7	1.0105		10:12	1.0095

Table A.3: Hydrometer reading of the site of KU1 2022

		Page (4)	Date 29/9/2022
Laboratory of soil mechanics		Hydrometer Test	Project num.
Sample		August Part 1 2022	
Research		GTK	
Cup No.		E14	
Tube No.		7	
Depth	**m**	3-3.1	
Weight of sample for Hydrometer	**g**	50	

Time	Date	at	T	Hyd-Reading	at	T	Hyd-Reading
1 min	29.9.2022	10:12	23.4	1.0318			
6 min	29.9.2022		23.4	1.0317			
19 min	29.9.2022		23.4	1.0316			
1 h	29.9.2022		23.4	1.0314			
5 h	29.9.2022		23.4	1.0291			
1 day	30.9.2022	10:12	23	1.0248			
4 days	2.10.2022	10:08	22.8	1.0195			
8 days	6.10.2022	11:23	23.3	1.0165			
16 days	14.10.2022	9:33	22.9	1.0134			
26 days	24.10.2022	16:00	22.9	1.0110			
35 days	2.11.2022	9:21	22.6	1.0103			
42 days	9.11.2022	10:12	22.7	1.0094			

Table A.4: Hydrometer reading of the site of KU1 2022

		Page (1)		Date 4/10/2022			
Laboratory of soil mechanics		Hydrometer Test		Project num.			
Sample		August Part 2 2022					
Research		GTK					
Cup No.		E21		E3			
Tube No.		I		II			
Depth	**m**	0.15-0.25		0.65-0.75			
Weight of sample for Hydrometer	**g**	50		50			

Time	Date	at	T	Hyd-Reading	at	T	Hyd-Reading
1 min	4.10.2022	10:57	22.7	1.0304		22.7	1.0305
6 min	4.10.2022		22.7	1.0269		22.7	1.0295
19 min	4.10.2022		22.7	1.0247		22.7	1.0271
1 h	4.10.2022		22.7	1.0225		22.7	1.0243
5 h	4.10.2022		22.7	1.0185		22.7	1.0205
1 day	5.10.2022	10:57	22.7	1.0145		22.7	1.0155
4 days	8.10.2022	15:45	22.8	1.0105		22.8	1.0120
10 days	14.10.2022	17:20	23.8	1.0085		23.8	1.0095
20 days	24.10.2022	14:40	22.5	1.0073		22.5	1.0075

Table A.5: Hydrometer reading of the site of KU4 2022

		Page (2)	Date 4/10/2022
Laboratory of soil mechanics		Hydrometer Test	Project num.
Sample		August Part 2 2022	
Research		GTK	
Cup No.		E20	E5
Tube No.		III	IV
Depth	**m**	1.15-1.25	1.65-1.75
Weight of sample for Hydrometer	**g**	50	50

Time	Date	at	T	Hyd-Reading	at	T	Hyd-Reading
1 min	4.10.2022	10:57	22.7	1.0313		22.7	1.0320
6 min	4.10.2022		22.7	1.0290		22.7	1.0306
19 min	4.10.2022		22.7	1.0265		22.7	1.0285
1 h	4.10.2022		22.7	1.0239		22.7	1.0260
5 h	4.10.2022		22.7	1.0207		22.7	1.0217
1 day	5.10.2022	10:57	22.7	1.0157		22.7	1.0175
4 days	8.10.2022	15:45	22.8	1.0122		22.8	1.0135
10 days	14.10.2022	17:20	23.8	1.0098		23.8	1.0111
20 days	24.10.2022	14:40	22.5	1.0075		22.5	1.0085

Table A.6: Hydrometer reading of the site of KU4 2022

	Page (3)	Date 4/10/2022
Laboratory of soil mechanics	Hydrometer Test	Project num.
Sample	August Part 2 2022	
Research	GTK	
Cup No.	P79	L1
Tube No.	V	VI
Depth m	2.15-2.25	2.65-2.75
Weight of sample for Hydrometer g	50	50

Time	Date	at	T	Hyd-Reading	at	T	Hyd-Reading
1 min	4.10.2022	10:57	22.7	1.0319		22.7	1.0327
6 min	4.10.2022		22.7	1.0307		22.7	1.0322
19 min	4.10.2022		22.7	1.0290		22.7	1.0314
1 h	4.10.2022		22.7	1.0270		22.7	1.0305
5 h	4.10.2022		22.7	1.0234		22.7	1.0270
1 day	5.10.2022	10:57	22.7	1.0186		22.7	1.0223
4 days	8.10.2022	15:45	22.8	1.0143		22.8	1.0170
10 days	14.10.2022	17:20	23.8	1.0115		23.8	1.0135
20 days	24.10.2022	14:40	22.5	1.0083		22.5	1.0115

Table A.7: Hydrometer reading of the site of KU4 2022

		Page (4)	Date 4/10/2022
Laboratory of soil mechanics		Hydrometer Test	Project num.
Sample		August Part 2 2022	
Research		GTK	
Cup No.		P38	P75
Tube No.		VII	VIII
Depth	**m**	3.15-3.25	3.65-3.75
Weight of sample for Hydrometer	**g**	50	50

Time	Date	at	T	Hyd-Reading	at	T	Hyd-Reading
1 min	4.10.2022	10:57	22.7	1.0316		22.7	1.0315
6 min	4.10.2022		22.7	1.0304		22.7	1.0305
19 min	4.10.2022		22.7	1.0292		22.7	1.0295
1 h	4.10.2022		22.7	1.0277		22.7	1.0285
5 h	4.10.2022		22.7	1.0245		22.7	1.0264
1 day	5.10.2022	10:57	22.7	1.0207		22.7	1.0226
4 days	8.10.2022	15:45	22.8	1.0162		22.8	1.0185
10 days	14.10.2022	17:20	23.8	1.0134		23.8	1.0155
20 days	24.10.2022	14:40	22.5	1.0113		22.5	1.0075

Table A.8: Hydrometer reading of the site of KU4 2022

	Page (1)	Date
Laboratory of soil mechanics	Determination of solid density	Project num.

Sampling Location: GTK

Project: Reza August 2022 Part 1

Point:

AST No.	Tube No.	Depth m	Pycnometer No.	Pycnometer g	Pyc+dry sample g	Dry sample m_k g	Temp T °C	Pyc+Sample+ Water+cup m_b g	Pyc+water+ cup m_a g	$m_k + m_a - m_b$	ρ_w g/cm3	ρ_s g/cm3	Mean value
	1	0-0.1	1461	29.57	34.43	4.86	22	138.23	135.12	1.75	0.998	2.77	2.76
			1373	28.86	34.76	5.9	22	138.82	135.05	2.13	0.998	2.761	
	2	0.5-0.6	1106	17.66	21.1	3.39	20.30	75.37	73.22	1.24	0.998	2.726	2.73
			1069	18.67	22.41	3.74	20.30	76.96	74.59	1.37	0.998	2.732	
	3	1-1.1	1180	17.56	22.3	4.74	20.30	76.88	73.85	1.71	0.998	2.767	2.76
			1148	19.25	23.7	4.45	20.30	79.01	76.18	1.62	0.998	2.75	
	4	1.5-1.6	1148	19.25	23.56	4.31	22	78.92	76.15	1.54	0.998	2.787	2.78
			1307	18.06	21.73	3.67	22	76.84	74.49	1.32	0.998	2.769	
	5	2-2.1	1037	18.35	22.83	4.48	20.30	78.51	75.65	1.62	0.998	2.757	2.73
			1307	18.06	21.49	3.43	20.30	76.67	74.51	1.27	0.998	2.701	
	6	2.5-2.6	1037	18.35	22.32	3.97	22	78.18	75.63	1.42	0.998	2.787	2.78
			57	19.55	23.49	3.94	22	77.2	74.68	1.42	0.998	2.775	
	7	3-3.1	107	17.99	20.9	2.91	22	74.14	72.27	1.04	0.998	2.789	2.77
			1030	17.8	21.53	3.73	22	76.64	74.26	1.35	0.998	2.761	

Table A.9: Solid density of the site of KU1 2022

	Page (1)	Date
Laboratory of soil mechanics	Determination of solid density	Project num.

Sampling Location: GTK

Project: Reza August 2022 Part 2

Point:

AST No.	Tube No.	Depth m	Pycnometer No.	Pycnometer g	Pyc+dry sample g	Dry sample m_k g	Temp T °C	Pyc+Sample+ Water+cup m_b g	Pyc+water+ cup m_a g	$m_k + m_a - m_b$	ρ_w g/cm3	ρ_s g/cm3	Mean value
	I	0.15-0.25	1148	19.25	23.15	3.9	20.6	78.66	76.17	1.41	0.998	2.758	2.76
			1307	18.35	21.55	3.2	20.6	77.69	75.65	1.16	0.998	2.757	
	II	0.65-0.75	1022	19.45	23.84	4.39	20.30	78.04	75.25	1.60	0.998	2.75	2.74
			1030	17.8	22.1	4.26	20.30	76.98	74.28	1.56	0.998	2.72	
	III	1.15-1.25	50	19.55	22.95	3.4	20.30	77.68	75.53	1.25	0.998	2.71	2.75
			84	17.15	20.37	3.22	20.30	73.38	71.31	1.15	0.998	2.783	
	IV	1.65-1.75	1307	18.06	21.93	3.87	20.6	76.99	74.50	1.38	0.998	2.789	2.79
			1030	17.8	21.15	3.35	20.6	76.43	74.28	1.20	0.998	2.793	
	V	2.15-2.25	68	18.89	22.28	3.39	20.6	77.97	75.78	1.20	0.998	2.817	2.82
			1069	18.67	23	4.33	20.6	77.38	74.58	1.53	0.998	2.819	
	VI	2.65-2.75	1022	19.45	22.81	3.36	20.6	77.41	75.24	1.19	0.998	2.814	2.82
			84	17.15	20.55	3.4	20.6	73.51	71.31	1.20	0.998	2.825	
	VII	3.15-3.25	13	15.75	18.66	2.91	20.6	71.31	69.44	1.04	0.998	2.794	2.79
			50	19.55	22.96	3.41	20.6	77.72	75.53	1.22	0.998	2.791	
	VIII	3.65-3.75	107	17.99	20.9	2.91	20.3	74.15	72.29	1.05	0.998	2.761	2.77
			68	18.89	23.26	4.37	20.3	78.58	75.79	1.58	0.998	2.769	

Table A.10: Solid density of the site of KU4 2022

	Page (1)	Date
Laboratory of soil mechanics	Determination of organic content	Project num.

Sampling Location: GTK

Project: Reza August 2022 Part 1

Point:

AST No.	Tube No.	Depth m	Cup No.	Cup g	Weight of cup+ Dry sample at 150° B_k g	Dry sample At 150° m_k g	Weight of cup+ Dry sample at 800° B_h g	After burning Bk-Bh=Hh g	After burning Hk %	Water Crystal K_v %	Clay % <0.002 mm %	Humus H_m %
	1		19	24.6	39.2	14.6	38.54	0.66	4.52	3.84	88	0.68
			2	18.51	31.18	12.67	30.61	0.57	4.50	3.84	88	0.66
	2		7	38.3	78.96	40.66	77.1	1.85	4.55	3.55	78	1
			8	37.16	79.09	41.93	77.18	1.91	4.56	3.55	78	1
	3		30	12.59	23.54	10.95	22.98	0.56	5.11	3.49	76	1.62
			35	11.79	22.92	11.13	22.35	0.57	5.12	3.49	76	1.63
	4		15	26.34	43.83	17.49	43.03	0.8	4.57	3.67	82	0.91
			12	25.49	44.73	19.24	43.85	0.88	4.57	3.67	82	0.91
	5		13	25.71	44.03	18.32	43.24	0.79	4.31	3.81	87	0.5
			18	21.11	39.97	18.86	39.14	0.83	4.4	3.81	87	0.59
	6		6	22.55	36.87	14.32	36.31	0.56	3.91	3.84	88	0.07
			1	19.93	33.83	13.9	33.27	0.56	4.03	3.84	88	0.19
	7		Q1	16.08	35.5	19.37	34.7	0.8	4.13	3.81	87	0.32
			Q2	14.07	31.87	17.8	31.05	0.82	4.61	3.81	87	0.79

Table A.11: Organic content of the site of KU1 2022

	Page (1)	Date
Laboratory of soil mechanics	Determination of organic content	Project num.

Sampling Location: GTK

Project: Reza August 2022 Part 2

Point:

AST	Tube	Depth	Cup		Weight of cup+ Dry sample at 150°	Dry sample At 150°	Weight of cup+ Dry sample at 800°	After burning		Water	Clay % <0.002 mm	Humus
No.	No.	m	No.	g	B_k g	m_k g	B_h g	Bk-Bh=Hh g	Hk %	Crystal K_v %	%	H_m %
	I		12	25.49	41.79	16.3	40.95	0.84	5.15	2.71	49	2.44
			15	26.34	43.86	17.52	42.93	0.93	5.31	2.71	49	2.6
	II		18	21.11	41.13	20.02	40.13	1	5	2.89	55	2.11
			13	25.71	44.1	18.39	43.17	0.93	5.06	2.89	55	2.17
	III		1	19.93	35.01	15.08	34.28	0.73	4.84	2.94	57	1.90
			6	22.55	41.32	18.77	40.39	0.93	4.95	2.94	57	2.01
	IV		Q1	16.08	35.33	19.25	34.33	1	5.19	3.03	60	2.16
			Q2	14.07	29.58	15.51	28.79	0.79	5.09	3.03	60	2.06
	V		14	28.18	46.89	18.71	45.91	0.98	5.24	3.21	66	2.03
			19	24.6	43.65	19.05	42.68	0.97	5.09	3.21	66	1.89
	VI		30	12.59	22.95	10.36	22.49	0.46	4.44	3.55	78	0.89
			35	11.79	22.19	10.4	21.74	0.45	4.33	3.55	78	0.77
	VII		2	18.51	35.08	16.57	34.17	0.91	5.49	3.32	70	2.17
			17	18.74	36.27	17.53	35.27	1	5.70	3.32	70	2.38
	VIII		7	38.3	75.3	37	73.22	2.08	5.62	3.52	77	2.10
			8	37.16	74.43	37.27	72.34	2.09	5.61	3.52	77	2.08

Table A.12: Organic content of the site of KU4 2022

	Page (1)	Date 05-09-2022
Laboratory of soil mechanics	Fall cone test	Project num.

Sampling Location: Marine Clay
Project: GTK May 2022 Part 1
Point:

Tube num		1		2		3		4	
Plate num		1		2		3		4	
Depth	m	0.1-0.2		0.8-0.9		1.27-1.37		1.81-1.91	
Container num		E33		E35		E27		E29	
Container	g	249.15		243.75		242.04		243.04	
Container + moist sample	g	574.57		585.82		569.2		588.61	
Moist sample	g	325.42		342.07		327.16		345.57	
Container + dry sample	g	373.12		379.45		367.44		388.37	
Dry sample	g	123.97		135.7		125.4		145.33	
Water	g	201.45		206.37		201.76		200.24	
Water content	%	162.5		152.1		160.9		137.8	
Soil type (visual estimate)		clay		clay		clay		clay	
Colour		gray		gray		gray		gray	
Layering									
Notes									
Undist=undisturbed, Dist=disturbed		Undist	Dist	Undist	Dist	Undist	Dist	Undist	Dist
Cone	g	60	10	60	10	60	10	60	10
Penetration	mm 1	6.1	11.8	6.5	10.2	7	12.4	6.4	8.4
	2	6.2	11.8	6.9	10.2	8.6	12.4	4.8	8.4
	3	7.4	11.8	8.5	10.2	5.8	12.4	5.5	8.4
	4	6.6		7.7		8.2		6.2	
	5	6.3		7.4		9		6.6	
Average penetration i	mm	6.5	11.8	7.3	10.2	7.7	12.4	5.9	8.4
Undrained shear strength c_u	kPa	3.87	0.21	3.06	0.28	2.75	0.19	4.54	0.41
Sensitivity $S_t = c_u / c_{uR}$		18.4		10.9		14.5		11.1	
Height of the sample h	cm	10		10		10		10	
Sample	g	343.31		359.93		343.2		360.97	
Sampling tube area A	cm2	26.42079422		26.42079422		26.42079422		26.42079422	
Sample volume V (=hA)	cm^3	264.2079422		264.2079422		264.2079422		264.2079422	
Density ρ	g/cm^3	1.299		1.362		1.299		1.366	
Unit weight γ = ρ*g	kN/m^3	11.80		12.37		12.73		13.39	
Coefficient	a tai α								
Liquid limit w_L = aw = αw									

Table A.13: Fall Cone test data of the site May 2022 part 1-1

	Page (2)	Date 05-09-2022
Laboratory of soil mechanics	Fall cone test	Project num.

Sampling Location: Marine Clay
Project: May 2022 Part 1
Point:

Tube num		5		6		7		8	
Plate num		5		6		7		8	
Depth	m	2.28-2.38		2.77-2.87		1.27-1.37		3.77-3.87	
Container num		E1		E7		E5		E3	
Container	g	180.55		180.45		180.99		180.68	
Container + moist sample	g	521.07		532.36		521.35		540.99	
Moist sample	g	340.52		351.91		340.36		360.31	
Container + dry sample	g	325.6		330.04		330.3		344.96	
Dry sample	g	145.05		149.59		149.31		164.28	
Water	g	195.47		202.32		191.05		196.03	
Water content	%	134.8		135.2		128		119.3	
Soil type (visual estimate)		clay		clay		clay		clay	
Colour		gray with black lines		gray with black lines		gray		gray with black lines	
Layering									
Notes									
Undist=undisturbed, Dist=disturbed		Undist	Dist	Undist	Dist	Undist	Dist	Undist	Dist
Cone	g	60	10	60	10	60	10	60	10
Penetration	mm 1	3.9	8	3.9	7.8	7.3	8	4.3	6.2
	2	4.6	8	4.8	7.8	6.4	8	3.9	6.2
	3	5.1	8	5.2	7.8	3.1	8	4.3	6.2
	4	5.5		4.8		5.9		4.3	
	5	5.6		3.6		6.2		3	
Average penetration i	mm	4.9	8	4.5	7.8	5.8	8	4	6.2
Undrained shear strength c_u	kPa	5.96	0.46	6.96	0.48	4.67	0.46	8.87	0.76
Sensitivity $S_t = c_u / c_{uR}$		12.9		14.5		10.2		11.7	
Height of the sample h	cm	10		10		10		10	
Sample	g	356.46		364.53		358.1		372.36	
Sampling tube area A	cm2	26.42079422		26.42079422		26.42079422		26.42079422	
Sample volume V (=hA)	cm^3	264.2079422		264.2079422		264.2079422		264.2079422	
Density ρ	g/cm^3	1.349		1.380		1.355		1.409	
Unit weight $\gamma = \rho * g$	kN/m^3	13.22		13.52		13.28		13.81	
Coefficient	a tai α								
Liquid limit w_L = aw = α w									

Table A.14: Fall Cone test data of the site May 2022 part 1-2

	Page (3)	Date 05-09-2022
Laboratory of soil mechanics	Fall cone test	Project num.

Sampling Location: Marine Clay
Project: May 2022 Part 1
Point:

Tube num		9							
Plate num		9							
Depth	m	4.27-4.37							
Container num		E20							
Container	g	180.03							
Container + moist sample	g	551.73							
Moist sample	g	341.7							
Container + dry sample	g	358.62							
Dry sample	g	178.59							
Water	g	163.11							
Water content	%	91.3							
Soil type (visual estimate)		clay							
Colour		gray with black lines							
Layering									
Notes									
Undist=undisturbed, Dist=disturbed		Undist	Dist	Undist	Dist	Undist	Dist	Undist	Dist
Cone	g	60	10						
Penetration	mm 1	3.9	5.8						
	2	3.9	5.8						
	3	3.9	5.8						
	4	5.2							
	5	5.4							
Average penetration i	mm	4.5	58						
Undrained shear strength c_u	kPa	7.06	0.87						
Sensitivity $S_t = c_u / c_{uR}$		8.1							
Height of the sample h	cm	10							
Sample	g	382.21							
Sampling tube area A	cm2	26.42079422							
Sample volume V (=hA)	cm^3	264.2079422							
Density ρ	g/cm^3	1.447							
Unit weight γ = ρ*g	kN/m^3	14.18							
Coefficient	a tai α								
Liquid limit w_L = aw = αw									

Table A.15: Fall Cone test data of the site May 2022 part 1-3

	Page (1)	Date 05-09-2022
Laboratory of soil mechanics	Fall cone test	Project num.

Sampling Location: Marine Clay
Project: May 2022 Part 2
Point:

Tube num		I		II		III		IV	
Plate num		1		2		3		4	
Depth	m	0-0.1		0.38-0.48		0.88-0.98		1.38-1.48	
Container num		P28		P42		P47		E29	
Container	g	122.68		142.99		163.7		243.08	
Container + moist sample	g	396.82		473.25		509.25		602.63	
Moist sample	g	274.14		330.26		345.55		359.55	
Container + dry sample	g	199.99		280.99		316.68		402.79	
Dry sample	g	77.31		138		152.98		159.71	
Water	g	196.83		192.26		192.57		199.84	
Water content	%	254.6		139.3		125.9		125.1	
Soil type (visual estimate)		clay		clay		clay		clay	
Colour		Gray & black		gray		gray		gray	
Layering									
Notes									
Undist=undisturbed, Dist=disturbed		Undist	Dist	Undist	Dist	Undist	Dist	Undist	Dist
Cone	g	60	10	60	10	60	10	60	10
Penetration	mm 1	8.5	7.5	3.7	8	6.8	7.8	3.2	8.1
	2	12	7.5	3.6	8.6	6.1	8	4.4	8
	3	9.8	7.5	4.1	8.6	7.1	8	4	8.1
	4	9.1		3.8		5.7		5	
	5	9.1		4.2		7		3.2	
Average penetration i	mm	9.7	7.5	3.9	8.4	6.5	7.9	4	8.1
Undrained shear strength c_u	kPa	1.78	0.52	9.2	0.41	3.85	0.47	8.87	0.45
Sensitivity $S_t = c_u / c_{uR}$		3.4		22.4		8.3		19.6	
Height of the sample h	cm	10		10		10		10	
Sample	g	284.38		342.5		357.66		372.44	
Sampling tube area A	cm2	26.42079422		26.42079422		26.42079422		26.42079422	
Sample volume V (=hA)	cm^3	264.2079422		264.2079422		264.2079422		264.2079422	
Density ρ	g/cm^3	1.076		1.296		1.354		1.410	
Unit weight γ = ρ*g	kN/m^3	9.77		11.77		13.27		13.82	
Coefficient	a tai α								
Liquid limit w_L = aw = αw									

Table A.16: Fall Cone test data of the site May 2022 part 2-1

	Page (2)	Date 05-09-2022
Laboratory of soil mechanics	Fall cone test	Project num.

Sampling Location: Marine Clay
Project: May 2022 Part 2
Point:

Tube num		V		VI		VII		VIII	
Plate num		5		6		7		8	
Depth	m	1.88-1.98		2.38-2.48		2.88-2.98		3.38-3.48	
Container num									
Container	g	243.74		249.18		241.96		181.58	
Container + moist sample	g	595.65		608.83		610.11		563.98	
Moist sample	g	351.91		359.65		368.15		382.4	
Container + dry sample	g	406.8		408.53		422.4		366.94	
Dry sample	g	163.06		159.35		180.44		185.36	
Water	g	188.85		200.30		187.71		197.04	
Water content	%	115.8		125.7		104		106.3	
Soil type (visual estimate)		clay		clay		clay		clay	
Colour		gray		gray with blacl lines		gray		gray	
Layering									
Notes									
Undist=undisturbed, Dist=disturbed		Undist	Dist	Undist	Dist	Undist	Dist	Undist	Dist
Cone	g	60	10	60	10	60	10	60	10
Penetration	mm 1	4.9	7.6	2.8	7	4.9	5	3.1	6
	2	6	7.6	2.4	7	3.3	5	3.3	6
	3	5.2	7.6	3.2	7	4.8	5	3.3	6
	4	6.6		2.4		3.5		3.3	
	5	6.9		2.7		3		3.5	
Average penetration i	mm	5.9	7.6	2.6	7	3.9	5	3.3	6
Undrained shear strength c_u	kPa	4.52	0.51	14.32	0.6	9.13	1.18	11.84	0.81
Sensitivity $S_t = c_u / c_{uR}$		8.9		23.9		7.7		14.6	
Height of the sample h	cm	10		10		10		10	
Sample	g	362		369.83		379.68		393.81	
Sampling tube area A	cm2	26.42079422		26.42079422		26.42079422		26.42079422	
Sample volume V (=hA)	cm^3	264.2079422		264.2079422		264.2079422		264.2079422	
Density ρ	g/cm^3	1.370		1.4		1.437		1.491	
Unit weight γ = ρ*g	kN/m^3	13.43		13.72		14.08		14.61	
Coefficient	a tai α								
Liquid limit w_L = aw = αw									

Table A.17: Fall Cone test data of the site May 2022 part 2-2

	Page (1)	Date 22-09-2022
Laboratory of soil mechanics	Fall cone test	Project num.

Sampling Location: Marine Clay
Project: August 2022 Part 1
Point:

Tube num		1		2		3		4	
Plate num		1		2		3		4	
Depth	m	0-0.1		0.5-0.6		1-1.1		1.5-1.6	
Container num		E17		E23		E13		E4	
Container	g	185.7		183.03		186.22		180.09	
Container + moist sample	g	531.86		561.89		536.31		562.78	
Moist sample	g	346.16		378.86		350.09		382.69	
Container + dry sample	g	349.43		365.46		344.24		366.47	
Dry sample	g	163.73		182.43		158.02		186.38	
Water	g	182.43		196.43		192.07		196.31	
Water content	%	111.4		107.7		121.5		105.3	
Soil type (visual estimate)		clay		clay		clay		clay	
Colour		Gray & black		gray		Gray & black		gray	
Layering									
Notes									
Undist=undisturbed, Dist=disturbed		Undist	Dist	Undist	Dist	Undist	Dist	Undist	Dist
Cone	g	60	10	60	10	60	10	60	10
Penetration	mm 1	7.6	6	6.8	6	4.6	6.9	5.2	6.9
	2	6.7	6	7.2	6	6.6	6.9	5.6	6.5
	3	6.7	6	6.1	6	5.2	6.9	4.7	6.7
	4	7		6.5		4.4		6.1	
	5	6.7		6.4		3		5.5	
Average penetration i	mm	6.9	6	6.6	6	4.8	6.9	5.4	6.7
Undrained shear strength c_u	kPa	3.43	0.81	3.82	0.81	6.34	0.62	5.13	0.66
Sensitivity $S_t = c_u / c_{uR}$		4.2		4.7		10.2		7.8	
Height of the sample h	cm	10		10		10		10	
Sample	g	364.13		396.18		365.16		394	
Sampling tube area A	cm2	26.42079422		26.42079422		26.42079422		26.42079422	
Sample volume V (=hA)	cm^3	264.2079422		264.2079422		264.2079422		264.2079422	
Density ρ	g/cm^3	1.378		1.5		1.382		1.491	
Unit weight γ = ρ*g	kN/m^3	12.52		13.62		13.55		14.62	
Coefficient	a tai α								
Liquid limit w_L = aw = αw									

Table A.18: Fall Cone test data of the site August 2022 part 1-1

	Page (2)	Date 22-09-2022
Laboratory of soil mechanics	Fall cone test	Project num.

Sampling Location: Marine Clay
Project: August 2022 Part 1
Point:

Tube num		5		6		7			
Plate num		5		6		7			
Depth	m	2-2.1		2.5-2.6		3-3.1			
Container num		E18		E11		E14			
Container	g	184.93		180.92		179.45			
Container + moist sample	g	565.24		556.42		556.2			
Moist sample	g	380.31		375.5		376.75			
Container + dry sample	g	374.03		362.35		361.46			
Dry sample	g	189.1		181.43		182.01			
Water	g	191.21		194.07		194.74			
Water content	%	101.1		107		107			
Soil type (visual estimate)		clay		clay		clay			
Colour		gray		gray		gray			
Layering									
Notes									
Undist=undisturbed, Dist=disturbed		Undist	Dist	Undist	Dist	Undist	Dist	Undist	Dist
Cone	g	60	10	60	10	60	10		
Penetration	mm 1	4.1	6.2	4.3	7	4.3	6.5		
	2	4.4	6.2	5.1	7	4.7	6.5		
	3	4.4	6.2	5.2	7	4.6	6.5		
	4	5.1		5.2		4.2			
	5	3.1		6		4.5			
Average penetration i	mm	4.2	6.2	5.2	7	4.5	6.5		
Undrained shear strength c_u	kPa	8.09	0.76	5.53	0.6	7.06	0.7		
Sensitivity $S_t = c_u / c_{uR}$		10.6		9.2		10.1			
Height of the sample h	cm	10		10		10			
Sample	g	393.86		390.32		391.63			
Sampling tube area A	cm2	26.42079422		26.42079422		26.42079422			
Sample volume V (=hA)	cm^3	264.2079422		264.2079422		264.2079422			
Density ρ	g/cm^3	1.491		1.477		1.482			
Unit weight $\gamma = \rho * g$	kN/m^3	13.54		13.42		14.53			
Coefficient	a tai α								
Liquid limit w_L = aw = α w									

Table A.19: Fall Cone test data of the site August 2022 part 1-2

	Page (1)	Date 23-09-2022
Laboratory of soil mechanics	Fall cone test	Project num.

Sampling Location: Marine Clay
Project: August 2022 Part 2
Point:

Tube num		I		II		III		IV	
Plate num		1		2		3		4	
Depth	m	0.15-0.25		0.65-0.75		1.15-1.25		1.65-1.75	
Container num		E21		E3		E20		E5	
Container	g	185.91		180.67		180.03		180.99	
Container + moist sample	g	535.25		541.57		545.73		540.81	
Moist sample	g	349.34		360.9		365.7		359.82	
Container + dry sample	g	336.57		339.2		341.76		342.5	
Dry sample	g	150.66		158.53		161.73		161.51	
Water	g	198.68		202.37		203.97		198.31	
Water content	%	131.9		127.7		126.1		122.8	
Soil type (visual estimate)		clay		clay		clay		clay	
Colour		Gray black		gray		Gray & black		gray	
Layering									
Notes									
Undist=undisturbed, Dist=disturbed		Undist	Dist	Undist	Dist	Undist	Dist	Undist	Dist
Cone	g	60	10	60	10	60	10	60	10
Penetration	mm 1	7.5	6.5	5	7.8	6.4	7	4.1	7.1
	2	5.1	6.5	6.5	7.8	6.8	7	3.9	7.1
	3	6	6.5	5.1	7.8	6.5	7	4.1	7.1
	4	6.3		5		6.2		3.9	
	5	6.5		4.6		6.5		4.3	
Average penetration i	mm	6.3	6.5	5	7.8	6.5	7	4.1	7.1
Undrained shear strength c_u	kPa	4.11	0.7	5.77	0.48	3.91	0.6	8.44	0.59
Sensitivity $S_t = c_u / c_{uR}$		5.9		12		6.5		14.3	
Height of the sample h	cm	10		10		10		10	
Sample	g	358.37		369.97		375.92		369.17	
Sampling tube area A	cm2	26.42079422		26.42079422		26.42079422		26.42079422	
Sample volume V (=hA)	cm^3	264.2079422		264.2079422		264.2079422		264.2079422	
Density ρ	g/cm^3	1.356		1.4		1.423		1.397	
Unit weight γ = ρ*g	kN/m^3	12.32		12.72		13.95		13.69	
Coefficient	a tai α								
Liquid limit w_L = aw = αw									

Table A.20: Fall Cone test data of the site August 2022 part 2-1

	Page (2)	Date 23-09-2022
Laboratory of soil mechanics	Fall cone test	Project num.

Sampling Location: Marine Clay
Project: August 2022 Part 2
Point:

Tube num		V		VI		VII		VIII	
Plate num		5		6		7		8	
Depth	m	2.15-2.25		2.65-2.75		3.15-3.25		3.65-3.75	
Container num		P79		L1		P38		P75	
Container	g	149.38		184.81		150.1		160.57	
Container + moist sample	g	529.9		567.6		533.59		539.64	
Moist sample	g	380.52		382.79		383.49		379.07	
Container + dry sample	g	332.43		371.07		329.11		336.96	
Dry sample	g	183.05		186.26		179.01		176.39	
Water	g	197.47		196.53		204.48		202.68	
Water content	%	107.9		105.5		114.2		114.9	
Soil type (visual estimate)		clay		clay		clay		clay	
Colour		Gray with black lines		gray		Gray & black		Gray with black lines	
Layering									
Notes									
Undist=undisturbed, Dist=disturbed		Undist	Dist	Undist	Dist	Undist	Dist	Undist	Dist
Cone	g	60	10	60	10	60	10	60	10
Penetration	mm 1	4.85	6.8	3.9	5.8	5.1	5	3.7	5.2
	2	5.15	6.8	4	5.8	5.05	5	4.15	5.2
	3	5.75	6.8	4.2	5.8	4.55	5	3.85	5.2
	4	4.8		3.65		4.75		4	
	5	4.4		4.15		5.75		3.6	
Average penetration i	mm	5	6.8	4	5.8	5	5	3.9	5.2
Undrained shear strength c_u	kPa	5.85	0.64	8.79	0.87	5.76	1.18	9.3	1.09
Sensitivity $S_t = c_u / c_{uR}$		9.1		10.1		4.9		8.5	
Height of the sample h	cm	10		10		10		10	
Sample	g	389.45		393.58		392.06		388.74	
Sampling tube area A	cm2	26.42079422		26.42079422		26.42079422		26.42079422	
Sample volume V (=hA)	cm^3	264.2079422		264.2079422		264.2079422		264.2079422	
Density ρ	g/cm^3	1.474		1.490		1.484		1.471	
Unit weight γ = ρ*g	kN/m^3	14.45		14.60		14.54		14.42	
Coefficient	a tai α								
Liquid limit w_L = aw = αw									

Table A.21: Fall Cone test data of the site August 2022 part 2-2

Department of Civil Engineering		OEDOMETER TEST	Start time: 19.10.2022 Finish time: 28.10.2022	
Sampling place:	GTK		Sampling date:	Aug 2022
Testor:	Reza		Lab. No.:	6946
Tube No.:	3		Depth (m):	1.1-1.125
Specimen height (cm):	2		Section (cm^2)	

BEFORE TEST			AFTER TEST		
Specimen + ring (g)	93.32		Specimen height (mm)	10.9-9.6-9.96	
Ring (g)	38.09		Specimen mass (g)	34.6	
Specimen (g)	55.23		Container number	272	
Water content (%)	139		Container (g)	43.56	
Porosity (n_i)	79.12		Container + wet (g)	78.16	
Void ratio (e_i)	3.79		Container + dry (g)	66.61	
Saturation (S_{ri} %)	100		Water content (%)	50	
Density ($\rho_i, g/cm^3$)	1.38		Porosity (n_f)	58.85	
Grain density (ρ_s)	2.76		Void ratio (e_f)	1.43	
Water content close to specimen			Saturation (S_{rf} %)	96.6	
Container number	119		Density ($\rho_f, g/cm^3$)	1.7	
Container (g)	44.24		**Fall cone test**		
Container + wet (g)	121.17			Top	Bottom
Container + dry (g)	76.77		1st (mm)		5.3
Water content (%)	136		2nd (mm)		4.2
Fall cone test			3rd (mm)		4
	Top	Bottom	4th (mm)		4.6
1st (mm)			5th (mm)		4.4
2nd (mm)			Average (mm)		4.5
3rd (mm)			Strength (kPa)		
4th (mm)					
5th (mm)					
Average (mm)					
Strength (kPa)					

Table A.22: Oedometeric test for undisturbed sample, Lab No. 6946, depth 1.1-1.125 m

Department of Civil Engineering		OEDOMETER TEST	Start time: 19.10.2022 Finish time: 28.10.2022	
Sampling place:	GTK		Sampling date:	Aug 2022
Testor:	Reza		Lab. No.:	6947
Tube No.:	3		Depth (m):	1.125-1.15
Specimen height (cm):	2		Section (cm^2)	

BEFORE TEST			AFTER TEST		
Specimen + ring (g)	94.04		Specimen height (mm)	10.5-10.4-10.6	
Ring (g)	38.09		Specimen mass (g)	35.49	
Specimen (g)	55.95		Container number	281	
Water content (%)	141		Container (g)	43.15	
Porosity (n_i)	79		Container + wet (g)	78.64	
Void ratio (e_i)	3.762		Container + dry (g)	66.36	
Saturation (S_{ri} %)	100		Water content (%)	53	
Density ($\rho_i, g/cm^3$)	1.39		Porosity (n_f)	59.95	
Grain density (ρ_s)	2.76		Void ratio (e_f)	1.5	
Water content close to specimen			Saturation (S_{rf} %)	97	
Container number	39		Density ($\rho_f, g/cm^3$)	1.69	
Container (g)	20.96		**Fall cone test**		
Container + wet (g)	46.82			Top	Bottom
Container + dry (g)	31.96		1st (mm)		5.5
Water content (%)	135		2nd (mm)		6.9
Fall cone test			3rd (mm)		8.1
	Top	Bottom	4th (mm)		7.3
1st (mm)			5th (mm)		7.6
2nd (mm)			Average (mm)		7.08
3rd (mm)			Strength (kPa)		
4th (mm)					
5th (mm)					
Average (mm)					
Strength (kPa)					

Table A.23: Oedometeric test for undisturbed sample, Lab No. 6947, depth 1.125-1.15 m

Department of Civil Engineering		OEDOMETER TEST	Start time: 19.10.2022 Finish time: 28.10.2022	
Sampling place:	GTK		Sampling date:	Aug 2022
Testor:	Reza		Lab. No.:	6948
Tube No.:	VI		Depth (m):	2.75-2.775
Specimen height (cm):	2		Section (cm^2)	

BEFORE TEST			AFTER TEST		
Specimen + ring (g)	96.11		Specimen height (mm)	11.31-12.13-11.51	
Ring (g)	38.09		Specimen mass (g)	41.79	
Specimen (g)	58.02		Container number	20	
Water content (%)	115		Container (g)	42.46	
Porosity (n_i)	76		Container + wet (g)	84.25	
Void ratio (e_i)	3.193		Container + dry (g)	69.46	
Saturation (S_{ri} %)	100		Water content (%)	58	
Density ($\rho_i, g/cm^3$)	1.45		Porosity (n_f)	59.05	
Grain density (ρ_s)	2.83		Void ratio (e_f)	1.44	
Water content close to specimen			Saturation (S_{rf} %)	107	
Container number	1000		Density ($\rho_f, g/cm^3$)	1.79	
Container (g)	28.10		**Fall cone test**		
Container + wet (g)	43.92			Top	Bottom
Container + dry (g)	35.68		1st (mm)		6.6
Water content (%)	109		2nd (mm)		7.3
Fall cone test			3rd (mm)		8.4
	Top	Bottom	4th (mm)		7.4
1st (mm)			5th (mm)		8.5
2nd (mm)			Average (mm)		7.64
3rd (mm)			Strength (kPa)		
4th (mm)					
5th (mm)					
Average (mm)					
Strength (kPa)					

Table A.24: Oedometeric test for undisturbed sample, Lab No. 6948, depth 2.75-2.775 m

Department of Civil Engineering		OEDOMETER TEST	Start time: 19.10.2022 Finish time: 28.10.2022	
Sampling place:	GTK		Sampling date:	Aug 2022
Testor:	Reza		Lab. No.:	6949
Tube No.:	VI		Depth (m):	2.775-2.8
Specimen height (cm):	2		Section (cm^2)	

BEFORE TEST			AFTER TEST		
Specimen + ring (g)	96.30		Specimen height (mm)	11.89-12.25-12.05	
Ring (g)	38.09		Specimen mass (g)	42.03	
Specimen (g)	58.21		Container number	185	
Water content (%)	113		Container (g)	45.57	
Porosity (n_i)	75.87		Container + wet (g)	87.60	
Void ratio (e_i)	3.145		Container + dry (g)	72.88	
Saturation (S_{ri} %)	100		Water content (%)	54	
Density ($\rho_i, g/cm^3$)	1.45		Porosity (n_f)	60	
Grain density (ρ_s)	2.83		Void ratio (e_f)	1.5	
Water content close to specimen			Saturation (S_{rf} %)	101.7	
Container number	56		Density ($\rho_f, g/cm^3$)	1.74	
Container (g)	31.53		**Fall cone test**		
Container + wet (g)	48.89			Top	Bottom
Container + dry (g)	39.97		1st (mm)		7.9
Water content (%)	106		2nd (mm)		6.6
Fall cone test			3rd (mm)		7.5
	Top	Bottom	4th (mm)		7.6
1st (mm)			5th (mm)		7
2nd (mm)			Average (mm)		7.32
3rd (mm)			Strength (kPa)		
4th (mm)					
5th (mm)					
Average (mm)					
Strength (kPa)					

Table A.25: Oedometeric test for undisturbed sample, Lab No. 6949, depth 2.775-2.8 m

Department of Civil Engineering		OEDOMETER TEST	Start time: 1.11.2022 Finish time: 10.11.2022	
Sampling place:	GTK		Sampling date:	Aug 2022
Testor:	Reza		Lab. No.:	6954
Tube No.:	V		Depth (m):	2.25-2.275
Specimen height (cm):	2		Section (cm^2)	

BEFORE TEST			AFTER TEST		
Specimen + ring (g)	97.09		Specimen height (mm)	11.83-11.03-11.25	
Ring (g)	38.07		Specimen mass (g)	42.03	
Specimen (g)	59.02		Container number	6	
Water content (%)	109.5		Container (g)	22.6	
Porosity (n_i)	75.29		Container + wet (g)	64.63	
Void ratio (e_i)	3.048		Container + dry (g)	50.76	
Saturation (S_{ri} %)	100		Water content (%)	49.25	
Density ($\rho_i, g/cm^3$)	1.47		Porosity (n_f)	56.52	
Grain density (ρ_s)	2.85		Void ratio (e_f)	1.3	
Water content close to specimen			Saturation (S_{rf} %)	108	
Container number	31		Density ($\rho_f, g/cm^3$)	1.85	
Container (g)	27.05		**Fall cone test**		
Container + wet (g)	79.04			Top	Bottom
Container + dry (g)	52.28		1st (mm)		5.8
Water content (%)	106		2nd (mm)		5.5
Fall cone test			3rd (mm)		8
	Top	Bottom	4th (mm)		6.4
1st (mm)			5th (mm)		6.3
2nd (mm)			Average (mm)		6.4
3rd (mm)			Strength (kPa)		
4th (mm)					
5th (mm)					
Average (mm)					
Strength (kPa)					

Table A.26: Oedometeric test for undisturbed sample, Lab No. 6954, depth 2.25-2.275 m

Department of Civil Engineering		OEDOMETER TEST	Start time: 1.11.2022 Finish time: 10.11.2022	
Sampling place:	GTK		Sampling date:	Aug 2022
Testor:	Reza		Lab. No.:	6955
Tube No.:	V		Depth (m):	2.30-2.325
Specimen height (cm):	2		Section (cm^2)	

BEFORE TEST			AFTER TEST		
Specimen + ring (g)	96.91		Specimen height (mm)	12.33-12.27-11.22	
Ring (g)	38.07		Specimen mass (g)	41.72	
Specimen (g)	58.84		Container number	365	
Water content (%)	113		Container (g)	56.96	
Porosity (n_i)	75.8		Container + wet (g)	98.68	
Void ratio (e_i)	3.136		Container + dry (g)	84.52	
Saturation (S_{ri} %)	100		Water content (%)	51	
Density ($\rho_i, g/cm^3$)	1.47		Porosity (n_f)	59.5	
Grain density (ρ_s)	2.85		Void ratio (e_f)	1.47	
Water content close to specimen			Saturation (S_{rf} %)	99.6	
Container number	38		Density ($\rho_f, g/cm^3$)	1.75	
Container (g)	21.64		**Fall cone test**		
Container + wet (g)	56.56			Top	Bottom
Container + dry (g)	38.67		1st (mm)		7.3
Water content (%)	105		2nd (mm)		6.6
Fall cone test			3rd (mm)		8.6
	Top	Bottom	4th (mm)		7.7
1st (mm)			5th (mm)		7.4
2nd (mm)			Average (mm)		7.52
3rd (mm)			Strength (kPa)		
4th (mm)					
5th (mm)					
Average (mm)					
Strength (kPa)					

Table A.27: Oedometeric test for undisturbed sample, Lab No. 6955, depth 2.3-2.325 m

Department of Civil Engineering		OEDOMETER TEST	Start time: 1.11.2022 Finish time: 10.11.2022	
Sampling place:	GTK		Sampling date:	Aug 2022
Testor:	Reza		Lab. No.:	6956
Tube No.:	VII		Depth (m):	3.25-3.275
Specimen height (cm):	2		Section (cm^2)	

BEFORE TEST			AFTER TEST		
Specimen + ring (g)	95.90		Specimen height (mm)	12.20-11.45-10.65	
Ring (g)	38.07		Specimen mass (g)	40.47	
Specimen (g)	57.83		Container number	272	
Water content (%)	117		Container (g)	43.56	
Porosity (n_i)	76.17		Container + wet (g)	84.03	
Void ratio (e_i)	3.197		Container + dry (g)	70.15	
Saturation (S_{ri} %)	100		Water content (%)	52	
Density ($\rho_i, g/cm^3$)	1.44		Porosity (n_f)	58.29	
Grain density (ρ_s)	2.79		Void ratio (e_f)	1.398	
Water content close to specimen			Saturation (S_{rf} %)	104	
Container number	61		Density ($\rho_f, g/cm^3$)	1.77	
Container (g)	25.02		**Fall cone test**		
Container + wet (g)	58.96			Top	Bottom
Container + dry (g)	40.95		1st (mm)		7.5
Water content (%)	111		2nd (mm)		5.5
Fall cone test			3rd (mm)		6.6
	Top	Bottom	4th (mm)		7.1
1st (mm)			5th (mm)		7.5
2nd (mm)			Average (mm)		6.84
3rd (mm)			Strength (kPa)		
4th (mm)					
5th (mm)					
Average (mm)					
Strength (kPa)					

Table A.28: Oedometeric test for undisturbed sample, Lab No. 6956, depth 3.25-3.275 m

Department of Civil Engineering		OEDOMETER TEST	Start time: 1.11.2022 Finish time: 10.11.2022	
Sampling place:	GTK		Sampling date:	Aug 2022
Testor:	Reza		Lab. No.:	6957
Tube No.:	VII		Depth (m):	3.275-3.3
Specimen height (cm):	2		Section (cm^2)	

BEFORE TEST			AFTER TEST		
Specimen + ring (g)	95.67		Specimen height (mm)	11.26-11.25-11.44	
Ring (g)	38.07		Specimen mass (g)	39.55	
Specimen (g)	57.6		Container number	20	
Water content (%)	121		Container (g)	42.46	
Porosity (n_i)	76.67		Container + wet (g)	82.01	
Void ratio (e_i)	3.285		Container + dry (g)	68.50	
Saturation (S_{ri} %)	100		Water content (%)	52	
Density ($\rho_i, g/cm^3$)	1.44		Porosity (n_f)	58.78	
Grain density (ρ_s)	2.79		Void ratio (e_f)	1.426	
Water content close to specimen			Saturation (S_{rf} %)	101.5	
Container number	52		Density ($\rho_f, g/cm^3$)	1.75	
Container (g)	28.03		**Fall cone test**		
Container + wet (g)	63			Top	Bottom
Container + dry (g)	44.53		1st (mm)		7
Water content (%)	112		2nd (mm)		6.6
Fall cone test			3rd (mm)		7.9
	Top	Bottom	4th (mm)		6.7
1st (mm)			5th (mm)		6.8
2nd (mm)			Average (mm)		7
3rd (mm)			Strength (kPa)		
4th (mm)					
5th (mm)					
Average (mm)					
Strength (kPa)					

Table A.29: Oedometeric test for undisturbed sample, Lab No. 6957, depth 3.275-3.3 m

Department of Civil Engineering			OEDOMETER TEST	Start time: 23.11.2022 Finish time: 2.12.2022	
Sampling place:	GTK			Sampling date:	Aug 2022
Testor:	Reza			Lab. No.:	6964
Tube No.:	I			Depth (m):	0.25-0.275
Specimen height (cm):	2			Section (cm^2)	
BEFORE TEST			**AFTER TEST**		
Specimen + ring (g)	92.06		Specimen height (mm)	8.52-9.54-9.23	
Ring (g)	38		Specimen mass (g)	32.02	
Specimen (g)	54.06		Container number	20	
Water content (%)	152		Container (g)	42.46	
Porosity (n_i)	80		Container + wet (g)	74.48	
Void ratio (e_i)	4.15		Container + dry (g)	63.92	
Saturation (S_{ri} %)	100		Water content (%)	49.2	
Density ($\rho_i, g/cm^3$)	1.35		Porosity (n_f)	57	
Grain density (ρ_s)	2.76		Void ratio (e_f)	1.34	
Water content close to specimen			Saturation (S_{rf} %)	101	
Container number	60		Density ($\rho_f, g/cm^3$)	1.76	
Container (g)	27.52		**Fall cone test**		
Container + wet (g)	57.64			Top	Bottom
Container + dry (g)	40.1		1st (mm)		4.4
Water content (%)	139		2nd (mm)		4.5
Fall cone test			3rd (mm)		4.5
	Top	Bottom	4th (mm)		4
1st (mm)			5th (mm)		4.5
2nd (mm)			Average (mm)		4.38
3rd (mm)			Strength (kPa)		
4th (mm)					
5th (mm)					
Average (mm)					
Strength (kPa)					

Table A.30: Oedometeric test for undisturbed sample, Lab No. 6964, depth 0.25-0.275 m

Department of Civil Engineering		OEDOMETER TEST	Start time: 23.11.2022 Finish time: 2.12.2022	
Sampling place:	GTK		Sampling date:	Aug 2022
Testor:	Reza		Lab. No.:	6965
Tube No.:	I		Depth (m):	0.275-0.3
Specimen height (cm):	2		Section (cm^2)	

BEFORE TEST			AFTER TEST		
Specimen + ring (g)	92.25		Specimen height (mm)	8.78-10.14-10.62	
Ring (g)	38		Specimen mass (g)	33.56	
Specimen (g)	54.25		Container number	262	
Water content (%)	145		Container (g)	40.77	
Porosity (n_i)	80		Container + wet (g)	74.33	
Void ratio (e_i)	3.98		Container + dry (g)	62.94	
Saturation (S_{ri} %)	100		Water content (%)	51	
Density ($\rho_i, g/cm^3$)	1.36		Porosity (n_f)	59	
Grain density (ρ_s)	2.76		Void ratio (e_f)	1.45	
Water content close to specimen			Saturation (S_{rf} %)	97.6	
Container number	1		Density ($\rho_f, g/cm^3$)	1.7	
Container (g)	27.84		**Fall cone test**		
Container + wet (g)	51.95			Top	Bottom
Container + dry (g)	38		1st (mm)		6.2
Water content (%)	137		2nd (mm)		5
Fall cone test			3rd (mm)		4.4
	Top	Bottom	4th (mm)		6.4
1st (mm)			5th (mm)		4.5
2nd (mm)			Average (mm)		5.3
3rd (mm)			Strength (kPa)		
4th (mm)					
5th (mm)					
Average (mm)					
Strength (kPa)					

Table A.31: Oedometeric test for undisturbed sample, Lab No. 6965, depth 0.275-0.3 m

Department of Civil Engineering			OEDOMETER TEST	Start time: 23.11.2022 Finish time: 2.12.2022	
Sampling place:	GTK			Sampling date:	Aug 2022
Testor:	Reza			Lab. No.:	6966
Tube No.:	III			Depth (m):	1.4-1.425
Specimen height (cm):	2			Section (cm^2)	
BEFORE TEST			**AFTER TEST**		
Specimen + ring (g)	94.65		Specimen height (mm)	10.37-10.81-9.54	
Ring (g)	38		Specimen mass (g)	36.26	
Specimen (g)	56.65		Container number	231	
Water content (%)	132		Container (g)	42.84	
Porosity (n_i)	77.8		Container + wet (g)	79.10	
Void ratio (e_i)	3.51		Container + dry (g)	67.20	
Saturation (S_{ri} %)	100		Water content (%)	48.8	
Density ($\rho_i, g/cm^3$)	1.42		Porosity (n_f)	56.7	
Grain density (ρ_s)	2.75		Void ratio (e_f)	1.31	
Water content close to specimen			Saturation (S_{rf} %)	102	
Container number	145		Density ($\rho_f, g/cm^3$)	1.77	
Container (g)	31.65		**Fall cone test**		
Container + wet (g)	65.31			Top	Bottom
Container + dry (g)	46.45		1st (mm)		3.9
Water content (%)	127		2nd (mm)		4
Fall cone test			3rd (mm)		4.8
	Top	Bottom	4th (mm)		4
1st (mm)			5th (mm)		3.5
2nd (mm)			Average (mm)		4.04
3rd (mm)			Strength (kPa)		
4th (mm)					
5th (mm)					
Average (mm)					
Strength (kPa)					

Table A.32: Oedometeric test for undisturbed sample, Lab No. 6966, depth 1.4-1.425 m

Department of Civil Engineering			OEDOMETER TEST	Start time: 23.11.2022 Finish time: 2.12.2022	
Sampling place:	GTK			Sampling date:	Aug 2022
Testor:	Reza			Lab. No.:	6967
Tube No.:	III			Depth (m):	1.425-1.45
Specimen height (cm):	2			Section (cm^2)	
BEFORE TEST			**AFTER TEST**		
Specimen + ring (g)	94.44		Specimen height (mm)	10.93-10.36-10.16	
Ring (g)	38		Specimen mass (g)	36.41	
Specimen (g)	56.54		Container number	269	
Water content (%)	133		Container (g)	43.47	
Porosity (n_i)	77.9		Container + wet (g)	79.88	
Void ratio (e_i)	3.53		Container + dry (g)	67.75	
Saturation (S_{ri} %)	100		Water content (%)	49.9	
Density ($\rho_i, g/cm^3$)	1.41		Porosity (n_f)	57.8	
Grain density (ρ_s)	2.75		Void ratio (e_f)	1.37	
Water content close to specimen			Saturation (S_{rf} %)	100	
Container number	119		Density ($\rho_f, g/cm^3$)	1.74	
Container (g)	29.94		**Fall cone test**		
Container + wet (g)	75.22			Top	Bottom
Container + dry (g)	49.98		1st (mm)		4.5
Water content (%)	126		2nd (mm)		4.4
Fall cone test			3rd (mm)		5.9
	Top	Bottom	4th (mm)		5
1st (mm)			5th (mm)		5
2nd (mm)			Average (mm)		4.96
3rd (mm)			Strength (kPa)		
4th (mm)					
5th (mm)					
Average (mm)					
Strength (kPa)					

Table A.33: Oedometeric test for undisturbed sample, Lab No. 6967, depth 1.425-1.45 m

Department of Civil Engineering			**OEDOMETER TEST**	**Start time:** 8.12.2022 **Finish time:** 17.12.2022	
Sampling place:	GTK			Sampling date:	Aug 2022
Testor:	Reza			Lab. No.:	6972
Tube No.:	Remoulded			Depth (m):	2.65-2.665
Specimen height (cm):	1.5			Section (cm^2)	
BEFORE TEST			**AFTER TEST**		
Specimen + ring (g)	67.57		Specimen height (mm)		
Ring (g)	29.55		Specimen mass (g)		
Specimen (g)	38.02		Container number		
Water content (%)			Container (g)		
Porosity (n_i)			Container + wet (g)		
Void ratio (e_i)			Container + dry (g)		
Saturation (S_{ri} %)			Water content (%)		
Density ($\rho_i, g/cm^3$)			Porosity (n_f)		
Grain density (ρ_s)			Void ratio (e_f)		
Water content close to specimen			Saturation (S_{rf} %)		
Container number	159		Density ($\rho_f, g/cm^3$)		
Container (g)	28.98		**Fall cone test**		
Container + wet (g)	37.99			Top	Bottom
Container + dry (g)	34.34		1st (mm)		
Water content (%)	68		2nd (mm)		
Fall cone test			3rd (mm)		
	Top	Bottom	4th (mm)		
1st (mm)			5th (mm)		
2nd (mm)			Average (mm)		
3rd (mm)			Strength (kPa)		
4th (mm)					
5th (mm)					
Average (mm)					
Strength (kPa)					

Table A.34: Oedometeric test for remoulded sample, Lab No. 6972, depth 2.65-2.665 m

Department of Civil Engineering		OEDOMETER TEST	Start time: 8.12.2022 Finish time: 17.12.2022	
Sampling place:	GTK		Sampling date:	Aug 2022
Testor:	Reza		Lab. No.:	6973
Tube No.:	Remoulded		Depth (m):	2.77-2.785
Specimen height (cm):	1.5		Section (cm^2)	

BEFORE TEST			AFTER TEST		
Specimen + ring (g)	68		Specimen height (mm)		
Ring (g)	29.55		Specimen mass (g)		
Specimen (g)	38.45		Container number		
Water content (%)			Container (g)		
Porosity (n_i)			Container + wet (g)		
Void ratio (e_i)			Container + dry (g)		
Saturation (S_{ri} %)			Water content (%)		
Density ($\rho_i, g/cm^3$)			Porosity (n_f)		
Grain density (ρ_s)			Void ratio (e_f)		
Water content close to specimen			Saturation (S_{rf} %)		
Container number	43		Density ($\rho_f, g/cm^3$)		
Container (g)	27.60		**Fall cone test**		
Container + wet (g)	34.60			Top	Bottom
Container + dry (g)	31.72		1st (mm)		
Water content (%)	69.9		2nd (mm)		
Fall cone test			3rd (mm)		
	Top	Bottom	4th (mm)		
1st (mm)			5th (mm)		
2nd (mm)			Average (mm)		
3rd (mm)			Strength (kPa)		
4th (mm)					
5th (mm)					
Average (mm)					
Strength (kPa)					

Table A.35: Oedometeric test for remoulded sample, Lab No. 6973, depth 2.77-2.785 m

	Page (1)	Date 29/11/2022
Laboratory of soil mechanics	Triaxial Test	Project num.

Sampling Location: GTK
Project: August part 2
Tube: Remoulded sample
Laboratory Number: 6971

Depth: - 2.5-2.6 m
Cell: 244 (30 kPa)

Before the Test		
Sample Preparation		
Cradle	g	340.54
Cradle + Moist Sample	g	650.93
Membrane (0.1-0.5 cm thickness)	g	11.06
Water Content around the Sample		
Cup Number		50
Cup	g	42.50
Cup + Moist Sample	g	73.48
Cup + Dry Sample	g	60.81
Water Content	%	69
Testing of Porosity of Porous Stone		
Time Corresponding to 10 cm Pressure Height Difference		
Lower Porous Stone	s	40
Upper porous Stone	s	64

After the Test		
Immediately after a bit		
Moist Sample + Papers	g	295.25
Papers	g	1.30

Sample Measurements		
Diameter	**Height**	**Diameter**
48.82	89.22	49.17
49.64	88.23	49.35
49.62	88.58	49.49
49.05		48.64
48.79		47.94

Cone Test		
	Cone Weight g	100
	Bottom	**Top**
Penetration mm	6.5	5.6
	6	5.6
	5.5	5.9
	5.6	6.2
	5.9	6.1
Average	5.9	5.88
Cu		

Water Content				
	Bottom	**Middle B**	**Middle T**	**Top**
Cup Number	50	267	272	281
Cup g	42.50	42.98	43.56	43.15
Cup + Moist Sample	69.68	179.33	151.02	64.76
Cup + Dry Sample	59.60	128.85	111.09	56.60
Water Content %	59.2	58.8	59.1	60.6

Table A.36: Triaxial test for remoulded sample, Lab No. 6971, depth 2.5-2.6 m

	Page (1)	Date 8/12/2022
Laboratory of soil mechanics	Triaxial Test	Project num.

Sampling Location: GTK
Project: August part 2
Tube: Remoulded sample
Laboratory Number: 6974
Depth: - 2.67-2.77 m
Cell: 242 (60 kPa)

Before the Test

Sample Preparation

Cradle	g	340.54
Cradle + Moist Sample	g	659.46
Membrane (0.2-0.5 cm thickness)	g	11.59

Water Content around the Sample

Cup Number		183
Cup	g	44.30
Cup + Moist Sample	g	78.50
Cup + Dry Sample	g	65.4
Water Content	%	62

Testing of Porosity of Porous Stone

Time Corresponding to 10 cm Pressure Height Difference

Lower Porous Stone	s	54
Upper porous Stone	s	44

After the Test

Immediately after a bit

Moist Sample + Papers	g	294.31
Papers	g	1.56

Sample Measurements

Diameter	Height	Diameter
50.10	85.57	48.95
50.25	86.45	50.72
49.8	86.02	50.49
50.23		50.09
48.01		48.8

Cone Test

	Cone Weight g	100
	Bottom	**Top**
Penetration mm	3.6	4.1
	4	4.4
	3.9	4.1
	3.8	4
	4.2	4.3
Average	3.9	4.18
Cu		

Water Content

	Bottom	Middle B	Middle T	Top
Cup Number	54	353	305	20
Cup g	41.93	57.30	55.01	42.46
Cup + Moist Sample	63.43	197.66	164.82	62.10
Cup + Dry Sample	55.91	149.20	126.56	55.12
Water Content %	53.8	52.7	53.5	55

Table A.37: Triaxial test for remoulded sample, Lab No. 6974, depth 2.67-2.77 m

	Page (1)	Date 8/12/2022
Laboratory of soil mechanics	Triaxial Test	Project num.

Sampling Location: GTK
Project: August part 2
Tube: Remoulded sample
Laboratory Number: 6975
Depth: - 2.79-2.89 m
Cell: 244 (90 kPa)

Before the Test

Sample Preparation

Cradle	g	340.54
Cradle + Moist Sample	g	655.20
Membrane (0.2-0.5 cm thickness)	g	10.89

Water Content around the Sample

Cup Number		284
Cup	g	42.23
Cup + Moist Sample	g	75.14
Cup + Dry Sample	g	62.45
Water Content	%	62.8

Testing of Porosity of Porous Stone

Time Corresponding to 10 cm Pressure Height Difference

Lower Porous Stone	s	42
Upper porous Stone	s	61

After the Test

Immediately after a bit

Moist Sample + Papers	g	285.95
Papers	g	1.51

Sample Measurements

Diameter	Height	Diameter
49.8	85.13	49.53
50.3	85.51	50.17
50.02	84.2	50.1
49.9		49.78
49.72		49.61

Cone Test

	Cone Weight g	100
	Bottom	**Top**
Penetration mm	3.1	3
	3.4	3.5
	3.5	3.7
	3.3	3.6
	3.3	3.4
Average	3.32	3.44
Cu		

Water Content

	Bottom	Middle B	Middle T	Top
Cup Number	231	355	359	50
Cup g	42.84	56.98	56.68	42.50
Cup + Moist Sample	66.39	190.16	160.79	64.94
Cup + Dry Sample	58.44	145.88	125.90	57.27
Water Content %	51	49.8	50.4	51.9

Table A.38: Triaxial test for remoulded sample, Lab No. 6975, depth 2.79-2.89 m

	Page (1)	Date 20/10/2022
Laboratory of soil mechanics	Triaxial Test	Project num.

Sampling Location: GTK
Project: August part 1
Tube: 3
Laboratory Number: 6950
Depth: 1.15-1.25 m
Cell: 242 (30 kPa)

Before the Test		
Sample Preparation		
Cradle	g	340.44
Cradle + Moist Sample	g	619.05
Membrane (0.3-0.5 cm thickness)	g	11.55
Water Content around the Sample		
Cup Number		231
Cup	g	42.84
Cup + Moist Sample	g	139.90
Cup + Dry Sample	g	87.07
Water Content	%	119
Testing of Porosity of Porous Stone		
Time Corresponding to 10 cm Pressure Height Difference		
Lower Porous Stone	s	52
Upper porous Stone	s	43

After the Test		
Immediately after a bit		
Moist Sample + Papers	g	239.05
Papers	g	1.65

Sample Measurements		
Diameter	**Height**	**Diameter**
49.4	82.5	48.4
49.4	81.2	49.9
51	81.9	51.2
49.6		49.3
49.4		48

Cone Test		
	Cone Weight g	100
	Bottom	**Top**
Penetration mm	9.8	7.1
	9.6	8
	9.1	7.6
	8.3	8.1
	7.7	8.7
Average	8.9	7.9
Cu		

Water Content		
	Bottom	**Top**
Cup Number	183	333
Cup g	44.30	42.96
Cup + Moist Sample	157.85	164.10
Cup + Dry Sample	104.69	106.89
Water Content %	88	89

Table A.39: Triaxial test for Undisturbed sample, Lab No. 6950, depth 1.15-1.25 m

	Page (1)	Date 20/10/2022
Laboratory of soil mechanics	Triaxial Test	Project num.

Sampling Location: GTK
Project: August part 1
Tube: 3
Laboratory Number: 6951
Depth: 1.25-1.34 m
Cell: 244 (60 kPa)

Before the Test		
Sample Preparation		
Cradle	g	340.44
Cradle + Moist Sample	g	599.95
Membrane (0.2-0.3 cm thickness)	g	8.45
Water Content around the Sample		
Cup Number		262
Cup	g	40.77
Cup + Moist Sample	g	104.67
Cup + Dry Sample	g	69.02
Water Content	%	126
Testing of Porosity of Porous Stone		
Time Corresponding to 10 cm Pressure Height Difference		
Lower Porous Stone	s	40
Upper porous Stone	s	47

After the Test		
Immediately after a bit		
Moist Sample + Papers	g	205.61
Papers	g	1.12

Sample Measurements		
Diameter	**Height**	**Diameter**
47.5	70.33	47.52
49.61	69.69	50.79
50.02	70.82	50.39
47.59		48.2
46.1		46.1

Cone Test		
	Cone Weight g	100
	Bottom	**Top**
Penetration mm	5.3	4.6
	5.9	5.6
	6.1	4.8
	6.7	6
	7.2	6.8
Average	6.24	5.56
Cu		

Water Content		
	Bottom	**Top**
Cup Number	356	360
Cup g	57.65	55.61
Cup + Moist Sample	153.28	161.85
Cup + Dry Sample	110.71	114.56
Water Content %	80	80

Table A.40: Triaxial test for Undisturbed sample, Lab No. 6951, depth 1.25-1.34 m

	Page (1)	Date 26/10/2022
Laboratory of soil mechanics	Triaxial Test	Project num.

Sampling Location: GTK
Project: August part 1
Tube: 3
Laboratory Number: 6952

Depth: 1.35-1.427 m
Cell: 242 (90 kPa)

Before the Test		
Sample Preparation		
Cradle	g	340.44
Cradle + Moist Sample	g	560.81
Membrane (0.2-0.3 cm thickness)	g	10.83
Water Content around the Sample		
Cup Number		471
Cup	g	29.14
Cup + Moist Sample	g	73.27
Cup + Dry Sample	g	49.18
Water Content	%	120
Testing of Porosity of Porous Stone		
Time Corresponding to 10 cm Pressure Height Difference		
Lower Porous Stone	s	52
Upper porous Stone	s	66

After the Test		
Immediately after a bit		
Moist Sample + Papers	g	165.08
Papers	g	0.75

Sample Measurements		
Diameter	**Height**	**Diameter**
50.33	46.57	49.2
50.6	47.57	50.03
51.6	48.24	50.08
49.3		49.8
49.1		49.3

Cone Test		
	Cone Weight g	100
	Bottom	**Top**
Penetration mm	4.1	4.2
	4.3	4.4
	4	4.3
	4.5	4.9
	4.3	4.4
Average	4.24	4.44
Cu		

Water Content		
	Bottom	**Top**
Cup Number	281	20
Cup g	43.15	42.46
Cup + Moist Sample	132.51	115.28
Cup + Dry Sample	95.22	85.13
Water Content %	71.6	70.6

Table A.41: Triaxial test for Undisturbed sample, Lab No. 6952, depth 1.35-1.427 m

	Page (1)	Date 26/10/2022
Laboratory of soil mechanics	Triaxial Test	Project num.

Sampling Location: GTK
Project: August part 2
Tube: VI
Laboratory Number: 6953

Depth: 2.8-2.9 m
Cell: 244 (30 kPa)

Before the Test

Sample Preparation

Cradle	g	340.44
Cradle + Moist Sample	g	634.29
Membrane (0.2-0.3 cm thickness)	g	11.12

Water Content around the Sample

Cup Number		263
Cup	g	37.21
Cup + Moist Sample	g	61.86
Cup + Dry Sample	g	49.51
Water Content	%	100

Testing of Porosity of Porous Stone

Time Corresponding to 10 cm Pressure Height Difference

Lower Porous Stone	s	40
Upper porous Stone	s	64

After the Test

Immediately after a bit

Moist Sample + Papers	g	270.01
Papers	g	0.75

Sample Measurements

Diameter	Height	Diameter
48.6	81	50.1
50.5	80.5	52.3
50.48	80	50.82
49.1		51.85
49.08		51.38

Cone Test

	Cone Weight g	100
	Bottom	**Top**
Penetration mm	7.5	9.3
	7.6	7.3
	7.7	6.7
	6.9	7.4
	6.4	7.7
Average	7.22	7.68
Cu		

Water Content

	Bottom	Middle B	Middle T	Top
Cup Number	355	272	284	314
Cup g	56.98	43.56	42.23	52.65
Cup + Moist Sample	83.03	136.86	160.26	81.82
Cup + Dry Sample	70.79	93.62	105.26	68.11
Water Content %	88.6	86.3	87	88.7

Table A.42: Triaxial test for Undisturbed sample, Lab No. 6953, depth 2.8-2.9 m

	Page (1)	Date 3/11/2022
Laboratory of soil mechanics	Triaxial Test	Project num.

Sampling Location: GTK
Project: August part 2
Tube: VI
Laboratory Number: 6958

Depth: 2.9-3 m
Cell: 242 (60 kPa)

Before the Test

Sample Preparation

Cradle	g	340.44
Cradle + Moist Sample	g	634.11
Membrane (0.3-0.5 cm thickness)	g	12.18

Water Content around the Sample

Cup Number		159
Cup	g	28.98
Cup + Moist Sample	g	78.49
Cup + Dry Sample	g	54.16
Water Content	%	96.6

Testing of Porosity of Porous Stone

Time Corresponding to 10 cm Pressure Height Difference

Lower Porous Stone	s	46
Upper porous Stone	s	42

After the Test

Immediately after a bit

Moist Sample + Papers	g	254.49
Papers	g	0.98

Sample Measurements

Diameter	Height	Diameter
49.78	77.28	48.47
51.69	77.43	51.52
50.15	77.50	52.55
50.62		50.13
49.62		49.8

Cone Test

	Cone Weight g	100
	Bottom	**Top**
Penetration mm	4.7	4.5
	4.3	5.7
	4.2	4.9
	4.4	4.2
	4.6	4.5
Average	4.44	4.76
Cu		

Water Content

	Bottom	Middle B	Middle T	Top
Cup Number	281	50	262	148
Cup g	43.15	42.50	40.77	44
Cup + Moist Sample	69.40	171.61	119.85	63.69
Cup + Dry Sample	58.13	117.56	86.58	55.2
Water Content %	75.22	72	72.6	75.8

Table A.43: Triaxial test for Undisturbed sample, Lab No. 6958, depth 2.9-3 m

	Page (1)	Date 3/11/2022
Laboratory of soil mechanics	Triaxial Test	Project num.

Sampling Location: GTK
Project: August part 2
Tube: VI
Laboratory Number: 6959

Depth: 3-3.1 m
Cell: 244 (90 kPa)

Before the Test

Sample Preparation

Cradle	g	340.44
Cradle + Moist Sample	g	632.74
Membrane (0.3-0.5 cm thickness)	g	11.98

Water Content around the Sample

Cup Number		107
Cup	g	31.82
Cup + Moist Sample	g	64.59
Cup + Dry Sample	g	47.52
Water Content	%	108.7

Testing of Porosity of Porous Stone

Time Corresponding to 10 cm Pressure Height Difference

Lower Porous Stone	s	42
Upper porous Stone	s	65

After the Test

Immediately after a bit

Moist Sample + Papers	g	225.25
Papers	g	0.66

Sample Measurements

Diameter	Height	Diameter
47.69	73.44	47.82
49.26	73.10	49.31
51.88	73.21	51.54
49.31		49.28
45.76		46.59

Cone Test

	Cone Weight g	100
	Bottom	**Top**
Penetration mm	4.5	4.3
	4	4.2
	4.2	4.5
	4.5	4
	4.4	4.3
Average	4.32	4.26
Cu		

Water Content

	Bottom	Middle B	Middle T	Top
Cup Number	231	307	341	314
Cup g	42.84	53.34	58	52.65
Cup + Moist Sample	60.48	159.28	141.09	69.46
Cup + Dry Sample	53.07	115.39	106.58	62.39
Water Content %	72.4	70.7	71	72.6

Table A.44: Triaxial test for Undisturbed sample, Lab No. 6959, depth 3-3.1 m

	Page (1)	Date 25/11/2022
Laboratory of soil mechanics	Triaxial Test	Project num.

Sampling Location: GTK
Project: August part 2
Tube: I
Laboratory Number: 6968

Depth: 0.3-0.4 m
Cell: 242 (30 kPa)

Before the Test

Sample Preparation

Cradle	g	340.62
Cradle + Moist Sample	g	614.43
Membrane (0.1-0.5 cm thickness)	g	10.76

Water Content around the Sample

Cup Number		60
Cup	g	27.52
Cup + Moist Sample	g	83.41
Cup + Dry Sample	g	51.56
Water Content	%	132

Testing of Porosity of Porous Stone

Time Corresponding to 10 cm Pressure Height Difference

Lower Porous Stone	s	
Upper porous Stone	s	

After the Test

Immediately after a bit

Moist Sample + Papers	g	222.65
Papers	g	1.99

Sample Measurements

Diameter	Height	Diameter
47.82	77.40	47.6
48.4	78.26	48.1
49.90	77.98	49.96
48.02		48.2
45.1		46

Cone Test

	Cone Weight g	100
	Bottom	**Top**
Penetration mm	4.5	5.5
	4.5	5.5
	5.2	4.8
	4.6	4.9
	4.7	4.6
Average	4.7	5.06
Cu		

Water Content

	Bottom	Middle B	Middle T	Top
Cup Number	37	269	20	145
Cup g	28.06	43.46	44.46	31.65
Cup + Moist Sample	51.2	144.13	116.48	51.18
Cup + Dry Sample	40.14	96.86	82.37	41.88
Water Content %	91.5	88	89.9	90.9

Table A.45: Triaxial test for Undisturbed sample, Lab No. 6968, depth 0.3-0.4 m

	Page (1)	Date 25/11/2022
Laboratory of soil mechanics	Triaxial Test	Project num.

Sampling Location: GTK
Project: August part 2
Tube: I
Laboratory Number: 6969
Depth: 0.4-0.5 m
Cell: 244 (60 kPa)

Before the Test		
Sample Preparation		
Cradle	g	340.62
Cradle + Moist Sample	g	615
Membrane (0.1-0.5 cm thickness)	g	12.46
Water Content around the Sample		
Cup Number		145
Cup	g	31.65
Cup + Moist Sample	g	73.39
Cup + Dry Sample	g	50.15
Water Content	%	125
Testing of Porosity of Porous Stone		
Time Corresponding to 10 cm Pressure Height Difference		
Lower Porous Stone	s	
Upper porous Stone	s	

After the Test		
Immediately after a bit		
Moist Sample + Papers	g	211.50
Papers	g	1.41

Sample Measurements		
Diameter	**Height**	**Diameter**
46.87	75.51	46.25
46.06	75.11	47.98
49.82	75.07	49.73
47.78		48.49
46.6		46.71

Cone Test		
	Cone Weight g	100
	Bottom	**Top**
Penetration mm	5.5	5.5
	5	4.6
	5.6	4.5
	4.5	5.2
	4.2	5.2
Average	4.96	5
Cu		

Water Content				
	Bottom	**Middle B**	**Middle T**	**Top**
Cup Number	159	333	54	13
Cup g	28.98	42.96	41.93	28.77
Cup + Moist Sample	46.60	137.10	115.49	51.55
Cup + Dry Sample	38.89	96.15	83.46	41.58
Water Content %	77.8	77	77.1	77.8

Table A.46: Triaxial test for Undisturbed sample, Lab No. 6969, depth 0.4-0.5 m

	Page (1)	Date 29/11/2022
Laboratory of soil mechanics	Triaxial Test	Project num.

Sampling Location: GTK
Project: August part 2
Tube: III
Laboratory Number: 6970

Depth: 1.45-1.55 m
Cell: 242 (30 kPa)

Before the Test		
Sample Preparation		
Cradle	g	340.54
Cradle + Moist Sample	g	611.13
Membrane (0.1-0.5 cm thickness)	g	10.63
Water Content around the Sample		
Cup Number		130
Cup	g	30.47
Cup + Moist Sample	g	70.16
Cup + Dry Sample	g	48.52
Water Content	%	120
Testing of Porosity of Porous Stone		
Time Corresponding to 10 cm Pressure Height Difference		
Lower Porous Stone	s	63
Upper porous Stone	s	50

After the Test		
Immediately after a bit		
Moist Sample + Papers	g	238.01
Papers	g	1.66

Sample Measurements		
Diameter	**Height**	**Diameter**
47.84	86.30	47.84
47.23	83.79	47.86
48.22	83.08	48.31
48.52		48.1
46.34		46.7

Cone Test		
	Cone Weight g	100
	Bottom	**Top**
Penetration mm	8.1	6.1
	8.1	8.6
	7.7	8.5
	8.5	9.7
	7.9	8.4
Average	8.06	8.26
Cu		

Water Content				
	Bottom	**Middle B**	**Middle T**	**Top**
Cup Number	269	54	333	20
Cup g	43.46	41.93	42.96	42.46
Cup + Moist Sample	69.09	145.34	126.06	64.72
Cup + Dry Sample	56.41	94.35	85.31	53.89
Water Content %	97.9	97.2	96.2	97.4

Table A.47: Triaxial test for Undisturbed sample, Lab No. 6970, depth 1.45-1.55 m

	Page (1)	Date 14/11/2022
Laboratory of soil mechanics	Triaxial Test	Project num.

Sampling Location: GTK
Project: August part 2
Tube: V
Laboratory Number: 6960
Depth: 2.325-2.425 m
Cell: 242 (30 kPa)

Before the Test

Sample Preparation

Cradle	g	340.46
Cradle + Moist Sample	g	627.37
Membrane (0.3-0.5 cm thickness)	g	11.01

Water Content around the Sample

Cup Number		267
Cup	g	42.97
Cup + Moist Sample	g	76.17
Cup + Dry Sample	g	59.03
Water Content	%	107

Testing of Porosity of Porous Stone

Time Corresponding to 10 cm Pressure Height Difference

Lower Porous Stone	s	51
Upper porous Stone	s	34

After the Test

Immediately after a bit

Moist Sample + Papers	g	255.45
Papers	g	1.43

Sample Measurements

Diameter	Height	Diameter
47.57	85.45	49.77
50.07	85.04	50.22
48.83	85.65	48.51
48.46		48.39
47.16		47.16

Cone Test

	Cone Weight	g	100
	Bottom		**Top**
Penetration	mm	5.1	4.6
		7	6
		7.1	5
		6	5.6
		5.5	5.9
Average		6.14	5.42
Cu			

Water Content

	Bottom	Middle B	Middle T	Top
Cup Number	307	314	341	365
Cup g	53.34	52.65	58	56.95
Cup + Moist Sample	74.78	167.94	151.88	77.84
Cup + Dry Sample	64.84	114.95	109.02	68.17
Water Content %	86.4	85	84	86

Table A.48: Triaxial test for Undisturbed sample, Lab No. 6960, depth 2.325-2.425 m

	Page (1)	Date 14/11/2022
Laboratory of soil mechanics	Triaxial Test	Project num.

Sampling Location: GTK
Project: August part 2
Tube: V
Laboratory Number: 6961

Depth: 2.425-2.525 m
Cell: 244 (60 kPa)

Before the Test

Sample Preparation

Cradle	g	340.46
Cradle + Moist Sample	g	625.26
Membrane (0.3-0.5 cm thickness)	g	12.43

Water Content around the Sample

Cup Number		186
Cup	g	44.98
Cup + Moist Sample	g	92.17
Cup + Dry Sample	g	67.89
Water Content	%	106

Testing of Porosity of Porous Stone

Time Corresponding to 10 cm Pressure Height Difference

Lower Porous Stone	s	54
Upper porous Stone	s	43

After the Test

Immediately after a bit

Moist Sample + Papers	g	242.38
Papers	g	1.29

Sample Measurements

Diameter	Height	Diameter
47.76	81.89	47.94
49.69	82.37	48.08
49.76	81.75	48.19
48.62		48.56
48.97		47.85

Cone Test

	Cone Weight g	100
	Bottom	**Top**
Penetration mm	5.8	5.1
	5.3	4
	5.7	5
	4.7	4.6
	6.1	6.9
Average	5.52	5.12
Cu		

Water Content

	Bottom	Middle B	Middle T	Top
Cup Number	281	148	262	20
Cup g	43.15	44	40.77	42.46
Cup + Moist Sample	71.28	146.43	128.14	64.47
Cup + Dry Sample	58.89	101.89	89.87	54.73
Water Content %	78.7	77	77.9	79

Table A.49: Triaxial test for Undisturbed sample, Lab No. 6961, depth 2.425-2.525 m

	Page (1)	Date 21/11/2022
Laboratory of soil mechanics	Triaxial Test	Project num.

Sampling Location: GTK
Project: August part 2
Tube: VII
Laboratory Number: 6962

Depth: 3.3-3.4 m
Cell: 242 (30 kPa)

Before the Test		
Sample Preparation		
Cradle	g	340.62
Cradle + Moist Sample	g	626.88
Membrane (0.3-0.5 cm thickness)	g	12.71
Water Content around the Sample		
Cup Number		269
Cup	g	43.46
Cup + Moist Sample	g	92.69
Cup + Dry Sample	g	67.53
Water Content	%	104
Testing of Porosity of Porous Stone		
Time Corresponding to 10 cm Pressure Height Difference		
Lower Porous Stone	s	
Upper porous Stone	s	

After the Test		
Immediately after a bit		
Moist Sample + Papers	g	251.43
Papers	g	1.84

Sample Measurements		
Diameter	**Height**	**Diameter**
45.95	84.75	45.89
50.14	84.67	50.2
51.04	83.57	50.5
48.76		48.02
46.03		46.1

Cone Test		
	Cone Weight g	100
	Bottom	**Top**
Penetration mm	5.5	8.3
	7.3	7.7
	4.6	7.4
	6.7	5.3
	4.9	4.6
Average	5.8	6.66
Cu		

Water Content

	Bottom	**Middle B**	**Middle T**	**Top**
Cup Number	37	333	54	159
Cup g	28.06	42.96	41.93	28.98
Cup + Moist Sample	49.80	157.12	135.82	46.82
Cup + Dry Sample	39.20	103.06	91.6	38.60
Water Content %	95	90	89	93.5

Table A.50: Triaxial test for Undisturbed sample, Lab No. 6962, depth 3.3-3.4 m

	Page (1)	Date 21/11/2022
Laboratory of soil mechanics	Triaxial Test	Project num.

Sampling Location: GTK
Project: August part 2
Tube: VII
Laboratory Number: 6963

Depth: 3.4-3.5 m
Cell: 244 (60 kPa)

Before the Test

Sample Preparation

Cradle	g	340.68
Cradle + Moist Sample	g	603.96
Membrane (0.3-0.5 cm thickness)	g	12.28

Water Content around the Sample

Cup Number		50
Cup	g	42.50
Cup + Moist Sample	g	90.45
Cup + Dry Sample	g	65.39
Water Content	%	109

Testing of Porosity of Porous Stone

Time Corresponding to 10 cm Pressure Height Difference

Lower Porous Stone	s	
Upper porous Stone	s	

After the Test

Immediately after a bit

Moist Sample + Papers	g	223.06
Papers	g	1.70

Sample Measurements

Diameter	Height	Diameter
46.79	76.84	46.83
48.03	74	47.85
49.08	75.56	49.68
48.30		46.86
47.02		46.03

Cone Test

	Cone Weight g	100
	Bottom	**Top**
Penetration mm	4.5	4.5
	4	4.2
	4.2	4.5
	4	4.2
	4.2	4.1
Average	4.18	4.3
Cu		

Water Content

	Bottom	Middle B	Middle T	Top
Cup Number	33	263	260	1000
Cup g	28.60	37.21	38.98	28.10
Cup + Moist Sample	52.29	141.04	113.72	46.02
Cup + Dry Sample	41.52	95.04	80.40	37.86
Water Content %	83.3	79.5	80.4	83.6

Table A.51: Triaxial test for Undisturbed sample, Lab No. 6963, depth 3.4-3.5 m

B. List of Figures

Figure 2-1 Map of the site 11
Figure 2-2 Hydrometer test 13
Figure 2-3 Hydrometer test for the site KU1 14
Figure 2-4 Hydrometer test for the site KU1 14
Figure 2-5 Pycnometer glass 15
Figure 2-6 Fall cone apparatus for undisturbed sample 16
Figure 2-7 Fall cone apparatus for remoulded sample 17
Figure 2-8 Comparison between theoretical and experimental values by different researchers 18
Figure 2-9 Yield surface in MMC Model 20
Figure 2-10 Yield surface in S-CLAY1 Model (Koskinen M., 2014)**Error! Bookmark not defined.**
Figure 2-11 definition of $p'm$ (Koskinen M., 2014) ..... **Error! Bookmark not defined.**
Figure 2-12 Position of critical state line ..... **Error! Bookmark not defined.**
Figure 2-13 Position of v in the above formula ..... **Error! Bookmark not defined.**
Figure 2-14 determination of p' at destructuration part 26
Figure 2-15 Wykeham Farrance system for Triaxial test 29
Figure 2-16 New point B for correct calculation 31
Figure 3-1 KU1 For the depth 181-196 cm 34

Figure 3-2 KU1 For the depth 335-350 cm 34
Figure 3-3 KU4 For the depth 168-183 cm 35
Figure 3-4 KU4 For the depth 400-415 cm 35
Figure 3-5 Sampling profile 36
Figure 3-6 Physical property of the KU2 site 37
Figure 3-7 Physical property of the KU3 site 38
Figure 3-8 Physical property of the KU1 site 38
Figure 3-9 Physical property of the KU4 site 39
Figure 3-10 Comparison of Undrained shear strength for undisturbed samples by different researchers for different k 40
Figure 3-11 Comparison of Undrained shear strength for remoulded samples by different researchers for different k 40
Figure 3-12 Uniaxial test for consolidating remoulded sample 42
Figure 3-13 Oedometric test without pore pressure sensor 42
Figure 3-14 Oedometric test with pore pressure sensor 43
Figure 3-15 The Oedometric result for the depth 0.26 m and the site Kytö (KU 4) 44
Figure 3-16 The Oedometric result for the depth 0.29 m and the site Kytö (KU 4) 44
Figure 3-17 The Oedometric result for the depth 1.11 m and the site Kytö (KU 1) 45
Figure 3-18 The Oedometric result for the depth 1.14 m and the site Kytö (KU 1) 45
Figure 3-19 The Oedometric result for the depth 1.41 m and the site Kyto (KU 4) 46
Figure 3-20 The Oedometric result for the depth 1.44 m and the site Kyto (KU 4) 46
Figure 3-21 The Oedometric result for the depth 2.26 m and the site Kyto (KU 4) 47
Figure 3-22 The Oedometric result for the depth 2.31 m and the site Kyto (KU 4) 47
Figure 3-23 The Oedometric result for the depth 2.76 m and the site Kyto (KU 4) 48
Figure 3-24 The Oedometric result for the depth 2.79 m and the site Kyto (KU 4) 48
Figure 3-25 The Oedometric result for the depth 3.26 m and the site Kyto (KU 4) 49
Figure 3-26 The Oedometric result for the depth 3.29 m and the site Kyto (KU 4) 49
Figure 3-27 The Oedometric result for the depth 2.66 m and the site Kyto (KU 4) (Remoulded sample) 50

Figure 3-28 The Oedometric result for the depth 2.78 m and the site Kyto (KU 4) (Remoulded sample) 50

Figure 3-29 Representation of the in-situ vertical stress by Oedometric test and by calculations 51

Figure 3-30 Stress path (p',q) diagram for CIUC 6953-6958-6959 54

Figure 3-31 Behavior of deviatoric stress and pore pressure wrt axial strain 55

Figure 3-32 Specimen before and after Triaxial test 55

Figure 4-1 Statistics results on penetration depth 57

Figure 4-2 Error estimation of penetration depth 58

Figure 4-3 Probability mass function and Cumulative density function for four penetration 60

Figure 4-4 Position of each shape 66

Figure 4-5 Values of water content at 0.5 cm at the top (square shape), 0.5 cm at the bottom (circle shape), 4.5 cm at the middle top (triangle shape) and 4.5 cm at the middle bottom (diamond shape) 67

Figure 4-6 Comparison of different methods 68

C. List of Symbols

A	Area of the sample, cm^2
h	Height of the sample, cm
d	Diameter of the sample, cm
S_u	Undrained shear strength, kPa
S_{uR}	Remoulded undrained shear strength, kPa
V	Sample volume, cm^3
ρ_b	Bulk density, g/cm^3
ρ_s	Dry density, g/cm^3
ρ_w	Water density, g/cm^3
γ	Unit weight, kN/m^3
γ_w	Unit weight of water, kN/m^3
i	Penetration depth, mm
W	Water content, %
S_t	Sensitivity
H_m	Organic content, %
z	Depth, m
T	Temperature, $°C$
η	Water viscosity, mPa.s
R_h	True hydrometer reading

R_0	Reading in the reference solution
R_d	Modified hydrometer reading
H_r	Effective depth, mm
d_i	Equivalent particle diameter, mm
K	Cone factor
n	Porosity, %
S_{ri}	Initial degree of saturation, %
S_{rf}	Final degree of saturation, %
ν	Poisson ratio
e_i	Initial void ratio
e_f	Final void ratio
M	Critical state value of the stress ratio in triaxial space
κ	Slope of the swelling line in $ln - p' - v$ plane
λ	Slope of the normal compression line in $ln\ p' - v$ plane
ε_d	Shear strain, %
ε_d^e	Elastic component of shear strain, %
ε_d^p	Plastic component of shear strain, %
ε_v	Volumetric strain, %
ε_v^e	Elastic component of volumetric strain, %
ε_v^p	Plastic component of volumetric strain, %
$\varepsilon_1, \varepsilon_3$	Principal strains, %
a_v	Coefficient of compressibility, cm^2/kg
m_v	Coefficient of volume compressibility, cm^2/kg
E_{oed}	Oedometer modulus, kPa
C_v	Coefficient of consolidation, cm^2/s
K_v	Coefficient of permeability, cm/s
t	Time, sec
σ_1	Total vertical stress, kPa

σ_3	Total horizontal stress, kPa
C_c	Compression index
p'	Effective mean stress, kPa
q	Deviatoric stress, kPa
P'_0	Initial isotropic hardening parameter, kPa
P'_{CSL}	Effective stress in the critical state line, kPa
q_{CSL}	Deviatoric stress in the critical state line, kPa
P'_m	Size of the yield curve, kPa
G_s	Specific gravity of grains
γ'	Effective unit weight, kN/m^3
v	Specific volume
v_{CSL}	Specific volume at the critical state line
G	Shear modulus, kPa
K_0	Earth pressure coefficient
α	Scalar value of fabric tensor, defines the orientation of the yield curve